Fermi National Accelerator Laboratory

FN-492

Particle Properties on an ABACUS*

Dan Green
Fermi National Accelerator Laboratory
P.O. Box 500, Batavia, Illinois 60510

August 1988

Operated by Universities Research Association Inc. under contract with the United States Department of Energy

Particle Properties on an ABACUS

by

Dan Green
Fermilab

August 1988

Introduction

"If I could remember the names of all these particles, I'd be a Botanist."

Enrico Fermi

In the present era, we are witnesses to the triumph of the Standard Model. However, that model in itself (i.e., confinement) implies that asymptotic states are composites. That being true, the situation is analagous to living in a world of chemical compounds, inferring that atoms exist, but being unable to break the chemical bond. In such a world, a working knowledge of chemistry is unavoidable. Similarly, a nodding acquaintance with hadrons is still essential to particle physicists, even though we "know" that they are composed of quarks. The goal of this set of lectures is to make the masses and decays of the hadron "zoo" explicable using back of the envelope (ABACUS) estimates. The "inspirations" of quantum chromodynamics (QCD) are used wherever possible.

An idiosyncratic list of references is given. Clearly, it is not meant as a complete bibliography. Figures and tables are freely taken from these references. As regards units, $\hbar = c = 1$ is used, but knowing that $\hbar c = 0.2$ GeV $\cdot$ fm $= 2 \times 10^{-14}$ GeV $\cdot$ cm $= \frac{2}{3} \times 10^{-24}$ GeV $\cdot$ sec one can convert any expression to more physical units. Finally in discussing composites, M will refer to composite mass while m refers to the constituent mass.

This note is meant to be a companion piece to FN-423, "FNAL Collider Physics on an Abacus." The same simple minded handwaving approach adopted herein was used in that note but addressing topics in Collider physics. In the same sense that the Lund Monte Carlo contains all of Collider physics, lattice engines can calculate all hadronic properties. Unfortunately, little physical insight follows in the wake of these tools.

The masses, quantum numbers, interactions, and decay modes of the "zoo" are tabulated[1] in the "Blue Book" which is carried by most practicing particle physicists. At the end of these lectures, few mysteries (albeit that topics are sketched in broad but shallow brush strokes) should remain. The outline is as follows; Section I is on Hadron Masses while Section II concerns itself with interactions and decays. Have a good day trip to the Hadron Zoo.

The aid of T. Gourlay and P. Hatcher is gratefully acknowledged. Their patience and good humor is also much appreciated.

Section I.
Hadron Masses

A. Hadron Non-Relativistic Binding

The constituents of the Standard Model are shown in Fig. A.1. They consist of three quark doublets and three generations of lepton doublets. The gauge bosons consist of the photon and the charged and neutral weak force carriers, the Z^0 and W bosons. If this were the whole story, life would be much simpler. However, we know that isolated quarks do not exist and therefore we must face up to the problem of hadrons whose constituents are the quarks themselves.

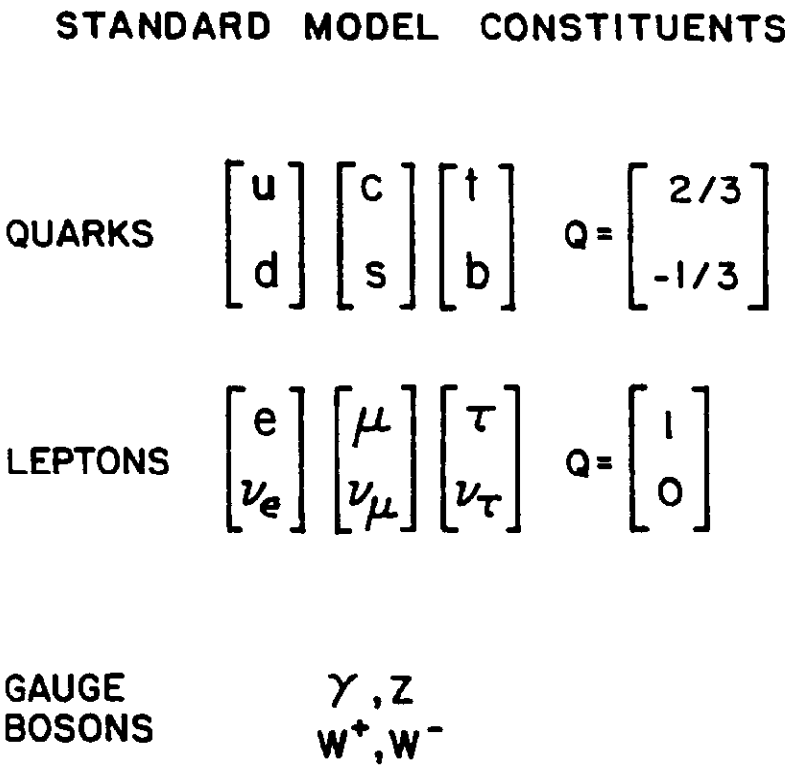

Fig. A.1: Constituents in the Standard Model.

To that end, let us first look at the hydrogen atom which is one of the few solveable problems in physics and something which we have a lot of experience with from undergraduate quantum mechanics. In the hydrogen atom there are only two scales of interest. There is the Yukawa wavelength λ , that is the mass scale, and there is another scale set by the dimensionless coupling constant which for the case of electromagnetism is usually called alpha. For a system acting under a power law potential the virial theorem is given in the equation below:

$$\begin{aligned} V(r) &= A/r^N \\ < T > &= \frac{N}{2} < V > \end{aligned} \qquad \text{(A.1)}$$

This relates the mean value of the kinetic energy and the mean value of the potential energy. Looking at Fig. A.2.a, it is easy to see that the amplitude involved in one photon exchange is proportional to α so it is not at all surprising that the binding energy is proportional to the square of that amplitude or α^2.

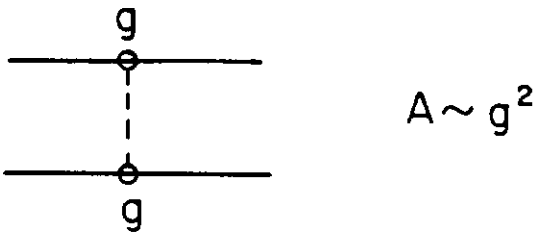

Fig. A.2.a: One photon exchange diagram for the hydrogen atom.

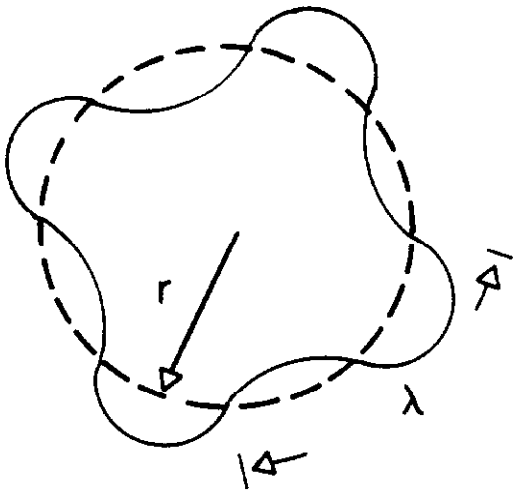

Fig. A.2.b: Standing wave stability condition for a deBroglie matter wave.

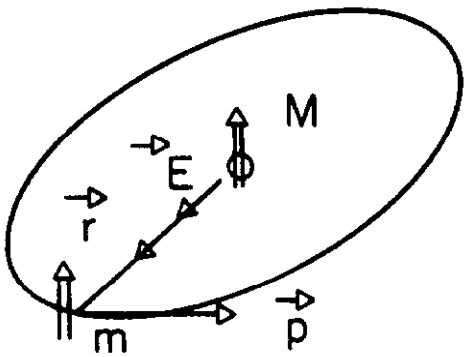

Fig. A.2.c: Spin-orbit vector diagram for moment alignment to $\vec{B}$ field.

The quantization condition for the deBroglie wavelength is shown pictorially in Fig. A.2.b and its given in equation form below:

$$\begin{aligned} \lambda_d &= 2\pi/p,\ \lambda\!\!\!^{-} \equiv 1/m \\ n\lambda_d &= 2\pi r \\ L &= n \end{aligned} \quad . \tag{A.2}$$

The condition can be understood as saying that a stable solution requires a standing wave which means that there are an integral number of deBroglie wavelengths around the orbit of

the hydrogen atom. This leads to the familiar quantization of orbital angular momentum. That being the case, we can derive an expression for the Bohr radius which is given in Eq. A.3 below:

$$\begin{aligned} T &= -V/2 \\ \frac{p^2}{2m} &= g^2/2r,\ L = rp = n \\ \frac{n^2}{2mr^2} &= g^2/2r,\ \alpha \equiv g^2 \qquad . \qquad \text{(A.3)} \\ r &= a = n^2\, \lambda\!\!\!^{-}/\alpha,\ a_o = \lambda\!\!\!^{-}/\alpha \\ E &= T + V = \frac{m}{2}\beta^2 \\ &= V/2 = \frac{m}{2}\left(\alpha^2/n^2\right) \equiv M \end{aligned}$$

We obtain the quantized energy levels as in the standard Bohr theory. Notice that the characteristic size of this bound system is the Yukawa mass scale of the constituents divided by the strength of the binding, α. This means that weakly bound systems are large. Note also that the scale of the binding energy is the mass scale times α^2. The velocity with respect to that of light or β is equal to α; this means we are indeed dealing with a nonrelativistic situation if the binding is weak.

So much for the basic binding mechanism, now let's look at some of the finer structure. We know that the electron has a spin so it possesses a magnetic moment. The basic electric binding, because of relativity, has implicit a magnetic field in the restframe of the electron due to the proton or nucleus current circulating about the electron. This is illustrated in Fig. A.2, and the energy associated with the alignment of the electron-spin magnetic moment to this magnetic field is shown in Eq. A.4:

$$
\begin{aligned}
M_{s0} &= -\vec{\mu}\cdot\vec{B} \\
\vec{B} &= \vec{\beta}\times\vec{E} \sim \vec{L} \\
\vec{E} &= (V/ga)\hat{r} \\
M_{s0} &\approx \left(\frac{g}{m}\right)\vec{S}\,[\beta M/ag] \\
\left|\vec{S}\right| &\sim 1 \\
\frac{M_{s0}}{M} &\sim \left(\frac{g}{m}\right)\left[\frac{\beta}{ag}\right] = \frac{\lambda\beta}{a} = \beta^2
\end{aligned}
\qquad . \qquad (A.4)
$$

The resultant spin-orbit splitting with respect to the main binding is proportional to β^2. Therefore, in a weak binding case where the velocities are low this is a perturbative correction to the main-binding effect and is generally known as spin-orbit splitting. Another small splitting effect is the spin-spin splitting due to the alignment of the electron-magnetic moment with the nuclear-magnetic moment. For heavy nuclei this is a small effect relative to the spin-spin splitting because the nuclear-magnetic moment relative to the electron-magnetic moment is down by the relative mass ratio.

What about angular momentum effects? So far we have been talking about S waves. The effect of angular momentum can be formulated as being due to a centrifugal potential and is shown in Eq. A.5 below:

$$
\begin{aligned}
f &= mv^2/r = L^2/(mr^3) \\
V_c &\sim \left[L^2/(2mr^2)\right] \\
L^2 &= \ell(\ell+1),\; L_z = p
\end{aligned}
\qquad . \qquad (A.5)
$$

The centrifugal force is derivable from the potential. In this case, we used the full quantization condition on the square of the angular momentum. The complete Schrödinger equation then states that the radial-kinetic energy plus the potential energy plus the centrifugal potential is equal to the total energy. Using the spherical harmonic wave function separation, the radial Schrödinger equation is as shown in Eq. A.6:

$$\left[\frac{p_r^2}{2m} + V + V_c\right] = E,\ \psi \equiv (u/r)Y_\ell^p$$
$$\left[-\frac{d^2/dr^2}{2m} + \frac{\ell(\ell+1)}{2mr^2} + V(r)\right]u = Eu \qquad (A.6)$$
$$E = E_o/n^2,\ E_o = \frac{m}{2}\alpha^2 = M$$

Without actually solving this equation one can study the properties of the solution at large and at small values of the radius. At large values of the radius the kinetic term dominates because the potential falls off. In that case, the solution is exponential in radius. Conversely, at small values of the radius, what is important is the kinetic term and the centrifugal potential since it goes like one over r^2 while the potential for Coulomb binding only goes as one over r. In that case, a power law for the wave function is easily seen to be a solution. Putting both of these together one can write down the Schrödinger solution as the product of those two times some unspecified polynomial. In fact, this is the correct solution as is known from undergraduate quantum mechanics:

$$r \to \infty \ : \ \frac{-1}{2m}\frac{d^2u}{dr^2} = (E_0/n^2)u$$
$$u \sim e^{-r/na_o}$$
$$r \to o \ : \ \left[-\frac{d^2u}{dr^2} + \frac{\ell(\ell+1)}{r^2}\right]u = o \qquad (A.7)$$
$$u \sim r^{\ell+1}$$
$$\therefore \quad \psi \sim r^\ell e^{-r/na_o}\left[h^{(r)}\right]Y_\ell^p$$

So what happens is that at large values of the radius the wave function falls off. That means we are bound and contained somewhere near the origin. The r^ℓ factor means that the centrifugal potential pushes out the wave function and that causes the r^ℓ behavior of the wave function near the origin. An important special case occurs for the lowest principle quantum number, S wave or l = 0 wave function which is a simple exponential. The normalization condition means that the wave function squared (the probability density) integrated over all space is equal to 1. That defines the coefficient in front as shown below:

$$\psi_{\ell=0}^{n=0} = \sqrt{\frac{1}{\pi a_0^3}}\, e^{-r/a_o}$$
$$|\psi(0)|^2 = \frac{1}{\pi a_o^3} \qquad (A.8)$$
$$= \alpha^3/\pi\lambda^{\,3}$$

Notice that the probability density at the origin goes like the inverse cubed power of the Bohr radius. This means that more weakly bound systems are less dense at the origin as one might expect. One should also note that the wave function vanishes at the origin except for S waves.

Finally, let's go back and look at the spin-spin interaction. In this case, we will be following a derivation which was originally made by Fermi. Suppose you have a uniform surface charge density which is rotating with some angular frequency. This surface charge density can be broken up into a series of infinitesimal current loops. We know that current loops cause a dipole magnetic field and we can sum all the current loops over the surface of the rotating sphere. When we do that we find we have a dipole field outside and a uniform field inside. The interaction of that field with a point particle of magnetic moment density $\vec{M}_2$ results in an interaction energy as given below:

$$\begin{aligned} \vec{B}_{in} &= \frac{8\pi}{3V}\vec{\mu}_1, \; V = \text{volume of 1} \\ M_{12} &= -\vec{\mu}\cdot\vec{B} = -\int \vec{B}_1\cdot\vec{M}_2 d\vec{r} \\ &= -\int \frac{8\pi}{3V}\vec{\mu}_1\cdot\vec{M}_2 d\vec{r} \\ &\simeq -\frac{8\pi}{3}\vec{\mu}_1\cdot\vec{M}_2(0) \end{aligned} \qquad (A.9)$$

Since we are dealing with S states the interaction energy with the dipole is only inside and we can approximate particles 2's magnetic moment density with its value at the origin. That value is given below:

$$\begin{aligned} \vec{M}_2(0) &= \frac{e_2}{m_2}\,\vec{S}_2\,|\psi_{12}(0)|^2 \\ \vec{\mu}_1 &\sim \frac{e_1}{m_1}\,\vec{S}_1 = \frac{e_1}{2m_1}\,\vec{\sigma}_1 \\ M_{12} &= \frac{8\pi}{3}\left(\frac{e_1e_2}{m_1m_2}\right)|\psi_{12}(0)|^2\vec{S}_1\cdot\vec{S}_2 \\ &= \frac{8\pi}{3}(\vec{\mu}_1\cdot\vec{\mu}_2)\,|\psi_{12}(0)|^2 \end{aligned} \qquad (A.10)$$

The resultant spin-spin interaction energy is proportional to the wave function of the composite system at the origin. Note, this result is only good for S states. To get an order of magnitude estimate of the value of the spin-spin interaction energy we use our previous estimate for the wave function at the origin. Remember that the probability density has dimensions one over length cubed:

$$
\begin{aligned}
M_{ss} &\sim \left(\frac{g^2}{m^2}\right)\left(\frac{1}{a_o^3}\right) \\
&\sim \frac{\alpha}{m^2}\left(\alpha^3 m^3\right) = \alpha^4 m \ . \qquad \text{(A.11)} \\
\frac{M_{ss}}{M} &\sim \alpha^2
\end{aligned}
$$

The spin-spin interaction energy is equal dimensionally to the mass times α^4, and that's α^2 times the characteristic binding energy. If you recall the result for spin-orbit splitting, when the constituents are all of equal mass the spin-spin splitting is as important as the spin-orbit splitting. That is not the case for the hydrogen atom but it is certainly the case for positronium and for the composite quark anti-quark and three quark systems that we will be looking at later.

B. Current and Constituent Quarks

The evidence for the existence of quarks has been outlined in many books and it can be found in the references. For example, in electron-positron scattering one first found evidence of the existence of point-like partons in the proton. Somewhat later the power law behavior of the transverse-momentum spectrum of secondaries seen in high-energy hadron colliders was used as evidence for the observation of Rutherford-like scattering of partons within the hadrons. The necessity of binding quark systems together implies the existence of some vector boson analogous to the photon. In addition, the momentum sum rule which must be satisfied by the partons in electron-proton deep-inelastic scattering tells you that the total momentum carried by the quarks in the proton is only about half of all of the momentum. That is additional evidence for the existence of this vector gluon. Finally, the comparison between electron-proton and neutrino-proton scattering validates the charge assignments given to the quarks. For reasons which will become more clear later, quarks are assumed to come in three colors. Color is the strong force "charge." There are then nine possible color anti-color gluon combinations. However, color confinement means there are no free gluons and so the color singlet which would not be confined is not allowed. This means that in the Standard Model there is an octet of colored gluons.

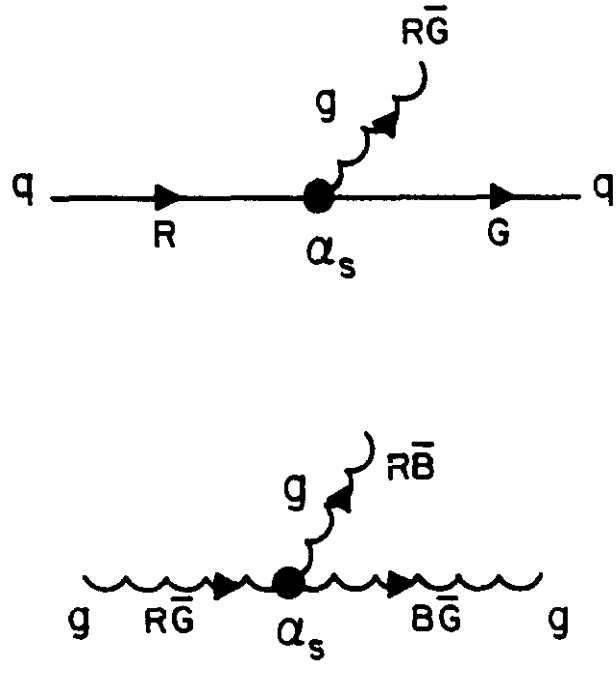

Fig. B.1: Quark-gluon and triple gluon couplings.

Looking at Fig. B.1, this means that gluons are "charged." They themselves are colored and so that leads to a natural question. Do gluons bind to one another, i.e., do glueballs exist? There is no particular reason why with non-Abelian couplings that glueballs should not exist. There is a whole cottage industry of lattice calculations which indeed predict the lowest lying glueball states. Since gluon couplings are not radically different from quark couplings, you expect that the lightest glueball will be on the same mass scale as the typical meson or about 1 GeV. The quantum numbers are predicted also. However, there is no convincing evidence yet for glueball candidates and we will speak no more on this topic.

To begin looking at quark anti-quark systems let's recall some of the results from positronium which is the bound state of an electron and a positron under electromagnetic interactions. The charge conjugation quantum number of such a state is $(-1)^{S+1}$ while the parity is $(-1)^{L+1}$ The two spins couple together to a spin zero or spin one. For S states, the parity is negative and the charge conjugation is either minus one for spin zero or plus one for spin one. Since the charge conjugation quantum number for a system of n photons is $(-1)^n$, the singlet positronium can only decay to three photons while the triplet can decay to two photons. The lowest order Feynman diagram for these decays is shown in Fig. B.2.

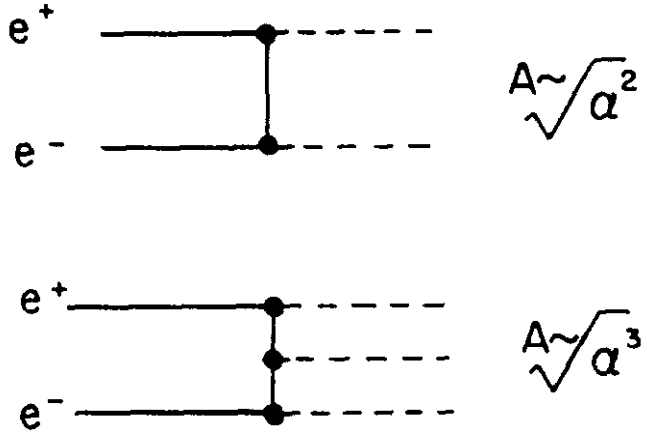

Fig. B.2: Diagram for otho and para positronium annihilation.

Clearly the singlet decay width is down by a factor of α just from coupling constant arguments. Exact formulae are given in Eq. B.1:

$$\begin{aligned}\Gamma(^1S_o \rightarrow \gamma\gamma) &= \frac{4\alpha^2}{M^2}|\psi(0)|^2 \\ \Gamma(^3S_1 \rightarrow \gamma\gamma\gamma) &= \frac{4\alpha^3}{M^3}|\psi(0)|^2\left\{\frac{4(\pi^2-9)}{9\pi}\right\}\end{aligned} \qquad (B.1)$$

In these formulae the power of α can be read off the Feynman diagram. We expect electron and positron to annihilate by overlapping at the origin, so we expect the proportionality to the wave function at the origin squared since that is a probability density. Since the probability density is proportional to mass cubed, and since the decay width has the dimensions of mass, then the width is dimensionally α^2 times the wave function squared divided by the square of the mass. That form could be argued for on purely dimensional grounds. In fact, as seen below,

$$\begin{aligned}\Gamma &\sim \frac{\alpha^2}{M^2}|\psi(0)|^2 \\ &\sim \alpha^5 M \\ \Gamma/E &\sim \alpha^3\end{aligned} \quad , \qquad (B.2)$$

the singlet decay width is proportional to the fifth power of α times the mass which means that the width per binding energy is proportional to α^3. This means that for weak coupling the positronium states are extremely narrow on the scale of their binding energies. The faster positronium rate is measured to be $\Gamma_{OBS}(e^+e^-) = 5.3 \times 10^{-15}\ GeV$. The expected rate is $\Gamma \sim \alpha^5 M$ or $2 \times 10^{-14}\ GeV$ for $M = 1.0\ MeV$ (ignoring reduced masses). This confirmation of the calculation spurs us on to apply the picture to new physical systems.

What we would like to do is find a bound system of quark and anti-quark in nature which approximates the situation for positronium. Without going into a justification for that, let us look at the ψ meson and assert that this is a bound state of a charmed and anti-charm quark system. Assuming that the binding is weak, we will take half of the ψ mass to be the charmed quark mass of about 1.5 GeV. This means the Yukawa wavelength is about 0.12 fermis and the first Bohr radius is the Yukawa length over α for strong interactions (α_s). The radius is about 0.4 fermis for an α_s of 0.3. Let's try to get a confirmation of that α_s by looking at the data in Table B.1.

Table B.1.
Charmonium Mass Splitting

$$\left.\begin{aligned} M_\psi - M_{\eta_c} &= 3.097 - 2.980\ GeV \\ M_\chi(2^{++}) - M_\chi(1^{++}) &= 3.558 - 3.510\ GeV \\ M_\chi(1^{++}) - M_\chi(0^{++}) &= 3.510 - 3.415\ GeV \end{aligned}\right\} \sim (\alpha_s)^2 M$$

$$\Gamma(\psi) = 63\ KeV$$

The spin-spin splitting between the ψ and the η_c gives an estimator of α_s since the spin-spin splitting we saw in Section A is proportional to $(\alpha_s)^2$. That gives us an estimator of α_s of about 0.44. Similarily, looking at Table B.1 the spin-orbit splitting, which is proportional to β^2 which for Coulomb binding is equal to α^2 gives us a comparable estimate for α_s.

At least we are self consistent in that we assume nonrelativistic binding and we get an α_s which is not too large. The decay rate for the ψ into anything is measured to be 63 kilovolts. We use the results given above in Eq. B.1, for Coulomb binding and also assume Coulomb binding to estimate the wave function at the origin. We find that, approximating the ψ total width as the triplet S decay into three gluons, solving for α_s gives us that the triplet width is proportional to the mass of the ψ and proportional to α_s to the sixth power. Putting in the numbers leads to an α_s of 0.22. This example is certainly encouraging because it tells us that ψ, n_c, and χ states behave as if they were composed of a quark anti-quark system bound together by gluons with the strength which is of order 0.2 which means we have a nonrelativistic system.

Having fortified ourselves with an example which works, we will now go on and attempt to construct the hadrons. All of the hadrons are formed from three fundamental constituent quarks up, down, and strange. The idea is to explain the multiplets of hadrons in the nonrelativistic quark model. We want to explain the quantum numbers, masses, decay widths, and decay branching ratios. The quantum numbers of the six types of quarks are given in Table B.2.

Table B.2.
Quantum Numbers of Three Quark Generations

A. QUANTUM NUMBERS

Each quark has spin 1/2. The additive quantum numbers (other than baryon number = 1/3) of the known (and presumed) quarks are shown in the table.

	Quark type (flavor)					
Quantum number	*d*	*u*	*s*	*c*	*b*	*t*
Q — electric charge	$-\frac{1}{3}$	$+\frac{2}{3}$	$-\frac{1}{3}$	$+\frac{2}{3}$	$-\frac{1}{3}$	$+\frac{2}{3}$
I_z — *z*-component of isospin	$-\frac{1}{2}$	$+\frac{1}{2}$	0	0	0	0
S — strangeness	0	0	−1	0	0	0
C — charm	0	0	0	+1	0	0
B — bottomness	0	0	0	0	−1	0
T — topness	0	0	0	0	0	+1

First let's add the spins of a quark and an anti-quark together. Now of course we know the answer to this, spin half plus spin half gives you a singlet spin zero and a triplet spin one. This means that a quark and anti-quark system will give you pseudoscalar mesons and vector mesons. However, it is instructive to look at this in a graphical way as shown in Fig. B.3.a where we have a fundamental doublet representation with spin-up and spin-down. When we add spin-half plus spin-half, you can do this pictorially by putting the center of gravity of one fundamental doublet on top of the other doublet. Then you find you have a triplet and a singlet where the top and the bottom of the triplet are easily seen to be up up and down down as shown in Fig. B.3.b. In the case of quarks, we have two additive quantum numbers which are the third component of isotopic spin and the strangeness. Fundamental representations of SU(3) for the 3 quarks and anti-quarks are shown in Fig. B.3.c.

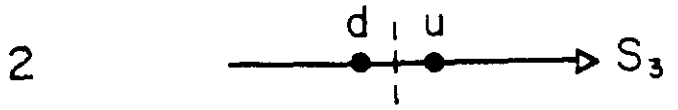

Fig. B.3.a: Locations for fundamental SU(2) representation.

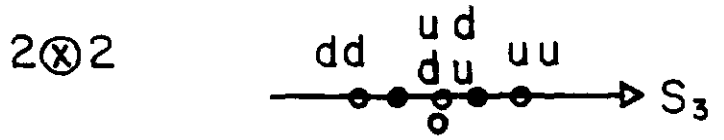

Fig. B.3.b: Formation of $2 \otimes 2$.

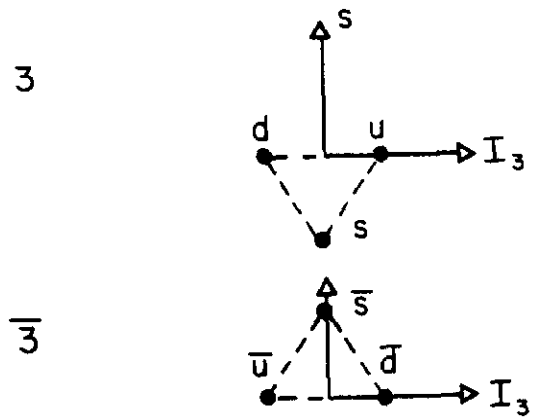

Fig. B.3.c: Locations for fundamental SU(3) representations.

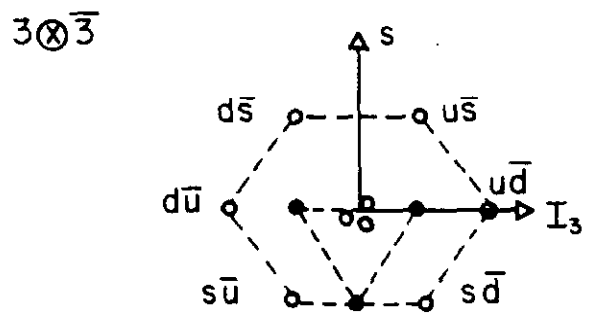

Fig. B.3.d: Formation of $3 \otimes \bar{3}$.

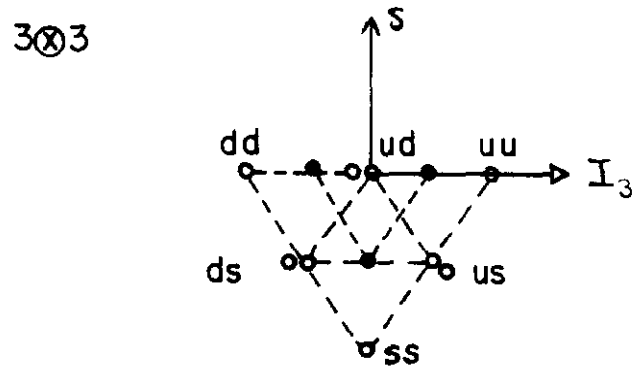

Fig. B.3.e: Formation of $3 \otimes 3$.

There are two fundamental representations for quarks and anti-quarks. Let's find the SU(3) representations of $3 \otimes \bar{3}$. This is done graphically in Fig. B.3.d. There are obviously nine possible quark anti-quark combinations and one visualizes them in the analogous way by putting the $\bar{3}$ representation on top of each element of the 3 representation. It is extremely easy to read off the quark and anti-quark content of all of the states on the periphery. Its quite easy to see that the decomposition leads to a singlet and an octet. Similarily the folding of $3 \otimes 3$ for a two quark system leads to a sextet and an anti-triplet as shown in Fig. B.3.e. If we combine them with yet another quark we would find the three quark baryon representations:

$$\begin{aligned} 2 \otimes 2 &= 1 \oplus 3 \\ 3 \otimes \bar{3} &= 1 \oplus 8 \\ 3 \otimes 3 &= 6 \oplus \bar{3} \\ 3 \otimes 3 \otimes 3 &= 1 \oplus 8 \oplus 8 \oplus 10 \end{aligned} \quad . \tag{B.3}$$

To make the identification with the multiplets of the quark and anti-quark system, we look at the meson entries to the particle properties tables shown in Table B.3.

Table B.3.
Meson Summary.

Particle	$I^G(J^{PC})$ [a] — *estab.*	Mass M (MeV)	Full width Γ (MeV)	Partial decay modes: Mode	Fraction(%) [Upper limits (%) are 90% CL]		p [b] (MeV/c)
NONFLAVORED MESONS							
$\pi^\pm$	$1^-(0^{-+})$	139.57	0.0	See Stable Particle Summary Table			
π^0		134.96	7.57 ± 0.32 eV				
η	$0^+(0^{-+})$	548.8 ± 0.6	*1.05* ± *0.15* keV	Neutral	70.9	See Stable Particle	
				Charged	29.1	Summary Table	
$\rho(770)$	$1^+(1^{--})$	770 [§] ± 3 [§]	153 ± 2 MeV	$\pi\pi$	≈ 100		358
				$\pi\gamma$	0.046 ± 0.005		372
				$\mu^+\mu^-$	0.0067 ± 0.0012 [d]		370
Γ_{ee} = (*6.9* ± *0.3*) keV				e^+e^-	0.0045 ± 0.0002 [d]		384
				$\eta\gamma$	seen		189
M and Γ from neutral mode.				For upper limits, see footnote *e*			
$\omega(783)$	$0^-(1^{--})$	782.6 ± 0.2 S=1.1*	9.8 ± 0.3	$\pi^+\pi^-\pi^0$	89.6 ± 0.5		327
				$\pi^0\gamma$	8.7 ± 0.5		380
				$\pi^+\pi^-$	*1.7* ± *0.2*		366
				$\pi^0\mu^+\mu^-$	0.010 ± 0.002		349
Γ_{ee} = (*0.66* ± *0.04*) keV S=*1.2**				e^+e^-	0.0067 ± 0.0004	S=1.2*	391
				$\eta\gamma$	seen		199
				For upper limits, see footnote *f*			
$\eta'(958)$	$0^+(0^{-+})$	957.57 ± 0.25	0.24 ± 0.03	$\eta\pi\pi$	65.2 ± 1.6		231
				$\rho^0\gamma$	30.0 ± 1.6		170
				$\omega\gamma$	2.7 ± 0.5		159
				$\gamma\gamma$	1.9 ± 0.2		479
				$3\pi^0$	0.17 ± 0.04		430
				$\mu^+\mu^-\gamma$	0.009 ± 0.002		467
				For upper limits, see footnote *g*			
$f_0(975)$ *was S*(975)	$0^+(0^{++})$	975 [c] ± 4 S=1.4*	33 [c] ± 6	$\pi\pi$	78 ± 3		467
				$K\bar{K}$	22 ± 3		
$a_0(980)$ *was* $\delta(980)$	$1^-(0^{++})$	983 [h] ± 2	54 [h] ± 7	$\eta\pi$	seen		320
				$K\bar{K}$	seen		
$\phi(1020)$	$0^-(1^{--})$	1019.5 ± 0.1 S=1.2*	4.22 ± 0.13	K^+K^-	49.5 ± 1.5	S=1.9*	127
				$K_L K_S$	34.3 ± 0.9	S=1.3*	110
				$\pi^+\pi^-\pi^0$ (incl. $\rho\pi$)	14.9 ± 1.4	S=2.3*	462
				$\eta\gamma$	1.3 ± 0.1	S=1.1*	362
				$\pi^0\gamma$	0.131 ± 0.013		501
				e^+e^-	0.031 ± 0.001		510
Γ_{ee} = (*1.31* ± *0.06*) keV				$\mu^+\mu^-$	0.025 ± 0.003		499
				$\pi^+\pi^-$	0.02 ± 0.01		490
				For upper limits, see footnote *i*			
$h_1(1190)$ *was H*(1190)	$0^-(1^{+-})$	1190 ± 60	320 ± 50	$\rho\pi$	seen		327

The pseudoscalar mesons have a strange particle doublet and a nonstrange particle isotriplet as do the vector mesons. These are identified with the K or $K^\star$ and the π and ρ, respectively. The splitting in mass among members of given multiplet is due to SU(3) breaking. The splitting between multiplets, for example, between the pseudoscalar and vector mesons is due to spin-spin splitting. We will quantify these splits later. Certainly the predicted octet and singlet structure for pseudoscalar and vector mesons is a very encouraging sign that SU(3) is a reasonable symmetry scheme.

For the baryons we have a three-quark system and there are 27 possible combinations. We have asserted that this decomposes into a singlet, a symmetric octet, an anti-symmetric octet, and a decuplet. This is something one can continue in the style of Fig. B.3.e and prove for onself. As far as the spins go, a $\frac{1}{2} + \frac{1}{2}$ gives you a singlet and a triplet. Recoupling with a third spin half quark gives you total spin of $\frac{1}{2}$ or $\frac{3}{2}$. The parity is $(-1)^L$ so the S wave baryons have parity plus. That means one expects a $\frac{1}{2}^+$ octet and a $\frac{3}{2}^+$ decuplet. In fact when flavor SU(3) was originally proposed by Gell-Mann, the Ω^- was as yet undiscovered and it's prediction and subsequent discovery was considered a triumph for SU(3). The 0^- and 1^- meson octets, the $\frac{1}{2}^+$ octet and the $\frac{3}{2}^+$ decuplet are shown in Fig. B.4.

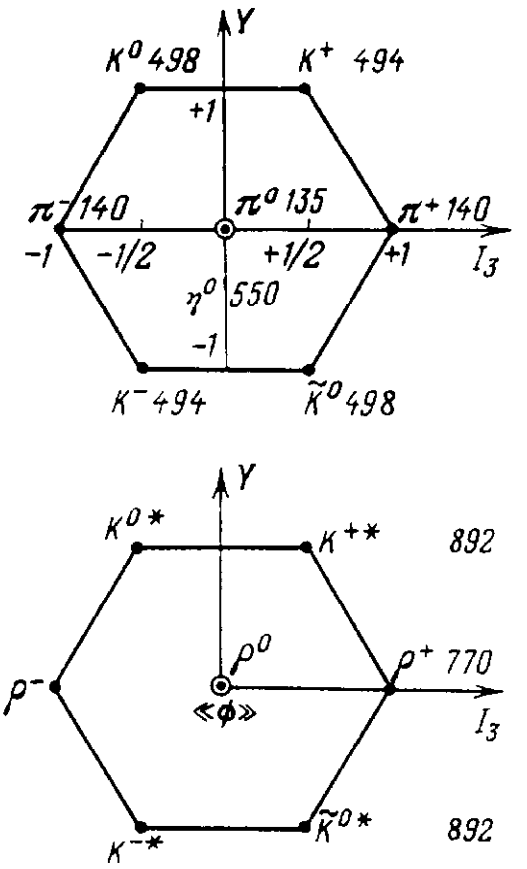

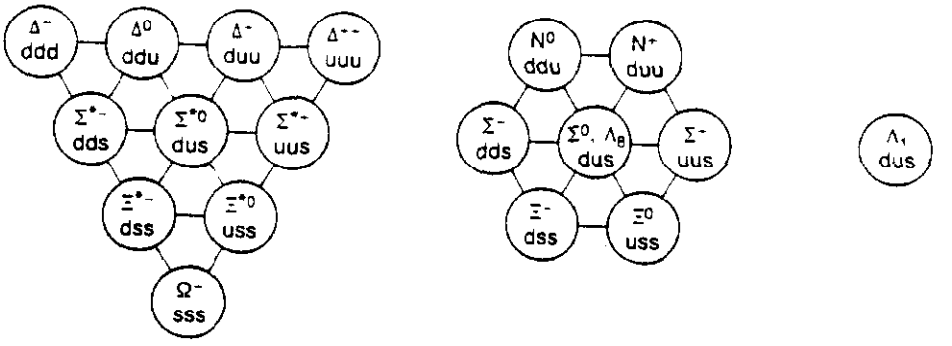

Fig. B.4: pseudoscalar mesons, vector mesons, octet, and decuplet baryons.

There is one problem, in the sense that looking at the Ω^- it consists of three strange quarks bound together. It is flavor symmetric. Since it consists of three identical Fermion quarks in an L = 0 state, it is spatially symmetric. The decuplet is spin $\frac{3}{2}$ so all spins have to be up. That is a spin symmetric wave function, and so the Ω^- is spin, space and flavor symmetric. Yet it is a system of three Fermions and must be totally anti-symmetric. In order to solve this problem another quantum number called color was postulated. Having started as an ad hoc way to save the spin/statistics theorem, it has become the charge of the strong force in the guise of quantum chromodynamics. Each quark comes in three colors; red, green, and blue. For example, the Ω^- is a strange red quark, a strange blue quark, and a strange green quark. It is color anti-symmetric and the complete wave function is totally anti-symmetric.

There remains the nagging problem of the relationship between current quarks and constituent quarks. A glance at Fig. B.5, which shows the interaction between an offshell photon with a quark in the proton, tells us that BJ's x variable is a measure of the momentum fraction carried by the proton if all the relevant mass scales are small with respect to the invariants q^2 and $\underline{p} \cdot q$. Thus deep-inelastic scattering and the scaling observed there implies that the mass scales associated with the quarks are small for these current interactions. But if that is so, then how is it that three quarks or a quark and anti-quark can make a system which has a mass of typically 1 GeV. To see that there is no paradox involved, let's imagine a system of N massless current quarks which is confined (by a mechanism we don't understand precisely) to a region of radius a. This confining "bag" has a phenomenological energy density B which is confining the system. The energy of such a system is the sum of kinetic terms

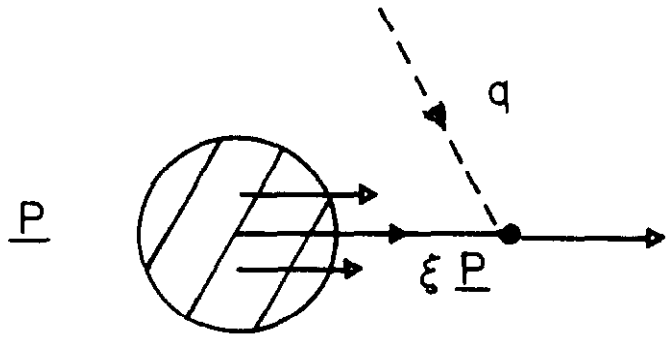

$$
\begin{aligned}
(\epsilon \underline{p} + q)^2 &= m^2 \\
\epsilon^2 M^2 + q^2 + 2\epsilon \underline{p} \cdot q - m^2 &= 0 \\
x_{B_j} &= -q^2/2\underline{p} \cdot q \simeq \epsilon
\end{aligned}
$$

Fig. B.5: Scattering of a virtual photon off a quark with momentum fraction ϵ.

and the bag energy itself, since all the energy contributes to the mass:

$$
\begin{aligned}
E &= \sum_i^n p_i + B\left(\frac{4\pi}{3}a^3\right) \\
\Delta x \Delta p &\sim 1 \\
p_i &\sim 1/a \\
E &\sim n/a + B\left(\frac{4\pi}{3}a^3\right)
\end{aligned}
\qquad \text{(B.4)}
$$

The uncertainty principle tells us that as we confine the system to smaller volume the momentum of the constituents goes up. That tells us that the kinetic term increases as the volume goes down whereas the energy associated with bag confinement has an opposite behavior. A stable system occurs at a minimum of the energy when the bag energy and the momentum associated with the confinement are balanced:

$$
\begin{aligned}
\partial E/\partial a &= 0 \\
a &= (N/4\pi B)^{\frac{1}{4}} \\
E_a \equiv M &= \frac{4}{3}(N/a)
\end{aligned}
\qquad \text{(B.5)}
$$

At this value of radius, the mass of this composite system is proportional to the number of constituents and inversely proportional to the confining radius. The confining radius depends on the bag parameter B.

As an example, if the mass is a proton mass and we take three constituents for N then we find that the size is 1.6 fermis. This is certainly a plausible number and that's the size needed to get a proton mass from confining three massless quarks to a certain volume of space. It is certainly compatible with the size that we get from the elastic electromagnetic form factor which is probing the distribution of charge inside the proton. It is also compatible with the pp cross section which is something like πa^2. If we take 40 millibarns, we find a radius of $a = 1.1\ fm$ which is again in the right ballpark.

What this means is that the constituent quark mass arises from the kinetic energy and the confining potential energy. The constituent mass is an effective mass somewhat analogous to the effective mass for electrons moving in a crystal. We have shown that the massless quark confined to a typical system of size 1 fermi acquires an effective mass of about 300 MeV. This analysis also warns us that the mass of a quark bound in a quark anti-quark meson is not necessarily the same constituent mass as the same quark bound in a three quark baryon. In order to understand the masses we clearly need to understand the dynamics. However, in the future we may gloss over this fact and assume that the up quark has some constituent mass which is independent of the binding situation. One should always keep in mind that this is an approximation which is clearly not true in general.

C. SU(N) and Hadron Multiplets, Electromagnetic Mass Splitting

Before starting with SU(3) multiplets, lets recall the situation with SU(2) isotopic spin multiplets. Remember that the proton and neutron have only a 1.2 MeV mass difference. The cause of this is the degeneracy of the up and the down quark; this is the basis for isotopic spin. Now obviously SU(3) symmetry is more badly broken because the Λ is split from the neutron by 176 MeV. The difference in quark content between those two is to replace a down quark in the neutron by a strange quark in the Λ. We expect that the main breaking in the SU(3) symmetry is mirrored in the fact that the strange quark is heavier than the up and down quarks.

For SU(2) the basis states are the up and down quarks and any state can be expanded in terms of up and down quarks. The generators are the Pauli spin matrices. They satisfy commutation relations and anti-commutation relations as given below:

$$\begin{aligned} u &= \begin{pmatrix} 1 \\ 0 \end{pmatrix}, d = \begin{pmatrix} 0 \\ 1 \end{pmatrix}, \chi = \begin{pmatrix} u \\ d \end{pmatrix} \\ \vec{\sigma} : \sigma_1 &= \begin{pmatrix} 0 & 1 \\ 1 & 0 \end{pmatrix}, \sigma_2 = \begin{pmatrix} 0 & -i \\ i & 0 \end{pmatrix}, \sigma_3 = \begin{pmatrix} 1 & 0 \\ 0 & -1 \end{pmatrix} \\ [\sigma_i, \sigma_j] &= 2i\, \epsilon_{ijk}\sigma_k \qquad . \qquad \text{(C.1)} \\ \{\sigma_i, \sigma_j\} &= 2\delta_{ij} \\ \vec{S} &= \vec{\sigma}/2 \end{aligned}$$

In general, one should recall that for SU(n) there are $n^2 - 1$ generators represented by hermitian traceless n by n matrices. In going to SU(3) the basis states are now up, down, and strange quarks and any general state χ can be expanded in terms of them. Now $n^2 - 1 = 8$ generators and they satisfy commutation and anti-commutation relations which are more complicated. The fundamental representation for those commutation relations are shown in Table C.1.

Table C.1.
Commutation and anti-commutation relations for the SU(3) generators λ_i.

$$\left[\lambda_a, \lambda_b\right] = 2if_{abc}\lambda_c$$
$$\left\{\lambda_a, \lambda_b\right\} = \tfrac{4}{3}\delta_{ab}I + 2d_{abc}\lambda_c$$

where I is a $d \times d$ unit matrix. The f_{abc} are odd under the permutation of any pair of indices, while the d_{abc} are even. The nonzero elements are

abc	f_{abc}	abc	d_{abc}	abc	d_{abc}
123	1	118	$1/\sqrt{3}$	355	1/2
147	1/2	146	1/2	366	−1/2
156	−1/2	157	1/2	377	−1/2
246	1/2	228	$1/\sqrt{3}$	448	$-1/(2\sqrt{3})$
257	1/2	247	−1/2	558	$-1/(2\sqrt{3})$
345	1/2	256	1/2	668	$-1/(2\sqrt{3})$
367	−1/2	338	$1/\sqrt{3}$	778	$-1/(2\sqrt{3})$
458	$\sqrt{3}/2$	344	1/2	888	$-1/\sqrt{3}$
678	$\sqrt{3}/2$				

In the fundamental 3-dimensional representation, the λ_a's are given by

$$\lambda_1 = \begin{pmatrix} 0 & 1 & 0 \\ 1 & 0 & 0 \\ 0 & 0 & 0 \end{pmatrix} \quad \lambda_2 = \begin{pmatrix} 0 & -i & 0 \\ i & 0 & 0 \\ 0 & 0 & 0 \end{pmatrix} \quad \lambda_3 = \begin{pmatrix} 1 & 0 & 0 \\ 0 & -1 & 0 \\ 0 & 0 & 0 \end{pmatrix}$$

$$\lambda_4 = \begin{pmatrix} 0 & 0 & 1 \\ 0 & 0 & 0 \\ 1 & 0 & 0 \end{pmatrix} \quad \lambda_5 = \begin{pmatrix} 0 & 0 & -i \\ 0 & 0 & 0 \\ i & 0 & 0 \end{pmatrix} \quad \lambda_6 = \begin{pmatrix} 0 & 0 & 0 \\ 0 & 0 & 1 \\ 0 & 1 & 0 \end{pmatrix}$$

$$\lambda_7 = \begin{pmatrix} 0 & 0 & 0 \\ 0 & 0 & -i \\ 0 & i & 0 \end{pmatrix} \quad \lambda_8 = \begin{pmatrix} 1/\sqrt{3} & 0 & 0 \\ 0 & 1/\sqrt{3} & 0 \\ 0 & 0 & -2/\sqrt{3} \end{pmatrix}$$

Looking at that table, it is fairly easy to see that the first three generators are the familiar isotopic spin generators from the SU(2) subgroup of SU(3). Those generators connect the up and the down segments of the state χ. The 4th and 5th generators and the 6th and 7th generators have been traditionally called the V spin and the U spin. V spin connects the up and strange quarks while U spin connects the down and strange quarks. The 8th generator is diagonal, as is λ_3, since there are two additive quantum numbers:

$$\begin{aligned} \chi &\rightarrow \begin{pmatrix} u \\ d \\ s \end{pmatrix} \\ \vec{F} &= \vec{\lambda}/2 \\ I_\pm &\approx F_1 \pm i\, F_2 \quad I_3 = F_3 \\ U_\pm &\approx F_6 \pm i\, F_7 \\ V_\pm &\approx F_4 \pm i\, F_5 \\ Y &= 2F_8/\sqrt{3} \end{aligned} \qquad . \tag{C.2}$$

The ladder operators are $I_\pm$, $U_\pm$, $V_\pm$. The two quantum numbers I_3, (third component of isotopic spin) and the hypercharge, Y, are related to charge Q, baryon number B, and strangeness S as follows:

$$\begin{aligned} Q &= I_3 + (B+S)/2 \\ &= I_3 + Y/2 \end{aligned} \tag{C.3}$$

The Gell-Mann/Nishijima formula is the name given to Eq. C.3. The action of the I, U and V ladder raising and lowering operators on the fundamental triplet representation of SU(3) is shown in Fig. C.1.

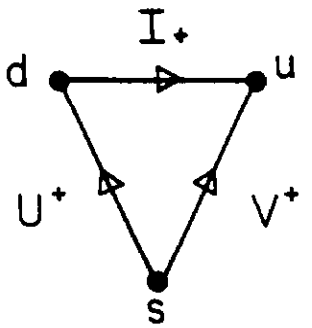

$\vec{I}$ $\lambda_{1,2,3}$ connects $\begin{pmatrix} u \\ d \end{pmatrix}$

$\vec{V}$ $\lambda_{4,5}$ connects $\begin{pmatrix} u \\ s \end{pmatrix}$

$\vec{U}$ $\lambda_{6,7}$ connects $\begin{pmatrix} d \\ s \end{pmatrix}$

Fig. C.1: Subgroup operators acting on the lowest dimensional (3) representation of SU(3).

At this point we want to look at a result we will need later in examining one gluon exchange among hadron constituents. We will start out in the SU(2) case because it is extremely familiar and then extend by analogy. In the SU(2) case what we are interested in is the expectation value of the square of the isotopic spin. One way to evaluate it is to use the fact that it is the same for all elements of a given representation. We then find the expectation value at the top of the ladder. One uses commutation relations to evaluate the expectation value at the top of the ladder using the fact that the third component of isotopic spin is equal to I at that location. This technique is shown in Eq. C.4:

$$
\begin{aligned}
I^2 &= \sum_i^3 I_i I_i = \frac{1}{2}[I_+, I_-] + I_3^2 \\
[I_+, I_-] &= 2I_3 \\
< I^2 > &= I_3^2 + I_3 = I(I+1)
\end{aligned}
\quad . \tag{C.4}
$$

We find the familiar result that the expectation value of the square of the isotopic spin is I(I+1).

For SU(3) we proceed in a completely analogous way and some of the steps are outlined below:

$$
\begin{aligned}
F^2 = \sum_{i=1}^{8} F_i F_i \qquad &= \frac{1}{2}[I_+, I_-] + I_3^2 \\
&+ \frac{1}{2}[U_+, U_-] \\
&+ \frac{1}{2}[V_+ V_-] + F_8^2 \\
< F^2 > = I_3^2 + 2I_3 + F_8^2 &
\end{aligned}
\quad . \tag{C.5}
$$

In this case we need the commutators for the I, U, and V spin ladder operators. One operates on the "top" of the representation. For example, for the triplet, looking at Fig. C.1., that would be operating on the up quark state. The result shown in Eq. C.5 is similar to the result for SU(2). One has to remember to evaluate at the "corner" of the representation. Some results for the SU(3) length operator are given in the accompanying table and are easily worked out. Just for reference purposes one should note that the minimum value of this length occurs for singlet representations of SU(3). These results will be used in the next section.

Table C.2.

Expectation values for the "length" F^2 in lower dimensional SU(3) representations.

SU(3) rep	$< F^2 >$
1	0
3	$\frac{4}{3}$
$\bar{3}$	$\frac{4}{3}$
6	$\frac{10}{3}$
8	3
10	6

At this point we would like to complete the identification of the elements of the meson octet that we started in Section B. You remember, we combine quarks and anti-quarks to obtain a singlet plus an octet of pseudoscalar and vector mesons in S wave. When we were folding representations of 3 and $\bar{3}$ together we found that at the center location we had $s\bar{s}, u\bar{u}$, and $d\bar{d}$ overlapping one another in the strangeness/isotopic spin space area. One simplication comes because the strange quark is an isotopic singlet so the isovector pion (in the octet) has no strange content.

A word about anti-quarks in the phase conventions which have been adopted. These are illustrated in Fig. C.2.a. As you recall G parity is defined to be charge conjugation plus a rotation about the I_2 axis in isotopic spin space. It is so defined that for a system of n pions the G parity is $(-1)^n$. Performing these operations on a u quark it turns into a $\bar{d}$ anti-quark, whereas a d quark under G parity turns into a -$\bar{u}$ anti-quark. The doublets are u, d and $\bar{d}$, -$\bar{u}$. This phase is illustrated in Fig. C.2.a.

$$
\begin{aligned}
u &\xrightarrow{G} \bar{d} \qquad \begin{bmatrix} u \\ d \end{bmatrix}, \begin{bmatrix} \bar{d} \\ -\bar{u} \end{bmatrix} \\
d &\xrightarrow{G} -\bar{u}, \\
G(n\pi) &= (-1)^n \\
G &= Ce^{i\pi I_2}
\end{aligned}
$$

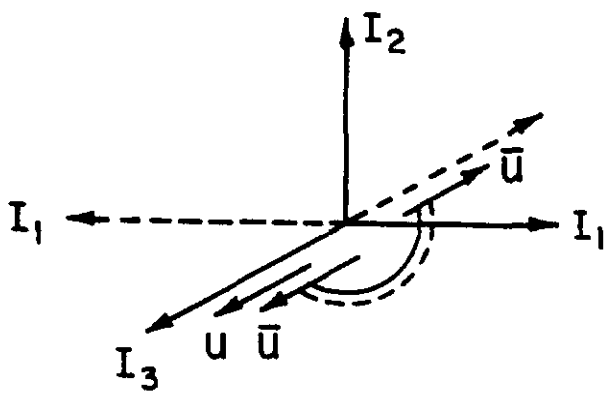

Fig. C.2.a: G parity operation acting on u and d quarks.

$$
\begin{aligned}
\underset{(S)}{\chi_1} &= \begin{cases} \uparrow\uparrow \\ \frac{1}{\sqrt{2}}\,(\uparrow\downarrow + \downarrow\uparrow) \\ \downarrow\downarrow \end{cases} \\
\underset{(A)}{\chi_0} &= \frac{1}{\sqrt{2}}(\uparrow\downarrow - \downarrow\uparrow)
\end{aligned}
$$

Fig. C.2.b: Spin states for $q\bar{q}$ composites.

As far as spin goes the combinations are a symmetric vector and an anti-symmetric scalar spin state. The composition in terms of quark and anti-quark are shown in Fig. C.2.b. Armed with this information one can find the SU(3) content of the multiply occupied origin containing $u\bar{u}$, $d\bar{d}$, and $s\bar{s}$. The singlet should be a flavorless equally weighted composite of all $q\bar{q}$ (suitably normalized), whereas the isovector part of the octet can be formed by reference to Fig. C.2.a using the G parity phase convention. Then the isosinglet element in the octet can be formed by constructing a state orthogonal to the first two states. The result of these operations is shown below:

$$
\begin{aligned}
|1> &= \frac{1}{\sqrt{3}}(u\bar{u} + d\bar{d} + s\bar{s}) \\
|8>_1 &= \frac{1}{\sqrt{2}}(-u\bar{u} + d\bar{d}) \qquad . \qquad \text{(C.6)} \\
|8>_0 &= \frac{1}{\sqrt{6}}(u\bar{u} + d\bar{d} - 2s\bar{s})
\end{aligned}
$$

An extended set of 16 such wave functions is given in the accompanying table where one is generalized to 4 quark possibilities, the up, down, strange, and charmed. In most of what follows we only need SU(3).

Table C.3.

Wave functions for the meson nonets, 0^- and 1^-.

Meson		*SU*(3) multiplicity	Wave function
15	K^+	8	$u\bar{s}$
	K^0	8	$d\bar{s}$
	π^+	8	$-u\bar{d}$
	π^0	8	$(u\bar{u} - d\bar{d})/\sqrt{2}$
	π^-	8	$d\bar{u}$
	η	8	$(u\bar{u} + d\bar{d} - 2s\bar{s})/\sqrt{6}$
	$\bar{K}^0$	8	$-s\bar{d}$
	K^-	8	$s\bar{u}$
	F^+	$\bar{3}$	$c\bar{s}$
	D^+	$\bar{3}$	$-c\bar{d}$
	D^0	$\bar{3}$	$c\bar{u}$
	$\bar{D}^0$	3	$-u\bar{c}$
	D^-	3	$-d\bar{c}$
	F^-	3	$-s\bar{c}$
	$\chi = \eta_c$	1	$(u\bar{u} + d\bar{d} + s\bar{s} - 3c\bar{c})/\sqrt{12}$
1	η'	1	$\frac{1}{\sqrt{3}}(u\bar{u} + d\bar{d} + s\bar{s} + c\bar{c})$

Meson	*SU*(3) multiplicity	Wave function
K^{*+}	8	$u\bar{s}$
K^{*0}	8	$d\bar{s}$
ρ^{+}	8	$-u\bar{d}$
ρ^{0}	8	$(u\bar{u}-d\bar{d})/\sqrt{2}$
ρ^{-}	8	$d\bar{u}$
$\bar{K}^{*0}$	8	$-s\bar{d}$
K^{*-}	8	$s\bar{u}$
ω	mixed	$(u\bar{u}+d\bar{d})/\sqrt{2}$
ϕ	mixed	$s\bar{s}$
J/ψ	mixed	$c\bar{c}$.
F^{*+}	$\bar{3}$	$c\bar{s}$
D^{*+}	$\bar{3}$	$-c\bar{d}$
D^{*0}	$\bar{3}$	$c\bar{u}$
$\bar{D}^{*0}$	3	$-u\bar{c}$
D^{*-}	3	$-d\bar{c}$
F^{*-}	3	$-s\bar{c}$

Having now found the SU(3) content of the quark anti-quark meson states lets apply this result to look at meson electromagnetic form factors. Since we have composite hadrons, we know there will be a form factor when the system is probed by photons via the electromagnetic interaction. As seen in Eq. C.7 below the amplitude for the electromagnetic interaction sandwiched between initial and final plane wave states gives you the Fourier transform of the charge distribution.

It is easy to imagine that one is measuring in such a situation the electromagnetic charge radius squared which is also defined below:

$$\begin{aligned} A &\approx \int e^{-ik_f z}\left(\frac{e\rho(r)}{r}\right) e^{ik_i z}\vec{dr} \sim < f|H|i > \\ &\sim e\int e^{iqr}\frac{\rho(r)}{r}\,\vec{dr} \qquad . \qquad \text{(C.7)} \\ < r^2_{em} > &\equiv \int \rho(r) r^2 \vec{dr} \end{aligned}$$

The data for these experiments is shown in Table C.4. One finds mean charge squared radii of order 1 fermi which is not surprising. We also find that the kaons have a smaller charge radius than the pions. What is most interesting is the neutral kaon has a negative charge radius. Lets try to see if we can explain this in a very simple fashion.

Table C.4.
Data on electromagnetic squared radius.

Particle	Beam Momentum (GeV/c)	$\langle r^2_{EM} \rangle$, fm^2	Reference
π^-	100	0.31 ± 0.04	Dally, et al. (1977)
	250	0.43 ± 0.03	Dally, et al. (1980a)
	Combined fit	0.39 ± 0.04	Dally, et al. (1980a)
K^-	250	0.28 ± 0.05	Tsyganov (1979) ; Dally, et al. (1980c)
	π^-/K^- Comparison	0.25 ± 0.05	Dally, et al. (1980b)
K^0	30 - 100	−0.054 ± 0.026	Molzon, et al. (1978)

First, we will define a center-of-mass coordinate for the quark and anti-quark system and the mean squared charge radius is then the deviation from the center-of-mass position squared weighted by the charge of the quark and anti-quark constituents. Doing a little bit of algebra we get the result shown in Eq. C.8:

$$
\begin{aligned}
\vec{R} &= \frac{(m_q \vec{r}_q + m_{\bar{q}} \vec{r}_{\bar{q}})}{(m_q + m_{\bar{q}})} = \text{C.M. Coordinate} \\
< r_{em}^2 > &= \left\langle \sum_i^2 e_i (r_i - R)^2 \right\rangle = \alpha \left\langle \sum_i^2 Q_i (r_i - R)^2 \right\rangle \\
\vec{\delta} &\equiv \vec{r}_q - \vec{r}_{\bar{q}} = \text{Relative Coordinate} \\
< r_{em}^2 > &= \frac{(Q_q m_{\bar{q}}^2 + Q_{\bar{q}} m_q^2) < \delta^2 >}{(m_q + m_{\bar{q}})^2}
\end{aligned}
\qquad . \qquad \text{(C.8)}
$$

Having done the algebra, let's assume SU(2) symmetry, i.e., the up and down quark have the same constituent mass and the strange quark is heavier by a factor γ. In that case, its easy to work out what the mean charge radius is for the case of π^+, K^+, and K^0:

$$
\begin{aligned}
m_u &= m_d \equiv m \\
m_s &\equiv \gamma m \\
< r_{em}^2 >_{\pi^+} &= < \delta^2 >_\pi /4 \\
< r_{em}^2 >_{K^+} &= < \delta^2 >_K (2\gamma^2 + 1)/3(1+\gamma)^2 \\
< r_{em}^2 >_{K^0} &= < \delta^2 >_K (-\gamma^2 + 1)/3(1+\gamma)^2 \\
\gamma &= 1.5 \\
\sqrt{< \delta^2 >_\pi} &\sim 1.25 fm, \sqrt{< \delta^2 >_K} \sim 1.0 fm
\end{aligned}
\qquad . \qquad \text{(C.9)}
$$

Right away it is easy to see why the K^0 has a negative square charge radius. That is because you have a light d quark which is orbiting around a heavier $\bar{s}$ quark and that light d quark is negatively charged. If the anti-quark mass is very large with respect to the quark mass than the mean charge radius just approaches a limit which is the quark charge times the mean squared relative coordinate. In other words, when you probe lightly into the charge distribution what you are seeing is the charge of the light objects which are orbiting out at large distances.

If we take a γ value of 1.5 this gives us a reasonable agreement with the observed ratio of the K^0 to K^+ charge radius, because in that case, that ratio is only a function of γ. One can try to push this a little farther and compare the π^+ to the K^+ and extract from that the ratio of the mean squared deviations. We find that the ratio of K^+ to π^+ is about $\frac{2}{3}$. We expect that kind of situation because you remember that the scale of the system size goes like one over the mass. In fact, putting in γ of 1.5 we can extract the mean separation to be 1.25 fermis for the pions and 1.0 fermi for the kaons. These sizes are also in reasonable agreement with our bag estimates of size.

Another electromagnetic effect we can look at with mesons is the electromagnetic mass difference. The mass differences for pions, kaons, D mesons, B mesons and some baryons is given in Table C.5.

Table C.5.

Electromagnetic mass splittings for mesons and baryons.

Hadron	$M^+ - M^0$ (MeV)
π	4.60
K	-4.05
D	4.7 ± 0.3
B	-4.0 ± 3.4
N	-1.29
Σ	-3.1
$\Sigma(\Sigma^0 - \Sigma^-)$	-4.9
$\Xi(\Xi^0 - \Xi^-)$	-6.5

In order to try to explain the data we will use an over simplified model which assumes that the electromagnetic mass is due to the fact that up and down masses are not exactly the same. There is an explicit SU(2) breaking and the quark and anti-quark have a mutual Coulomb interaction which causes another contribution to the mass splitting. We ignore hyperfine interactions in this approximation. An expression for the mass in this model is given in Eq. C.10:

$$\begin{aligned} M &= M_0 + n(m_d - m_u) + < Q_q Q_{\bar{q}} > M_c \\ Q_q &= \frac{2}{3}, -\frac{1}{3} \\ M_c &\sim < \alpha/a >= 2\ MeV \text{ for } a = 0.8\ fm \end{aligned} \quad . \tag{C.10}$$

We expect that for binding on the scale of one fermi, the parameter M_c for the Coulomb mass is going to be of order a few MeV. Using this expression for the mass of a composite $q\bar{q}$ meson and the wave functions which we just found for the meson octet states we can evaluate the masses for the π^+, π^0, K^+, and K^0:

$$\begin{aligned} M_{\pi^+} = M_{\pi^-} &= M_0 + (m_d - m_u) + \frac{2}{9} M_c \\ M_{\pi^0} &= M_0 + (m_d - m_u) - \frac{5}{18} M_c \\ M_{K^+} &= M_0 + (m_s - m_u) + \frac{2}{9} M_c \\ M_{K^0} &= M_0 + (m_s - m_u) - \frac{1}{9} M_c \\ &\quad -(m_d - m_u) \end{aligned} \quad . \tag{C.11}$$

For example, in the π^+ the $\frac{2}{9}$ expression is the $\frac{2}{3}$ u times the $\frac{1}{3}$ $\bar{d}$, whereas for the π^0 mass the factor $\frac{5}{18}$ is $\frac{1}{2} \times \left(\left(\frac{2}{3}\right)^2 + \left(\frac{1}{3}\right)^2\right)$ which reflects the equal mixing of $u\bar{u}$ and $d\bar{d}$ in the isovector π^0 wave function.

Solving for the mass differences as shown in Eq. C.12, we find the Coulomb mass parameter and the up and down quark constituent mass difference:

$$\begin{aligned} M_{\pi^+} - M_{\pi^0} &= M_c/2 \\ M_c &= 9.2MeV \\ M_{K^+} - M_{K^0} &= M_c/3 - (m_d - m_u) \\ m_u - m_d &= -7MeV \end{aligned} \quad . \tag{C.12}$$

As expected, the Coulomb mass parameter turns out to be of order MeV. We also find that the up and down quarks are degenerate on the scale of a few MeV. This result is clearly a reflection of the goodness of the isotopic-spin symmetry which we have assumed from the beginning. Twenty years ago we used to worry; the K^+ was heavier than the K^0 as expected for an internal net positive charged distribution. However, the neutron was heavier than the proton. This was a major puzzle. The Standard Model (which "explains" all) now tells us that this is so because the d quark is heavier than the u quark. Armed with this enlightment, we seem not to have advanced very far; the Standard Model says nothing about quark masses.

Using the π's and K's one can make a simple prediction for heavier flavor states. Replacing the up by a charm quark, one expects the D^+ to D^0 mass difference to be similar to the $\pi^+$to π^0 mass difference and replacing the strange quark by a b quark one expects the B^+ to B^0 mass difference to be similar to the K^+ to K^0 mass difference:

$$\begin{aligned} M_{D^+} - M_{D^0} &\stackrel{?}{=} M_{\pi^+} - M_{\pi^0}(u \to c) \\ M_{B^+} - M_{B^0} &\stackrel{?}{=} M_{K^+} - M_{K^0}(s \to b) \end{aligned} \quad . \tag{C.13}$$

A glance at the table shows us that these expectations are born out quite well.

We will now turn our attention to baryons. Let us begin by forming di-quarks in $3 \otimes 3$. When we did that in Section B, we found that $3 \otimes 3$ consisted of a sextet and an anti-triplet. The sextet is symmetric since it contains uu, dd, and ss on the periphery while the anti-triplet is anti-symmetric. It is easy by using ladder operators to step uu down or dd up in order to find the other elements of the sextet. The $\bar{3}$ states are orthogonal to the 6 states, by construction. These are shown in Table C.6.

Table C.6.

qq content of the $3 \otimes 3$ representations.

rep	qq	rep	qq
6	uu	$\bar{3}$	
(S)	$\frac{1}{\sqrt{2}}(ud + du)$	(A)	$\frac{1}{\sqrt{2}}(ud - du)$
	dd		
	$\frac{1}{\sqrt{2}}(us + su)$		$\frac{1}{\sqrt{2}}(us - su)$
	$\frac{1}{\sqrt{2}}(ds + sd)$		$\frac{1}{\sqrt{2}}(ds - sd)$
	ss		

Continuing on to form 3 quark states we cross $3 \otimes 3 \otimes 3$ as shown below:

$$\begin{aligned} 3 &\otimes (3 \otimes 3) \\ 3 &\otimes (6 \oplus \bar{3}) \\ 3 &\otimes 6 \oplus (1 \oplus 8) \\ (1 \oplus 8) &\oplus 8' \oplus 10(S) \end{aligned} \quad . \tag{C.14}$$

We get 9 states from $3 \otimes \bar{3}$ which are the familiar singlet plus octet. The decomposition of $3 \otimes 6$ gives us another octet and a decuplet which is completely symmetric. The reason we know the decuplet is completely symmetric is because it contains elements such as uuu, ddd, and sss and the symmetry of a representation is the same for all elements of that representation. One of the difficult points is that we only have eight physical baryons but we have two octets. The reason for that is that there are two ways to get to the octet. One is from a $3 \otimes \bar{3}$ and the other is from a $3 \otimes 6$ and the two octets have a mixed symmetry so there is a double counting between two octet elements and one physical baryon.

Perhaps a simpler way to see this is to look at the spin coupling which is needed for the 3 quark system. The representations are given in Eq. C.15 while the states are shown in Fig. C.3:

$$\begin{aligned} 2 \otimes 2 &= 1 \oplus 3 \\ 2 \otimes (2 \otimes 2) &= 2 \oplus (2 \oplus 4) \end{aligned} \quad . \tag{C.15}$$

When we couple spin $\frac{1}{2}$ to spin $\frac{1}{2}$ we get spin 0 and spin 1. Now obviously spin 1 is the symmetric state because you need, for example, both quarks in spin up states to get to spin 1 whereas spin 0 is anti-symmetric in the 2 quarks. Recoupling the third quark to the spin 1 we get a total spin $\frac{3}{2}$ which is again symmetric, as shown in Fig. C.3.a., for the 4 possible projections of spin $\frac{3}{2}$. For spin $\frac{1}{2}$, if the 2 quarks are coupled to spin 0 then we have an anti-symmetric situation with a third quark defining the spin projection. Whereas, if the 2 quarks are coupled in a symmetric spin 1 state, the system is recoupled with Clebsch-Gordon

coefficients one can find in the particle data tables to total spin $\frac{1}{2}$ in a symmetric way. It is these two possibilities that lead to a mixed symmetry spin state for total spin $\frac{1}{2}$ in the 3 quark system.

$$\chi^{\frac{3}{2}}_{(S)} = \left\{ \begin{array}{l} (\Uparrow\Uparrow)\Uparrow \\ [(\Uparrow\Uparrow)\Downarrow + (\Uparrow\Downarrow + \Downarrow\Uparrow)\Uparrow]/\sqrt{3} \\ [(\Downarrow\Downarrow)\Uparrow + (\Uparrow\Downarrow + \Uparrow\Downarrow)\Downarrow]/\sqrt{3} \\ (\Downarrow\Downarrow)\Downarrow \end{array} \right\} (S)$$

Fig. C.3.a: qqq spin coupling for $J^P = \frac{3}{2}^+$, symmetric.

$$\chi^{\frac{1}{2}}_{(Mixed)} = \left\{ \begin{array}{ll} (\Uparrow\Downarrow - \Downarrow\Uparrow)\Uparrow/\sqrt{2} & (A) \\ +[(\Uparrow\Downarrow + \Downarrow\Uparrow)\Uparrow - 2(\Uparrow\Uparrow)\Downarrow]/\sqrt{6} & (S) \\ (\Uparrow\Downarrow - \Downarrow\Uparrow)\Downarrow/\sqrt{2} & (A) \\ +[(\Uparrow\Downarrow + \Downarrow\Uparrow)\Downarrow - 2(\Downarrow\Downarrow)\Uparrow]/\sqrt{6} & (S) \end{array} \right.$$

Fig. C.3.b: $J^P = \frac{1}{2}^+$, mixed symmetry.

Looking at the spin subsystem, which is a system we are more familiar with from nonrelativistic quantum mechanics, should make the SU(3) wave functions for the baryons rather easier to understand. A full set of these wave functions for both octets and the decuplet are shown in Table C.7. The analogy between Fig. C.3.a and the Δ wave functions, and Fig. C.3.b and the proton and neutron wave functions should be obvious.

Table C.7.

Baryon decuplet and octet wave functions (zero charm).

Baryon	Wave function
Δ^{++}	uuu
Δ^{+}	$(uud + udu + duu)/\sqrt{3}$
Δ^{0}	$(udd + dud + ddu)/\sqrt{3}$
Δ^{-}	ddd
Σ^{*+}	$(uus + usu + suu)/\sqrt{3}$
Σ^{*0}	$(uds + usd + dus + dsu + sud + sdu)/\sqrt{6}$
Σ^{*-}	$(dds + dsd + sdd)/\sqrt{3}$
Ξ^{*0}	$(uss + sus + ssu)/\sqrt{3}$
Ξ^{*-}	$(dss + sds + ssd)/\sqrt{3}$
Ω^{-}	sss

Baryon	Wave function
	Octet 1
p	$(2uud - udu - duu)/\sqrt{6}$
n	$(udd + dud - 2ddu)/\sqrt{6}$
Λ^{0}	$\frac{1}{2}(usd + sud - dsu - sdu)$
Σ^{+}	$(2uus - usu - suu)/\sqrt{6}$
Σ^{0}	$(2uds + 2dus - usd - dsu - sud - sdu)/\sqrt{12}$
Σ^{-}	$(2dds - dsd - sdd)/\sqrt{6}$
Ξ^{0}	$(uss + sus - 2ssu)/\sqrt{6}$
Ξ^{-}	$(dss + sds - 2ssd)/\sqrt{6}$
	Octet 2
p	$(udu - duu)/\sqrt{2}$
n	$(udd - dud)/\sqrt{2}$
Λ^{0}	$(2uds - 2dus + sdu - dsu + usd - sud)/\sqrt{12}$
Σ^{+}	$(usu - suu)/\sqrt{2}$
Σ^{0}	$\frac{1}{2}(usd + dsu - sud - sdu)$
Σ^{-}	$(dsd - sdd)/\sqrt{2}$
Ξ^{0}	$(uss - sus)/\sqrt{2}$
Ξ^{-}	$(dss - sds)/\sqrt{2}$

Comparing the tables for the meson and baryon wave functions, one can see that in octet two for the baryons the anti-symmetrized quark-quark product state plays the role of the anti-quark to form the octet. In this sense, the di-baryon acts as if it were an anti-quark in terms of the flavor properties of the system.

What about predictions for electromagnetic interactions of baryons? In this case we will take a short cut and utilize one of the SU(2) subgroups, the U spin which we have referred to already. If we write down the electromagnetic current in Eq. C.16 we see that the photon obviously does not change the charge:

$$J_{\mu}^{\gamma} = e\left[\frac{2}{3}\bar{u}\gamma_{\mu}u - \frac{1}{3}(\bar{d}\gamma_{\mu}d + \bar{s}\gamma_{\mu}s)\right] = \sqrt{\alpha}\sum_{i}^{3} Q_i\bar{q}\gamma_{\mu}q \quad . \tag{C.16}$$

Looking at the fundamental triplet we recall that the U spin connects d and s. So U spin multiplets all have the same charge. That means that the electromagnetic current must be a U spin singlet in order that the photon, indeed, not change charge. The implication is that the electromagnetic contribution to the mass of the system must be the same for all U spin multiplet numbers because the photon is a U spin singlet. For the baryon octet the U spin multiplets are the p/Σ^+ doublet, the neutron/Σ^0/Ξ^0 triplet, and the Σ^-/Ξ^- doublet. That leads to the following relationships between Coulomb contributions to the hadron masses:

$$\begin{aligned} (M_c)_p &= (M_c)_{\Sigma^+} \\ (M_c)_n &= (M_c)_{\Sigma^0} = (M_c)_{\Xi^0} \\ (M_c)_{\Sigma^-} &= (M_c)_{\Xi^-} \end{aligned} \quad . \tag{C.17}$$

Solving this set of equations, we have the results shown in C.18:

$$\begin{aligned} M_p - M_n &= M_{\Sigma^+} - M_{\Sigma^-} + M_{\Xi^-} - M_{\Xi^0} \\ -1.3\ MeV &\stackrel{?}{=} -1.6\ MeV \end{aligned} \quad . \tag{C.18}$$

This relationship is quite well satisfied and is thus a good test of the symmetry for the octet baryons.

Following in this mode we have a prediction for another electromagnetic property, the magnetic moments of the baryons. Again the elements of the two U spin doublets and the U spin triplet all must have the same magnetic moment. Data for the octet magnetic moments is given in Table C.8 and one can see that these relationships are at least crudely correct.

Table C.8.
Baryon octet magnetic moments.

Particle	Experiment	Quark Model
n/p	-0.685	-0.67
Σ^+	2.38 ± 0.02	2.7
Σ^-	-1.11 ± 0.03	-1.1
Ξ^-	-1.85 ± 0.75	-0.50
Ξ^0	-1.25 ± 0.01	-1.4
$\Sigma^0 \to \Lambda$	1.8 ± 0.2	1.6

All moments are in units of μ_B. In the $\Sigma^0 \to \Lambda$ case, the moment describes the $M1$ transition $\Sigma^0 \to \Lambda\gamma$. The Σ^+ and Σ^- moment measurements are new: Σ^+: Ankenbrandt (1983); Σ^-: Hertzog (1983).

However, the U spin symmetry assumes that SU(3) is not broken and we know this is not the case. That being the situation, we will defer more detailed discussion of baryon magnetic moments until later when we can confront the problem of SU(3) symmetry breaking in order to get better agreement with the data:

$$\begin{aligned} \mu_{\Sigma^+} &\stackrel{?}{=} \mu_p, & 2.4 &\stackrel{?}{=} 2.8 \\ \mu_n = \mu_{\Sigma^0} &\stackrel{?}{=} \mu_{\Xi^0}, & -1.9 &\stackrel{?}{=} -1.2 \\ \mu_{\Sigma^-} &\stackrel{?}{=} \mu_{\Xi^-}, & -1.1 &\stackrel{?}{=} -1.9 \end{aligned} \quad . \tag{C.19}$$

D. QCD and Strong Mass Splitting

In this section, we will continue our studies of mass relationships in the SU(3) multiplets for meson and baryons. In particular, we will look at the strong mass splitting. In doing so we will attempt to use QCD inspired versions of the potentials in each case.

For example, in the vector meson octet the wave functions for the central members are:

$$\begin{aligned} |\rho^0> &= \frac{1}{\sqrt{2}}(-u\bar{u} + d\bar{d}) \\ |w_8> &= \frac{1}{\sqrt{6}}(u\bar{u} + d\bar{d} - 2s\bar{s}) \quad . \\ |w_1> &= \frac{1}{\sqrt{3}}(u\bar{u} + d\bar{d} + s\bar{s}) \end{aligned} \tag{D.1}$$

We have already derived these wave functions in Section C. We also know that SU(3) is rather badly broken because the masses of the multiplet members are not degenerate. This means that various SU(3) representations will mix. For example, the physical η and η' (which are isotopic-spin singlets and are both pseudoscalar) are, in fact, going to be mixtures of the SU(3) octet and singlet members.

We can get an idea of the magnitude of the SU(3) breaking just by counting strange quarks. The results for both the mesons and the baryons are shown in Table D.1 below. For the baryons this result is known as the decuplet equal spacing rule. One can see that a rough representation of the mass is obtained just by counting up the constituent quark masses, assigning the up and down quark the same mass of roughly 300 MeV, and assigning the strange quark a mass 150 MeV higher. For the vector octet and the baryon decuplet we get a reasonable representation of the masses just by counting the strange quarks in this way.

Table D.1.

Strange quark mass splitting.

Hadron	Mass (MeV)	N_S	ΔM (MeV)
ρ	770	0	—
$K^\star$	890	1	120
ϕ	1020	2	130
Δ	1250	0	—
$\Sigma^\star$	1380	1	130
$\Xi^\star$	1520	2	160
Ω	1670	3	150
$m_u \sim m_d \sim 300\ MeV$			
$m_s - m_u \sim 150\ MeV$			

Now let's look at the vector meson nonet, or octet plus singlet. The first observation, using the wave functions shown in D.1, is that if there were no mixing the physical ω would be the octet ω and would have $2s\bar{s}$ in the wave function. The physical singlet, the ϕ, would be the SU(3) singlet and would have $1s\bar{s}$ in the wave function. That is clearly not true because the ω has a mass of 783 MeV while the ϕ has a mass of 1,020 MeV. This means that we do indeed observe representation mixing due to SU(3) symmetry breaking. For example, we can set this up as a rotation as shown below.

$$\begin{aligned} \begin{pmatrix} |w> \\ |\phi> \end{pmatrix} &= \begin{pmatrix} \frac{1}{\sqrt{2}}(u\bar{u}+d\bar{d}) \\ s\bar{s} \end{pmatrix} \\ &= \begin{pmatrix} \sqrt{\frac{2}{3}} & \sqrt{\frac{1}{3}} \\ -\sqrt{\frac{1}{3}} & \sqrt{\frac{2}{3}} \end{pmatrix} \begin{pmatrix} |w_8> \\ |w_1> \end{pmatrix} . \qquad \text{(D.2)} \\ \tan\theta_1 &= \frac{1}{\sqrt{2}}, \theta_1 = 35^0 \end{aligned}$$

We picked the particular rotation angle of about 35^0 in order to achieve "ideal mixing." We do this for a couple of reasons. The physical ρ and ω are almost mass degenerate. That means the ω has to be rotated in such a fashion as to have no strange quarks. We also do it because the ϕ appears to behave as an almost pure $s\bar{s}$ state. Diagramatically the decays of the ϕ are shown in Fig. D.1. What is observed is that the ϕ seldom goes into $\rho\pi$ or 3 pions and prefers to go into a K^+K^- pair. In fact, the relative partial width into 3 πs for the ϕ and ω are only 7%. One can explain this on the basis that the K^+K^- decay proceeds via the two gluon annihilation diagram whereas the $\rho\pi$ decay proceeds via a three gluon annihilation diagram. This is called the OZI rule but in fact it is more of an observation

than a rule. It represents the cost of a higher power of the strong coupling constant in the amplitude.

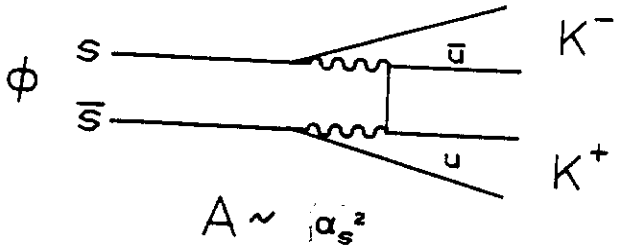

Fig. D.1.a: ϕ decay into K^+K^- via 2 gluon annihilation.

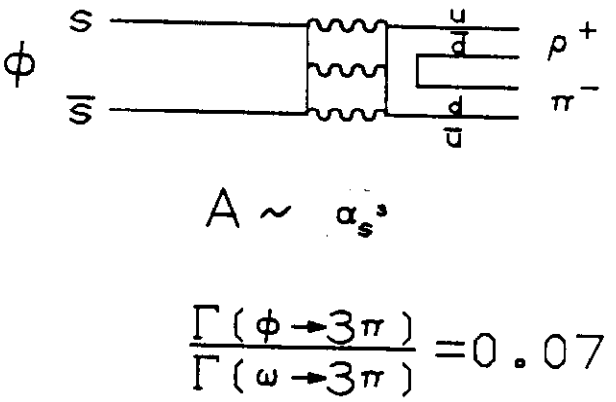

Fig. D.1.b: ϕ decay into $\rho\pi$ via OZI violating 3 gluon intermediate state.

This ideal mixing angle yields a pure $s\bar{s}$ ϕ and an ω and ρ which are degenerate, in agreement with observation. Using these wave functions we extract the mass relations for the vector octet given in Eq. D.3:

$$\begin{array}{rcll} & & M_1 + 2m & M_\omega \\ < V|H|V > & = & M_1 + m + m_s = & M_{K^*} \\ & & M_1 + 2m_s & M_\phi \\ m_u & \equiv & m_d \equiv m & \end{array} \quad . \tag{D.3}$$

Solving these equations, we have two constraints which are reasonably well satisfied as shown in Eq. D.4:

$$
\begin{aligned}
a)\ M_\phi - M_{K^*} &= M_{K^*} - M_\omega \\
&\simeq m_s - m = (\gamma - 1)m \\
130\ MeV &\stackrel{?}{=} 107\ MeV\ , \\
b)\qquad M_{K^*} &= (M_\omega + M_\phi)/2 \\
892\ MeV &\stackrel{?}{=} 901\ MeV\ .
\end{aligned}
\tag{D.4}
$$

Now we turn to the pseudoscalar meson nonet where the picture is somewhat more complicated. In this case, the π and the η are quite split in contrast to the ρ and ω so we expect that the mixing will not be ideal. Using the wave functions just as we did for the vector nonet we obtain the octet and singlet masses shown in Eq. D.5:

$$
\begin{aligned}
 & & M_o + 2m & & M_\pi \\
< P|H|P > &= & M_o + m + m_s & & M_K \\
 & & M_o + \tfrac{2m+4m_s}{3} &= & M_{\eta_8} \\
 & & M_o + \tfrac{4m+2m_s}{3} & & M_{\eta_1}
\end{aligned}
\quad . \tag{D.5}
$$

In Eq. D.6 we explicitly show SU(3) breaking. The strange and up quark mass difference connects the different SU(3) multiplets. The matrix element for octet and singlet mixing is:

$$
\begin{aligned}
< \eta_1|H|\eta_8 > &= \frac{1}{\sqrt{3}} < u\bar{u} + d\bar{d} + s\bar{s}|H|(u\bar{u} + d\bar{d} - 2s\bar{s}) > /\sqrt{6} \\
&= \frac{4}{\sqrt{18}}(m - m_s) \\
&= \frac{2\sqrt{2}}{3}m(1-\gamma) \\
&= M_{18}
\end{aligned}
\quad . \tag{D.6}
$$

Solving Eq. D.5, the singlet and octet pseudoscalar masses are quite close to the physical η and η' masses:

$$
\begin{aligned}
4M_K - M_\pi &= 3M_{\eta_8}, M_{\eta_8} = 613\ MeV \sim M_\eta = 550\ MeV \\
2M_K + M_\pi &= 3M_{\eta_1}, M_{\eta_1} = 1132\ MeV \sim M_{\eta'} \sim 960\ MeV
\end{aligned}
\quad . \tag{D.7}
$$

This means that while there is mixing, we expect it to be rather small. Now we will explicitly solve for the mixing angle as shown below in Eq. D.8:

$$\begin{pmatrix} |\eta> \\ |\eta'> \end{pmatrix} = \begin{pmatrix} \cos\theta_0 & \sin\theta_0 \\ -\sin\theta_0 & \cos\theta_0 \end{pmatrix} \begin{pmatrix} |\eta_8> \\ |\eta_1> \end{pmatrix}$$

$$\begin{pmatrix} M_\eta & 0 \\ 0 & M_{\eta'} \end{pmatrix} = \begin{pmatrix} \cos\theta_0 & \sin\theta_0 \\ -\sin\theta_0 & \cos\theta_0 \end{pmatrix} \begin{pmatrix} M_{\eta_8} & M_{18} \\ M_{18} & M_{\eta_1} \end{pmatrix} \begin{pmatrix} \cos\theta_0 & \sin\theta_0 \\ -\sin\theta_0 & \cos\theta_0 \end{pmatrix} . \quad \text{(D.8)}$$

$$\tan^2\theta_0 = \frac{4M_K - M_\pi - 3M_\eta}{3M_{\eta'} - 4M_K + M_\pi}$$

$$\theta_0 \sim 24^0$$

The octet and singlet states are rotated into the physical states. This is accompanied by a diagonalization of the mass matrix in the physical state representation. Solving for the angle, we find that the pseudoscalar mixing angle is 24^0.

This appears to be all right. However, there are certain relationships which are independent of the mixing. For example, the center-of-gravity of the nonet, as defined in Eq. D.9, is independent of mixing:

$$\begin{aligned} a)\ M_{\eta_1} + M_{\eta_8} &= 2M_K = M_\eta + M_{\eta'} \\ &\quad 992 = 1510\ MeV\ , \\ b)\ M_{w_1} + M_{w_8} &= 2M_{K^*} = M_w + M_\phi \\ &\quad 1780 = 1803\ MeV\ . \end{aligned} \quad \text{(D.9)}$$

For the vector nonet the center-of-gravity relation is very well satisfied, whereas for the pseudoscalar nonet it does not work at all. A failure like this normally means that we are forgetting something important. What we have assumed for representation mixing is that it is entirely driven by the strange/up quark mass difference. However, there are other physical processes which are going on. For example, flavor singlets like $s\bar{s}$ can annihilate into multigluons and reform in other flavors such as $u\bar{u}$. That means that the gluons, which are flavorless, also mix SU(3) representations. They are SU(3) singlets since gluons cannot carry any flavor. This is an effect which we have been ignoring up till now.

Since the gluons don't know about flavor, we will assume that the annihilation amplitude is an SU(3) invariant A. That means that the annihilation amplitude does not contribute to the octet mass nor to the octet/singlet mixing. It merely contributes to singlet mixing.

Therefore, the mass matrix is as shown in Eq. D.10 (see Eqs. D.5 and D.6):

$$\begin{aligned} M_{\eta_8} &= \frac{2m}{3}(1+2\gamma) \\ M_{\eta_1} &= \frac{2m}{3}(2+\gamma) \\ M_{18} &= \frac{2m}{3}\sqrt{2}(1-\gamma) \\ M &= \frac{2m}{3}\begin{bmatrix} (1+2\gamma) & \sqrt{2}(1-\gamma) \\ \sqrt{2}(1-\gamma) & (2+\gamma)+x \end{bmatrix} \\ x &= \frac{9A}{2m} \end{aligned} \quad . \tag{D.10}$$

This matrix has exactly the form previously given in Eqs. D.5 and D.6 with the addition of the SU(3) singlet annihilation amplitude due to annihilation into gluons. As you recall from the solution of the eigenvalue problem, the trace and the determinent of any matrix are invariants. That allows us to easily write down the trace and the determinent of the mass matrix in terms of the eigenvalues λ_1 and λ_2:

$$\begin{aligned} \lambda_1+\lambda_2 &= \frac{2m}{3}[3(1+\gamma)+x] \\ \lambda_1\lambda_2 &= \frac{4m^2}{9}[9\gamma+x(1+2\gamma)] \end{aligned} \quad . \tag{D.11}$$

If the annihilation amplitude A is 0, then the sum of the eigenvalues (which are the physical masses) which result from diagonalizing the mass matrix are a statement about the center-of-gravity of the nonet, D.12a:

$$\begin{aligned} a)\quad \lambda_1+\lambda_2 &= 2m(1+\gamma) = 2M_{K^*} = M_\omega + M_\phi \ , \\ b)\quad \lambda_1+\lambda_2 &= 2m(1+\gamma)+3A_1 = 2M_{K^*}+3A_1 \ , \\ c)\quad \lambda_1+\lambda_2 &= 2m(1+\gamma)+3A_0 = 2M_K+3A_0 \ , \\ d)\qquad A_1 &\sim 6.3\ MeV,\ A_0 \sim 172\ MeV \ . \end{aligned} \tag{D.12}$$

If the annihilation amplitude is non zero, one can solve for the amplitude necessary to make the center-of-gravity relationship work out. This is shown in Eqs. D.12 b and c. We find that for the vector nonet, A is only 6.3 MeV, while for the pseudoscalar nonet it is 172 MeV.

In the context of QCD we expect the annihilation amplitude to decrease rapidly with mass because we know that QCD is asymptotically free. This means that the coupling constant decreases as the mass increases. We also remember that a 0^- state can couple to 2 vector gluons but a 1^- state cannot. You will recall this from our discussion of positronium. Thus in this gluon annihilation model, we expect the vector amplitude to be suppressed with respect to the pseudoscalar amplitude because it costs another gluon or another factor of α_s in the amplitude squared. The implication is that we can, in a plausible fashion, explain the mass relations for the multiplet members within the pseudoscalar nonet. We do need singlet mixing but it is an effect that we expect in QCD. Moreover, the mass dependence and quantum number dependence of the annihilation amplitude appears to follow trends we would expect in QCD.

It appears that the quark anti-quark mesons in the lowest S waves can thus have their mass relations explained in a satisfactory way. Note that we have as yet said nothing about relating the pseudoscalar and vector states. What about higher angular momentum states? What can we say about them? The quantum numbers of such a state follow from non-relativistic quantum mechanics for bound states of fermions and anti-fermions. The parity is $(-1)^{L+1}$ and the charge conjugation quantum number is $(-1)^{L+S}$. That means we have a well defined sequence of quantum numbers. Any quantum numbers outside that model are called exotic. In fact, it is a justification for the quark model that no meson with exotic quantum numbers has yet been observed and substantiated. For example, a state $J^{PC} = o^{+-}$ has exotic quantum numbers. The expected series of quantum numbers for S, P, and D states are shown in Table D.2 along with the observed states. They fit nicely into the progression of nonets which one expects. For example, it looks as if almost all of the elements of the 4 nonets expected in P wave have been observed and fit into the repeating nonet structure.

Table D.2.

Orbital $q\bar{q}$ mesonic excitations
with spin-orbit factors shown.

L	S	J^{PC}	$< \vec{L} \cdot \vec{S} >$	Nonet			
0	0	0^{-+}	0	π	η	η'	K
	1	1^{--}		ρ	w	ϕ	K^*
1	0	1^{+-}	0	B			Q
		0^{++}	-2	δ	ϵ	S^*	κ
	1	1^{++}	-1	A_1	D		Q
		2^{++}	1	A_2	f	f'	K^*
2	0	2^{-+}	0	A_3			L
		1^{--}	-6				
	1	2^{--}	-2				
		3^{--}	4	g	ω		K^{**}

Let's look at the spin-orbit splitting that we talked about in Section A. The result (familiar from atomic physics) is:

$$\begin{aligned} \vec{J}^2 &= (\vec{L}+\vec{S})^2 = \vec{L}^2 + \vec{S}^2 + 2\vec{L}\cdot\vec{S} \\ < \vec{L}\cdot\vec{S} > &= [J(J+1) - L(L+1) - S(S+1)]/2 \end{aligned} \quad . \tag{D.13}$$

If we assume that the splitting among the P wave states is simply due to spin-orbit splitting, we can write down a relationship between the nonets in P wave. As shown below the isovector members of the 4 nonets in P wave seem to follow this relationship quite well.

$$\begin{aligned} a) \qquad (M_{2++} - M_{1++}) &\stackrel{?}{=} 2\,[M_{1++} - M_{0++}] \\ A_2(1310) - A_1(1100) &= 2[A_1(1100) - \delta(970)] \\ 210\ MeV &= 260\ MeV\ , \end{aligned} \tag{D.14}$$

$$\begin{aligned} b) \qquad M_{so}/M &\sim \left(\vec{L}\cdot\vec{S}\right)\alpha_S^2 \\ M_{2++} - M_{1++} &\sim 2\alpha_S^2 \bar{M} \\ \alpha_S &\sim 0.3\ . \end{aligned}$$

Referring to our previous derivation (Eq. A.4) we can relate the spin-orbit splitting to α_s as in Eq. D.14.b. We obtain a reasonable value of α_s using the 2^{++} to 1^{++} isovector masses. Note that M_{so} is $\sim 200\ MeV$. We can estimate spin-spin splitting from the meson

octets, $M_{ss} \sim M_{K^*} - M_K \sim 390\ MeV$. Hence, the spin-orbit and spin-spin splittings are comparable. This behavior is as expected for composite systems composed of equal mass constituents.

The spin orbit relations, although it is satisfying that they seem to be fulfilled, don't make any connections between the states with different L values. If we try to see if there is some simple relation we can plot the mass of the members of a nonet versus their total angular momentum J as seen in Fig. D.2.a. In that figure, we have picked elements of the recurrences of the ρ meson; ρ, A2, g, etc. In Fig. D.2.b we have looked at the higher excitations of the Δ^{++}.

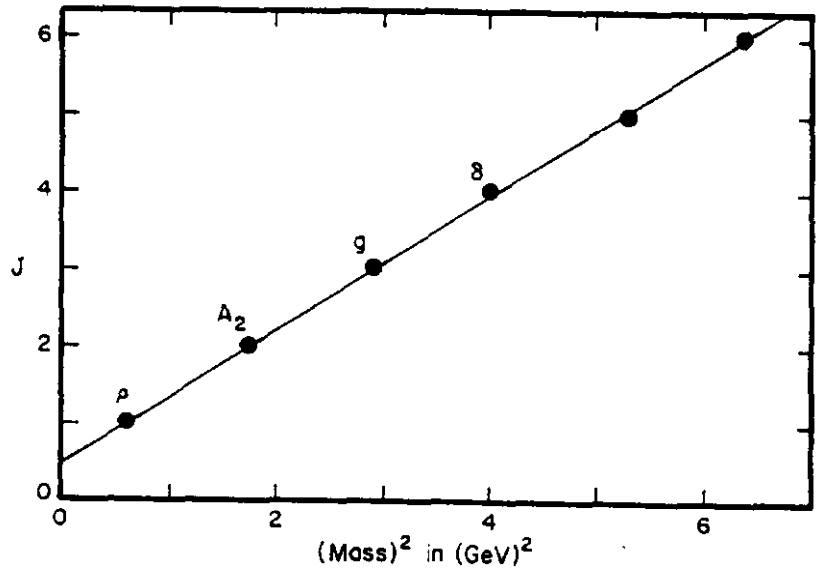

Fig. D.2.a: Orbital excitations of the ρ.

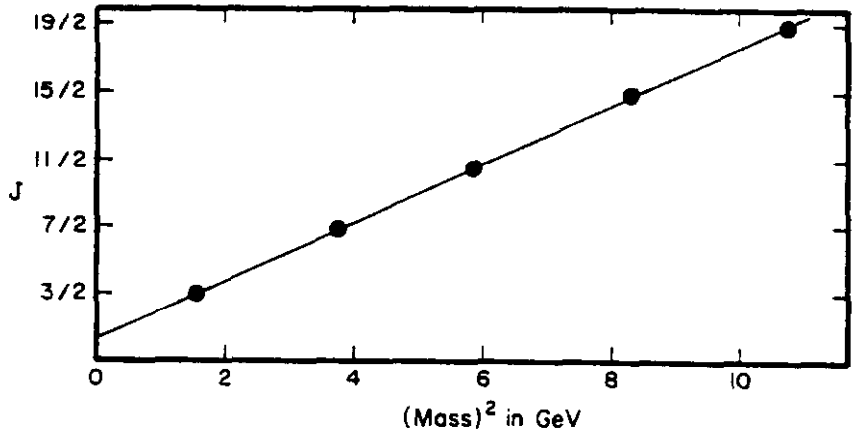

Fig. D.2.b: Orbital excitations of the Δ.

We observe that there seems to be a linear relationship between the angular momentum and the square of the mass. It also seems that the same slope works for both the mesons and the baryons. The slope appears to be about $(0.9\ \text{GeV})^{-2}$:

$$\begin{aligned} J &= \alpha + \alpha' M^2 \\ \alpha'_{q\bar{q}} &\cong \alpha'_{qqq} \cong 0.9\ GeV^{-2} \end{aligned} \qquad \text{(D.15)}$$

This is a very interesting set of relationships and one wonders if QCD can shed any light on them. One can make a picture of the quark and anti-quark bound together by gluons. QCD tells us that the gluons form a flux tube of flux lines which is flattened into a string. This is so because the gluons are themselves colored. Hence the flux lines attract one another and compress into a tube. In QED the photon is not charged and the effect does not occur. So, what we will do is assume a gluon string with a certain energy density per unit length k. This model is shown in Figure. D.3.

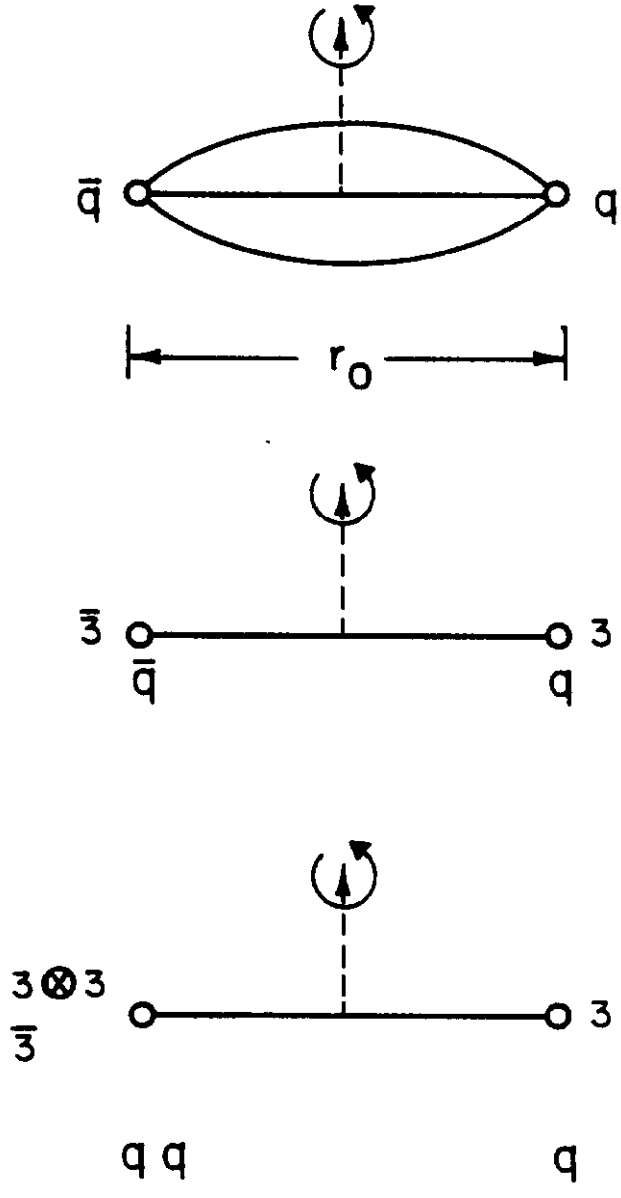

Fig. D.3: String picture for $\bar{q}q$ and qqq bound by gluon flux tube.

In that figure, we have assumed that the diquark at the end of the string is in a flavor $\bar{3}$ state which means that the quark anti-quark rotational properties should be very similar to the quark diquark rotational properties. We have then built in the fact that the Regge slope for mesons and baryons is the same. In this very simple string model we will assume massless quarks and that the ends of the string rotate at the speed of light at the maximum angular momentum. That means that the velocity as a function of the distance from the

center of the string is as given below:

$$\begin{aligned}
\beta(r) &= \frac{2r}{r_0} \\
M &= \int \gamma k dr = 2\int_0^{\ell/2} \frac{k dr}{\sqrt{1-\beta^2}} = \frac{k r_o \pi}{2} \\
L &= rp = \int r\gamma\beta dm = \int r\gamma\beta k dr \qquad . \qquad \text{(D.16)} \\
&= \frac{k r_0^2 \pi}{8} \\
J &\sim \left(\frac{1}{2\pi k}\right) M^2 \\
\alpha' &= \frac{1}{2\pi k}
\end{aligned}$$

The relativistic mass is just the energy density per unit length integrated over the lengths. Since the string has an angular velocity, the total system energy which is the total mass is as in Eq. D.16. Similarily the relationship between angular momentum and linear momentum is familiar but we use the correct relativistic expression for linear momentum. Since the slope of the Regge trajectories is a relationship between L and the square of the mass, it is easy to relate the Regge slope to the string tension. We will come back to their numerical relation later. For now it is sufficient to note that this simple picture explains the existence of the Regge trajectories and the fact that the Regge trajectories are the same for mesons and baryons. One can certainly consider that a phenomenological success for QCD.

At this point, we have reasonably successful explanations for the masses of the pseudoscalar and vector mesons and their orbital excitations. I will just assert that one can have a similar success with the octet and decuplet baryons and their excitations. However, we have yet to say anything about the relationship between, for example, the pseudoscalar and vector octet and the baryon octet and decuplet. In order to begin to study this relationship, we want to digress a moment and talk about one gluon exchange potentials. In QED the one photon exchange interaction energy is proportional to the product of the charges. That means that positronium is bound because the electron and positron have a negative energy and so the interaction is attractive whereas e^-e^- is unbound. For nuclei there is a similar SU(2) isospin relationship for the two nucleon system where you can have neutron neutron, proton proton or neutron proton. The isotopic interaction energy looks like the vector product of the isotopic spins of the constituents. That means that only the isoscalar is bound due to the one pion exchange. The deuteron is bound whereas pp and nn are unbound. These relationships are given below:

$a)$ QED

$$\begin{aligned} & & H_{EM} &\sim e_1 \cdot e_2 \\ e^+e^- & \text{ bound} & & H_{EM} \sim -1 \\ \left.\begin{matrix} e^-e^- \\ e^+e^+ \end{matrix}\right\} & \text{ unbound} & & H_{EM} \sim +1, \end{aligned} \tag{D.17}$$

$b)$ Isospin SU(2)

$$\begin{aligned} & & H_I &\sim \vec{I}_1 \cdot \vec{I}_2 \\ np & \text{ bound} & & H_I \sim -3(I=0) \\ \left.\begin{matrix} pp \\ np \end{matrix}\right\} & \text{ unbound} & & H_I \sim +1(I=1)\ . \end{aligned}$$

In QCD, we have quarks that come in three colors and eight gluons which can be thought of as containing a color and an anti-color. The vertex factor in one gluon exchange in QCD is shown in Fig. D.4. This one gluon exchange amplitude is proportional to some products of the square of the length of the generators in a given SU(3) representation. We have already evaluated these factors in Section B and we will use these results now.

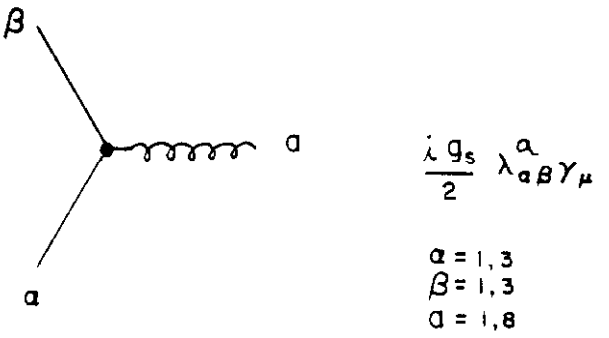

Fig. D.4.a: qqg vertex factors.

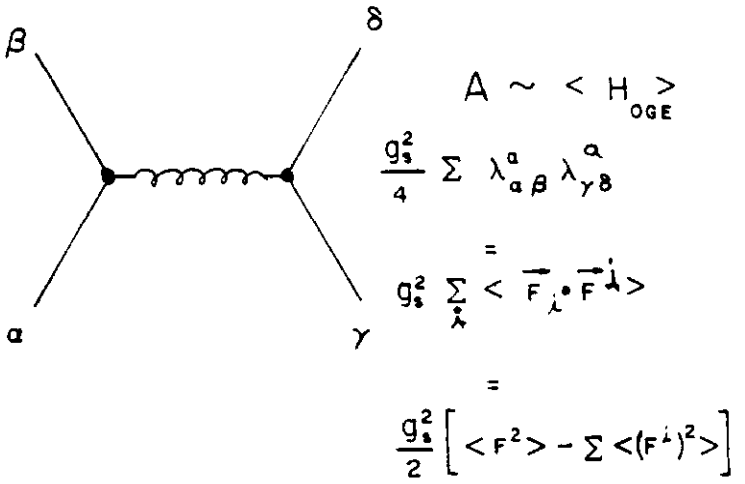

Fig. D.4.b: OGE diagram.

We have previously assumed that all hadrons are color singlets. For example, you can now (for amusement) prove to yourself that one gluon exchange is attractive in a singlet but repulsive in an octet. This is a posteriori justification for the idea that the quark anti-quark system is most bound in a color singlet. It is also amusing to show that while a diquark system can be in a $\bar{3}$ or a sextet, one gluon exchange is attractive in a $\bar{3}$ but repulsive in a sextet. This gives some justification for the idea that diquarks are in a $\bar{3}$ state and not in a sextet state. Similarly you can work out the fact that 3 quarks are in color singlets, octets, or decuplets but that the singlets are the most attractive. Of course one gluon exchange is not all that is happening in strong binding, but it gives us a warm feeling about our assumptions.

We can now look at quark anti-quark mesons under the assumption of 1 gluon exchange. We evaluate the QCD potential as shown below:

$$
\begin{aligned}
a) \qquad & \frac{g_S^2}{2}\left[< F_1^2 > - < F_3^2 > - < F_{\bar{3}}^2 >\right] \\
& \frac{g_S^2}{2}\left[0 - \frac{4}{3} - \frac{4}{3}\right] \\
& Vq\bar{q}(1) = -\frac{4}{3}\alpha_s/r \ , \qquad\qquad (D.18) \\
b) \qquad & \frac{g_S^2}{2}\left[< F_{\bar{3}}^2 > - < F_3^2 > - < F_3^2 >\right] \\
& Vqq(\bar{3}) = -\frac{2}{3}\alpha_s/r \ .
\end{aligned}
$$

These results mirror the idea (Eq. B.3) that the simplest colorless composites (most bound) can be made from three colors (red + blue + green = white) or from color/anti-color. What we find is that the quark anti-quark potential has a color factor minus 4/3 but otherwise looks essentially like the Coulomb interaction. In the case of baryons, we assume that the baryon is a color singlet. That means that any di-quark must be in a color $\bar{3}$ so that when convoluted with the other quark which is in a color triplet we get a color singlet baryon. That leads to a potential which is also attractive but which is only half as strong as the potential between quarks and anti-quarks. The main hadron binding is strong, due to multigluon effects. We will use our OGE results only to estimate perturbative splits.

As seen in Table D.3, spin-spin mass splittings for mesons are larger than those for baryons. This is just what we expect on the basis of gluon color factors. Even more striking, in the electromagnetic case we would have a quark anti-quark split of different sign from the quark-quark split because we are dealing with electromagnetic charge. For "color charge" the split for $q\bar{q}$ and for qq is attractive in both cases. This makes any problems one has in understanding the sign of the spin-spin splitting for qq and $q\bar{q}$ simply disappear. All quarks have color charge and that color charge is the same for quarks and anti-quarks.

Table D.3.

Spin-spin mass splitting
for mesons, 1^-, 0^- and baryons $\frac{3}{2}^+$, $\frac{1}{2}^+$.

$1^- - 0^-$	$\Delta M(MeV)$	$\frac{1}{\gamma_i\gamma_j}$
$M_\rho - M_\pi$	630	$\equiv 630 = \frac{4}{3}M_{ss}$
$M_{K^*} - M_K$	394	378
$M_D^* - M_D$	143	126
$M_{F^*} - M_F$	140	76
$M_{B^*} - M_B$	52	38
$\frac{3}{2}^+ - \frac{1}{2}^+$	$\Delta M(MeV)$	$3/(4\gamma_i\gamma_j)$
$M_\Delta - M_N$	293	472
$M_{\Sigma^*} - M_\Sigma$	191	280
$M_{\Xi^*} - M_\Xi$	215	168

m	=	300		1.0
m_s	=	500 MeV	$, \gamma =$	1.67
m_c	=	1500		5.0
m_b	=	5000		16.6

Let us now examine the spin-spin splitting between the pseudoscalar and vector octet. The departure point is the QED spin-spin splitting which we derived in Section A. We merely

replace the Coulomb charge by the color charge factors which we have already derived. We will absorb all of the factors into a spin-spin mass term except those factors which have values of order one, the spins and the color charges:

$$\begin{aligned} M_{QED} &= \frac{8\pi}{3} \frac{(e_i e_j)(\vec{S}_i \cdot \vec{S}_j)}{m_i m_j} |\psi(0)|^2 \\ M_{QCD} &\equiv \frac{-8\pi}{3} \frac{(\vec{F}_i \cdot \vec{F}_j)(\vec{S}_i \cdot \vec{S}_j)}{m_i m_j} \alpha_s |\psi(0)|^2 \\ M_{QCD} &\equiv \frac{(\vec{F}_i \cdot \vec{F}_i)(\vec{S}_i \cdot \vec{S}_j)}{\gamma_i \gamma_j} [M_{ss}] \\ M_{ss} &\equiv \frac{8\pi}{3} \frac{\alpha_s}{m^2} |\psi(0)|^2 \end{aligned} \quad . \tag{D.19}$$

We have already evaluated the spin and color factors in our previous discussion of one gluon exchange and spin-orbit splitting. The resultant split between the vector and pseudoscalar octets is shown in Eq. D.20:

$$\begin{aligned} < \vec{F}_q \cdot \vec{F}_{\bar{q}} > &= -\frac{4}{3} \\ < \vec{S}_q \cdot \vec{S}_{\bar{q}} > &= -\frac{3}{4}, S = 0 \\ &\quad \frac{1}{4}, S = 1 \\ M_1 - M_0 &= \frac{4}{3} \left(\frac{M_{ss}}{\gamma_i \gamma_j} \right) \end{aligned} \quad . \tag{D.20}$$

We can now write the π, ρ, K, and K^* masses in terms of an unbroken mass $\bar{M}$, the spin-spin mass splitting and the SU(3) breaking factor:

$$\begin{aligned} M_\pi &= \bar{M} - M_{ss} \\ M_\rho &= \bar{M} + M_{ss}/3 \\ M_K &= \bar{M} - M_{ss}/\gamma + (\gamma - 1)m \\ M_{K^*} &= \bar{M} + M_{ss}/3\gamma + (\gamma - 1)m \end{aligned} \quad . \tag{D.21}$$

Solving this set of equations we find the center-of-gravity for the mesons to be 617 MeV, a mass splitting of 480 MeV, and a strange to up quark mass splitting of 176 MeV:

$$\begin{aligned} \bar{M} &= (3M_\rho + M_\pi)/4 = 617\ MeV \\ M_{ss} &= 3(M_\rho - M_\pi)/4 = 480\ MeV \\ (\gamma - 1)m &= (3M_{K^*} + M_K)/4 - \bar{M} = 176\ MeV \end{aligned} \quad . \tag{D.22}$$

A glance at the table of spin-spin mass splittings shows you that a simple scaling in one over the product of the quark and anti-quark masses works well for scaling ρs to K^*s with the strange quark, ρs to Ds with the charm quark and ρs to Bs with the bottom quark. This spin-spin gluonic contribution has solved the long standing problem of why the pion mass was so small. The question is...why is the pion so light? And the answer appears to be that it is driven down in mass by the spin-spin QCD term. Another prediction is clearly that the F^* and B^* cannot decay into pions and have to decay electromagnetically into $F + \gamma$ and $B + \gamma$, respectively.

Taking the central mass $\bar{M}$ to be equal to 2m we find an m about 300 MeV and the strange quark at about 500 MeV. These are familiar values. Taking the value of the spin-spin mass term, assuming an α_s of 0.3, we find the wave function of the quark anti-quark system at the origin to be characterized by a length of 0.8 fermis. This is all very much the order-of-magnitude we expect from other considerations:

$$\begin{aligned} \bar{M} &= 2m,\ m = 308\ MeV,\ \gamma m = 484\ MeV \\ \alpha_s &= 0.3 \\ |\psi(0)|^2 &\sim (1/0.8\ fm)^3 \end{aligned} \quad . \tag{D.23}$$

What about the baryons? Clearly QCD relates the vector/pseudoscalar split in mesons to the decuplet/octet split in baryons. Taking the interaction to be the sum of two body interactions we can use the color factors which we have already derived in looking at the quark-quark potential:

$$\sum_{ij} < \vec{F}q_i \cdot \vec{F}q_j > = -\frac{2}{3} \quad . \tag{D.24}$$

$$M_B = \frac{2}{3}\sum_{ij} \frac{(\vec{S}_i \cdot \vec{S}_j)}{\gamma_i \gamma_j} M'_{ss}$$

The coupling of the 3 spins is such that, if all terms are equal, we can evaluate the Δ/nucleon mass split:

$$\begin{aligned} \vec{S} &= \vec{S}_1 + \vec{S}_2 + \vec{S}_3 \\ < \vec{S}_1 \cdot \vec{S}_2 \ \vec{S}_1 \cdot \vec{S}_3 + \vec{S}_2 \cdot \vec{S}_3 > &= \frac{S(S+1) - \frac{9}{4}}{2} \quad . \\ M_\Delta - M_N &= (\frac{2}{3}) M'_{ss} (\frac{6}{4}) = M'_{ss} \end{aligned} \tag{D.25}$$

This allows us to find the wave function (for baryons) at the origin again assuming $\alpha_s = 0.3$ and m = 300 MeV:

$$|\psi'(0)|^2 \ \sim \ (1/0.94 \ fm)^3 \quad . \tag{D.26}$$

This value is comparable to, but slightly larger than, the value we found for the mesons. A look back to Eq. B.5 leads us to expect the radius scaling $\sim 0.8 \ fm \ (\frac{3}{2})^{1/4} = 0.88 \ fm$.

What about baryons with strangeness? An evaluation of Eq. D.24 gives us the following result:

$$\begin{aligned} q_1 &= u, d, q_2 = u, d, q_3 = s \\ M_B &= \frac{2}{3} \left[< \vec{S}_1 \cdot \vec{S}_2 > + \frac{< (\vec{S}_1 + \vec{S}_2) \cdot \vec{S}_3 >}{\gamma} \right] M'_{ss} \\ < \vec{S}_1 \cdot \vec{S}_2 > &= \frac{1}{4} \\ < (\vec{S}_1 + \vec{S}_2) \cdot \vec{S}_3 > &= -1 \ (8) \\ &\quad + \frac{1}{2}, (10) \end{aligned} \quad . \tag{D.27}$$

For the Σ and Σ^* (uus), the uu are in a symmetric $S_{12} = 1$ state. This allows us to find $< \vec{S}_1 \cdot \vec{S}_2 >$. The fact that the octet has $S = \frac{1}{2}$ and decuplet has $S = \frac{3}{2}$ allows us to find the remaining terms:

$$
\begin{aligned}
M_{\Sigma} &= \bar{M}' + \frac{2}{3}M'_{ss}\left(\frac{1}{4} - \frac{1}{\gamma}\right) + (\gamma - 1)m \\
M_{\Sigma^*} &= \bar{M}' + \frac{2}{3}M'_{ss}\left(\frac{1}{4} + \frac{1}{2\gamma}\right) + (\gamma - 1)m \\
M_{\Sigma^*} - M_{\Sigma} &= \frac{M'_{ss}}{\gamma} \stackrel{?}{=} \frac{(M_{\Delta} - M_N)}{\gamma} \\
191 &\stackrel{?}{=} \frac{293}{1.5} = 195\ MeV
\end{aligned}
\qquad \text{(D.28)}
$$

One sees that the data agree rather well with our expectations. Clearly we could continue in this manner to find the splitting for all the baryons. However, it tells us little new.

A grand summary for the preceeding results of this section is supplied in Fig. D.5. Mesons and baryons are shown with a central mass $\bar{M}$. This level is split by spin-spin interactions, indicated by M_{ss}, into non-strange vectors (ρ), pseudoscalars (π) and $\frac{1}{2}^+(N)$, $\frac{3}{2}^+(\Delta)$. Note that splits for baryons are roughly half the meson splits as expected in QCD. Subsequent SU(3) breaking with $\gamma \neq 1$ has 2 effects; reduced spin-spin splitting (due to $1/m$ factors) and higher masses (due to $(\gamma-1)m$ factors). These two effects are indicated as $(m_s - m_u)$. Finally, singlets are indicated to indicate singlet/octet splits. It is clear that we have successfully described the major spectroscopic features of the low-lying mesons and baryons rather easily.

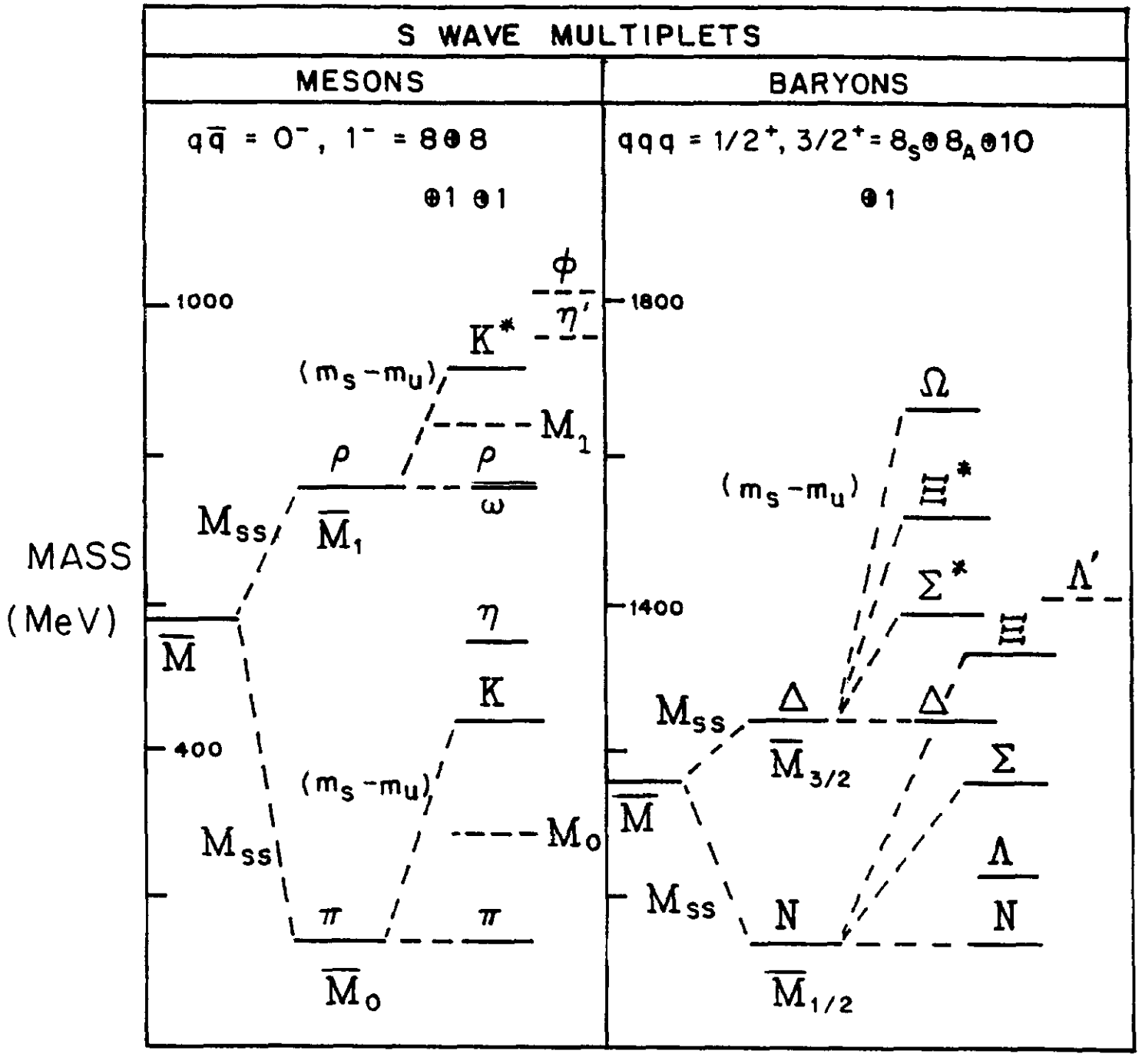

Fig. D.5: Meson and baryon multiplets with spin-spin and SU(3) splitting.

Clearly charm quark spectroscopy gives us a chance to apply much that we have learned. Taking a charm-quark mass of about 1500 MeV we can make various predictions. For example, it is obvious that the D^*/D mass splitting is reduced by the heaviness of the charm quark. We expect it to be very close to the threshold for D^* going to $D\pi$. In fact, it is observed that this reaction just barely goes. This means that the mass relations for the pseudoscalar and vector charmed mesons are something that we can essentially write down knowing what we know about the constituent masses and the spin-spin mass splitting. Heavy flavor spectroscopy has a long experimental history at Fermilab. Most recently E-691 has contributed dramatically to the worlds data on charmed-meson lifetimes and mixing limits.

What is a little less easy to confront with the data are the charmed baryons of which there are six with a single charmed quark. Clearly, the masses are not particularly well known and the decay modes are not at all well understood. Obviously it would be extremely useful to have new data on the charm-baryon spectra so that we could extend our knowledge of hadron spectroscopy. One can hope that that will come in the fullness of time with new experiments coming on-line.

Table D.4.
Charmed meson and baryon masses.

J^{PC}	Quark Content	Name	Mass[a] (MeV/c^2)	Lifetime (10^{-13} sec)	Width[a] (MeV)
Mesons					
0^{-+}	$c\bar{u}$	D^0	1864.6±0.6	$4.3^{+0.2}_{-0.2}$[b]	
	$c\bar{d}$	D^+	1869.3±0.6	$10.31^{+0.52}_{-0.44}$[b]	
	$c\bar{s}$	D_s (F)	1970.5±2.5	$3.5^{+0.6}_{-0.5}$[b]	
1^{--}	$c\bar{u}$	D^{*0}	2007.2±2.1		<5
	$c\bar{d}$	D^{*+}	2010.1±0.7		<2
	$c\bar{s}$	D^*_s (F^*)	2113. ± 8		
$1^+/2^{+?}$	$c\bar{d}$	D(2420)	2426. ± 6		75 +20
Baryons					
$1/2^+$	cud	Λ_c^+	2281.2±3.0	$1.9^{+0.5}_{-0.3}$[b]	
	cuu	Σ_c^{++}	$M(\Lambda_c^+)$+168.4 ± 0.5[d]		
	cdd	Σ_c^0	$M(\Lambda_c^+)$+165.8 ± 0.7[d]		
	cus	Ξ_c^+ (A^+)	2460 ±25	$4.8^{+2.9}_{-1.8}$[e]	
	css	Ω_c^0 (T^0)	2740 ±20		

Finally, what can we say about flavor singlet quark anti-quark states? Table D.5 shows the lowest lying states for $s\bar{s}$, $c\bar{c}$, and $b\bar{b}$.

Table D.5.
$q\bar{q}$ mesons, 0^- to 1^- radial excitations.

$q\bar{q}$		$\Delta M(MeV)$
$s\bar{s}$	$\phi(1020)$	
	$\phi(1685)$	665
$c\bar{c}$	$\psi(3097)$	
	$\psi(3686)$	589
$b\bar{b}$	$\Upsilon(9460)$	
	$\Upsilon(10023)$	563

First thing one notices is that the splitting between the first two excitations is effectively independent of the mass of the state. Let's look at how that might come about. If we look at the Schrödinger equation, we can make a connection between the level spacings and the force law which is responsible for the binding. We used the virial theorem in Section A where we derived the energy states of the hydrogen atom. We required the deBroglie relation and that there be a standing wave. In the equations below, we reproduce this calculation for general power law potential behavior. For example, one gluon exchange leads to the familiar result that the energy is proportional to the mass of the constituents and inversely proportional to the principle quantum number squared. For a string potential, we find that the mass dependence is extremely weak, it goes like $(m)^{-1/3}$.

$$\begin{aligned} V &\equiv A/r^N \\ E &= < T > + < V > \\ &= < T > (1 + 2/N) = < V > (\frac{N}{2} + 1) \\ &= \frac{n^2}{2mr^2}(1 + 2/N) \\ &= \frac{-n^2}{2m}(1 + 2/N)\left[\frac{< A >}{< V >}\right]^{2/N} \\ &= \frac{-n^2}{2m}(1 + 2/N)\left[\frac{A(1 + \frac{N}{2})}{E}\right]^{2/N} \\ E &= \left[\frac{n^2}{m}\right]^{\frac{N}{N+2}} (\text{Const}) \end{aligned} \qquad \text{(D.29)}$$

The actual behavior of the $c\bar{c}$ and $b\bar{b}$ systems is shown in more detail in Fig. D.6.

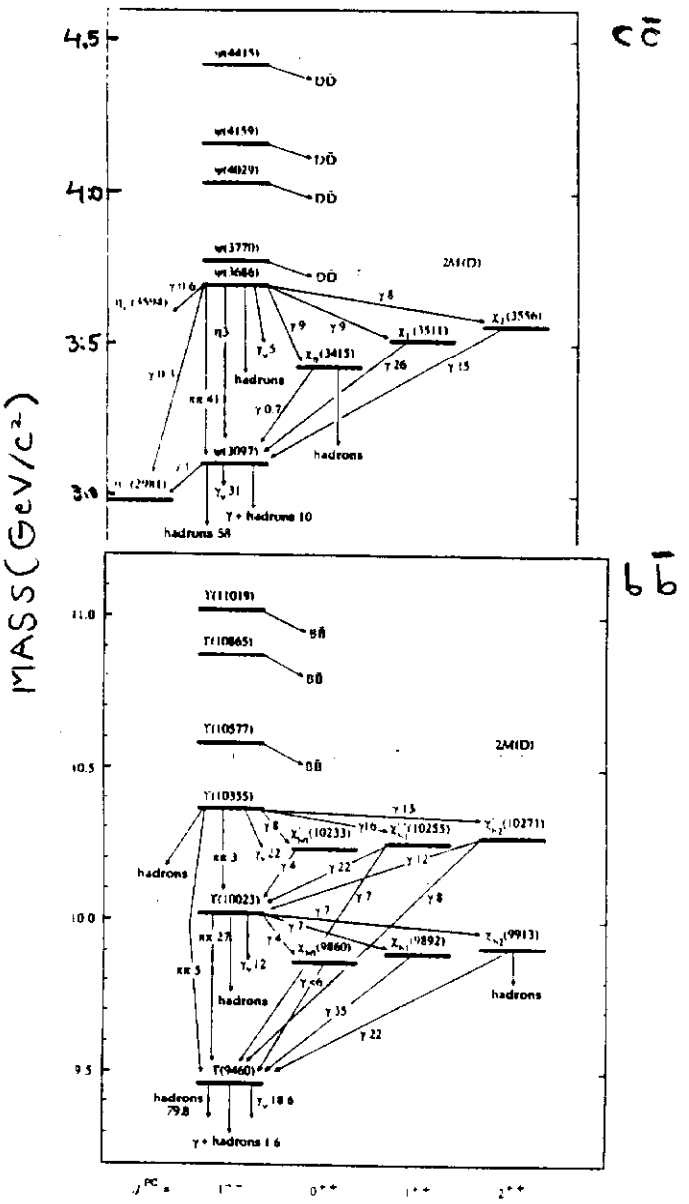

Fig. D.6: Level scheme for the $c\bar{c}$ and $b\bar{b}$ quarkonium states.

Again the level spacings are very similar and are essentially independent of the mass. The force seems to be flavor independent. You expect gluon color forces to be flavor and mass independent. Using the scaling laws from Eq. D.30 it looks as if the system has a mixture of one gluon exchange and confining string potentials. In fact, a potential which is a mix of those appears to work rather well:

$$\begin{aligned} a) \quad & \text{OGE, N} = -1,\ A = \alpha_s \\ & E = \left(\frac{mA^2}{2n^2}\right) = \frac{m\alpha_s^2}{2n^2}\ , \\ b) \quad & \text{String, N} = 1,\ \text{A} = \text{k} \\ & E = \left(\frac{9}{8m}\right)^{1/3}(kn)^{2/3}\ . \end{aligned} \tag{D.30}$$

Moreover, the two spectra are fit with α_s of about 0.2 which is a number we have come to expect. The fitted string tension is 0.16 GeV^2 which is very similar to that which we derived in looking at Regge trajectories. The resulting phenomenological potential given in Eq. D.31 is shown in Fig. D.7 along with the expectation value for the location of the states:

$$\begin{aligned} V_{q\bar{q}}(r) &= -\frac{4}{3}(\alpha_s/r) + kr \\ \alpha_s &\sim 0.2,\ k \sim 0.16\ GeV^2 \end{aligned}\ . \tag{D.31}$$

You recall that the lowest Bohr radius scales inversely with mass of the system and that subsequent levels scale proportional to the principle quantum number:

$$\begin{aligned} a_0 &\sim \lambda/\alpha_s \\ a &\sim na_0 \end{aligned}\ . \tag{D.32}$$

Looking at Fig. D.7, it is clear that the charmonium system does not probe the gluon region of the potential because it is not heavy enough whereas the $b\bar{b}$ states (being about 3 times heavier) move in about a factor of 3 in radius. They begin to probe the Coulomb part of the potential. Obviously the spectroscopy of the top quark (when and if it is discovered) will be defined by the gluonic part of the potential.

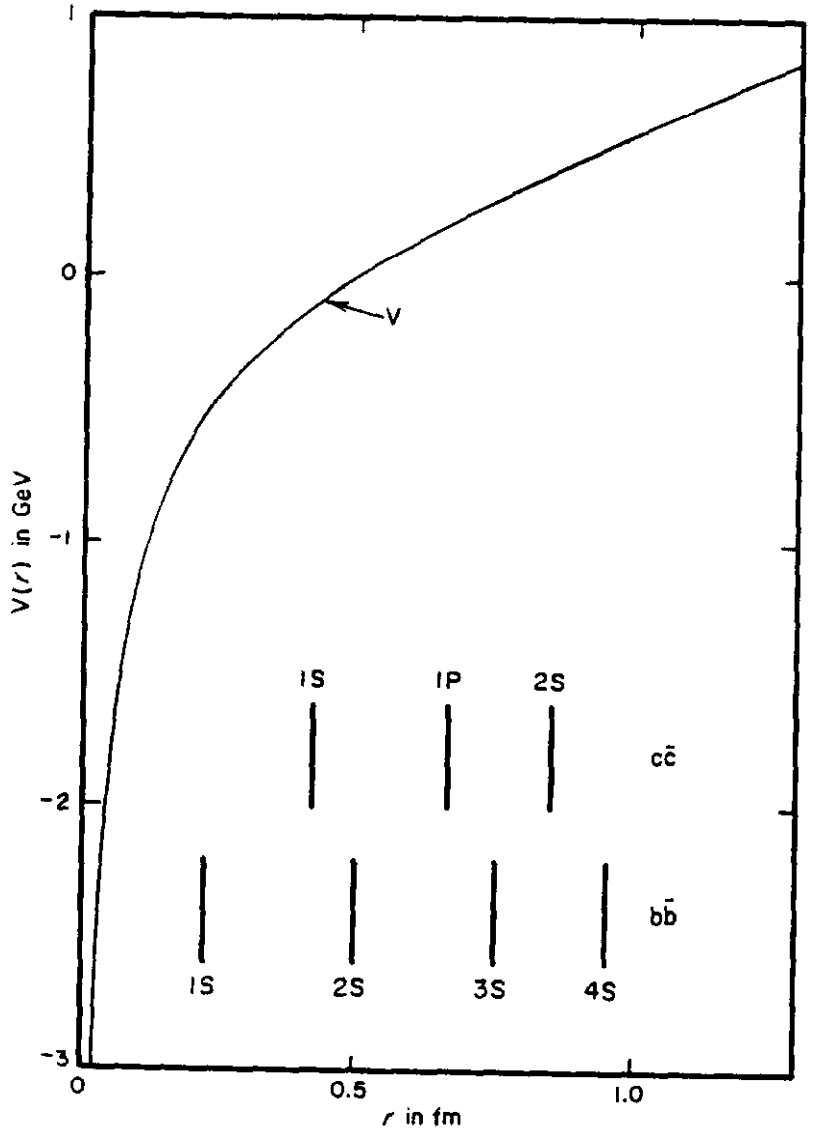

Fig. D.7: $V_{q\bar{q}}(r)$ and location of quarkonium states.

Section II.
Hadron Decays

A. Coupling Constants and Cross Sections

Having come to a reasonably successful explanation of the quark anti-quark and three quark systems (the systematics of their masses and their splittings) we now turn to their eventual fate, i.e., discussion of their decay modes. In order to begin, we need a working knowledge of the forces, the coupling constants, and some of the systematics of the cross sections. Let's begin the review of dynamics by talking about the dimensions of coupling constants and their definition. We start from the definition of the action as the time integral of the Lagrangian which is the four dimensional volume integral of the Lagrangian density. This means that the Lagrangian density has dimensions of mass to the 4th power:

$$\begin{aligned} S &= \int L dt = \int \mathcal{L} d^4x \\ [\mathcal{L}] &= [M]^4 \end{aligned} \qquad \text{(A.1)}$$

We now write the kinetic terms of the Lagrangian from the Dirac equation for fermions and from the Klein-Gordon equation for bosons. ψ denotes a fermion field and ϕ denotes a boson field. Looking at the kinetic terms we see that the dimensions of a fermion wave function is $[M]^{\frac{3}{2}}$ while the dimensions of a boson wave function is simply $[M]$:

$$\begin{aligned} \mathcal{L} &= \bar{\psi}\partial\psi, \ [\psi] = [M]^{\frac{3}{2}} \\ \mathcal{L} &= \partial\phi\partial\phi, \ [\phi] = [M] \end{aligned} \qquad \text{(A.2)}$$

Armed with this information, we can look at the Fermi interaction which is of the current-current form. We know that the current can be made up out of fermion bilinear operators, and that leads us to the conclusion that the Fermi coupling constant has dimensions of $[M]^{-2}$:

$$
\begin{aligned}
a) \qquad \mathcal{L} &= \frac{G}{\sqrt{2}} J_\mu J^\mu, \; J_\mu = \bar{\psi}\gamma_\mu\psi \\
[G] &= [M]^{-2} \; , \\
\\
b) \qquad \mathcal{L} &= g J_\mu A^\mu = g(\bar{\psi}\gamma_\mu\psi)\phi^\mu \\
[g] &= [M]^0 \\
\alpha, \alpha_s \; , \\
\\
c) \qquad \mathcal{L} &= g\phi^4 \; .
\end{aligned}
\tag{A.3}
$$

On the other hand, the QED or QCD Lagrangian is a current-field interaction with an associated dimensionless coupling constant called α or α_s. Finally, for completeness a ϕ^4 theory has a dimensionless coupling constant and that is why it is popular with theorists.

Let's look briefly at the comparison between the electromagnetic and the weak potentials. We will define a weak coupling constant g_w. We know that the Compton wavelength then leads to a Yukawa like potential or a propagator with a mass term. If we are in a situation where the q value is small with respect to the mass of the propagating boson, we can write an effective current-current interaction relating g_w to the Fermi constant:

$$
\begin{aligned}
V_{EM}(r) &= \alpha/r \\
\\
V_W(r) &= (g_W^2/r)e^{-r/\lambda w} \\
\\
V_W(q) &= g_W^2/(q^2 + M_W^2) \\
\\
\frac{G}{\sqrt{2}} &= g_W^2/8M_W^2 \equiv \alpha_W/8M_W^2
\end{aligned}
\tag{A.4}
$$

Looking at Eq. A.4, it is clear that if g_W^2 were of the same order as α, what would make the weak interactions weak would be the Yukawa exponential in the potential. For example, at a q value of 10 GeV the weak potential would still be roughly 10,000 times weaker than the electromagnetic potential.

Having looked at the coupling constants one can now consider the dynamics and the coupling scheme. First let's just look at electromagnetism and recall the free Dirac Lagrangian which is given in Eq. A.5: The interactions in electromagnetism are included by changing the derivative to the co-variant derivative which has the photon field in it. That leads to a standard $J_\mu \cdot A^\mu$ interaction term:

$$\begin{aligned} \mathcal{L} &= \bar{\psi}\,[\partial_\mu \gamma^\mu - m]\,\psi \\ \partial_\mu &\rightarrow D_\mu = \partial_\mu - ie\,A_\mu \quad . \\ \mathcal{L}_I &= -ie(\bar{\psi}\gamma_\mu\psi)A^\mu \end{aligned} \tag{A.5}$$

In the case of the weak interactions, we construct charge-changing interactions because we have seen β decays for many years. The attempt is to use the Gell-Mann Nishijima relationship but in this case for weak isospin and weak hypercharge. The gauge particles are a triplet of SU(2) bosons and a singlet of U(1) with coupling constants g_2 and g_1. One then writes down derivatives completely analogously to the minimal coupling scheme:

$$\begin{aligned} Q_W &= (I_3 + Y/2)_W \\ W^+, W^0, W^- &\quad , \quad SU(2), \;\; g_2 \\ B^0 &\quad , \quad U(1), \;\; g_1 \\ D_\mu &= \partial_\mu - \imath\left[g_1(Y/2)B^0_\mu + g_2\vec{I}\cdot\vec{W}_\mu\right] \\ e &\rightarrow gQ \end{aligned} \quad . \tag{A.6}$$

We want one of the physical bosons, the photon, to couple to charge. Since Q is not an SU(2) or U(1) generator we need to make a rotation of the neutral members of these two symmetry groups. If we do that we can demand that one of the rotated members couple to charge:

$$a) \qquad \begin{pmatrix} A \\ Z \end{pmatrix} = \begin{pmatrix} \cos\theta_W & \sin\theta_W \\ -\sin\theta_W & \cos\theta_W \end{pmatrix} \begin{pmatrix} B^0 \\ W^0 \end{pmatrix}$$

$$D = \partial - \imath \begin{bmatrix} (g_1 Y/2\cos\theta_W + g_2 I_3 \sin\theta_W)A + g_2(I^+W^- + I^-W^+) \\ (g_2 I_3 \cos\theta_W - g_1 Y/2 \sin\theta_W)Z \end{bmatrix} ,$$

$$g_1(Q - I_3)\cos\theta_W + g_2 I_3 \sin\theta_W \equiv Qe \tag{A.7}$$

$$b) \qquad g_1 \cos\theta_W = e$$

$$g_2 \sin\theta_W = e \; .$$

A pictorial way to visualize what is going on is given in Fig. A.1. Obviously, we will still have a neutral boson coupled to the weak charge. That means we are going to have charged and neutral currents in a unification scheme of electromagnetism and the weak interactions.

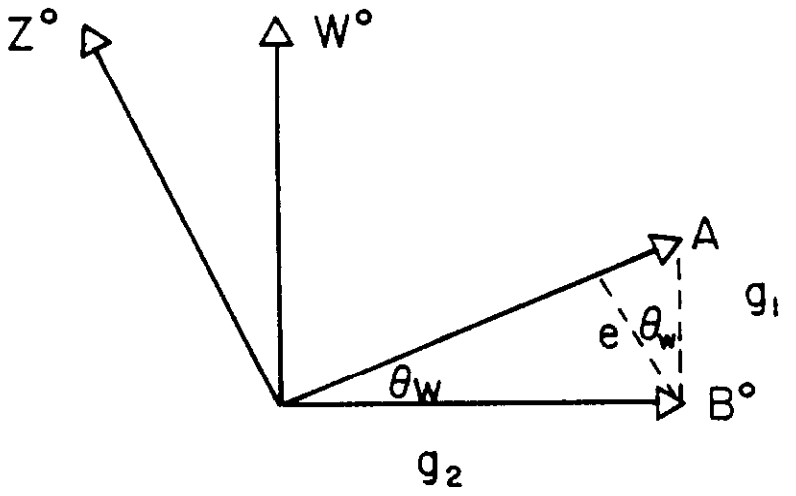

Fig. A.1: Rotation of the SU(2) and U(1) fields by θ_W to form the physical fields A and Z^0.

As one can see in Eq. A.8, one has a specified coupling of the neutral-current boson Z^0 in terms of charge, weak isotopic spin, and the Weinberg angle θ_W (which is measured elsewhere). Clearly g_2 is related to the more familiar charged weak decays.

$$
\begin{aligned}
a)\quad D &= \partial - \imath\left[eQA + g_2(I^+W^- + I^-W^+) + Z(-g_1(Q - I_3)\sin\theta_W + g_2 I_3 \cos\theta_W)\right] , \\
b)\qquad & -g_1 Q \sin\theta_W + g_1 I_3 \sin\theta_W + g_2 I_3 \cos\theta_W \\
&= \sqrt{g_1^2 + g_2^2}\left[-Q\sin^2\theta_W + I_3\sin^2\theta_W + I_3\cos^2\theta_W\right] \\
&= \sqrt{g_1^2 + g_2^2}\left[I_3 - Q\sin^2\theta_W\right] , \\
c)\quad D &= \partial - \imath\left[eQA + g_2(I^+W^- + I^-W^+) + \sqrt{g_1^2 + g_2^2}(I_3 - Q\sin^2\theta_W)Z\right] .
\end{aligned}
\tag{A.8}
$$

The specified couplings are the photon, which we are familiar with, the charged-weak current coupling constant g_2 and a weak-neutral current which is specified in terms of the Weinberg angle. What about masses in the theory? Recall the kinetic term in the weak isotopic doublet of scalars which are going to be the Higgs scalars. If we demand local gauge invariance then

the covariant derivative contains the photon, W, and the Z^0. If the vacuum has a condensate (or the Higgs field has a vacuum expectation value) then the kinetic term with this covariant derivative has contained within it terms which generate a mass for the W and Z. The photon is forced to be massless:

$$\begin{aligned} (\partial_\mu \phi)^*(\partial^\mu \phi) &\rightarrow (D_\mu \phi)^*(D^\mu \phi) \\ < \phi > &= \begin{pmatrix} 0 \\ \eta \end{pmatrix} \quad . \qquad \text{(A.9)} \\ (D_\mu \phi)^* (D_\mu \phi) &\sim \left(\frac{g_2^2}{2}\eta^2\right) \bar{W}W + \left(\frac{(g_1^2+g_2^2)}{2}\eta^2\right) \bar{Z}Z + \left[e^2(0)\right] \bar{A}A \end{aligned}$$

The W and Z masses are proportional to the vacuum expectation value of the Higgs field and are given below:

$$\begin{aligned} M_W &= g_2\eta/\sqrt{2} \\ M_Z &= \sqrt{g_1^2+g_2^2}\,\eta/\sqrt{2} \quad . \qquad \text{(A.10)} \\ M_Z &= M_W/\cos\theta_W \end{aligned}$$

In fact, the W and Z masses were predicted by measuring the Weinberg angle using data on weak-neutral current interactions. The vacuum expectation value can be related to the Fermi constant which is measured from β decay interactions and is 175 GeV. This is then the characteristic mass associated with the weak interactions. For example, the W and the Z masses are about 80 and 95 GeV, respectively:

$$\begin{aligned} M_W &= g_2\eta/\sqrt{2} \\ \frac{G}{\sqrt{2}} &= g_W^2/8M_W^2, g_2 = g_W \quad . \qquad \text{(A.11)} \\ \eta &= \frac{1}{\sqrt{G2\sqrt{2}}} = 175\ GeV \end{aligned}$$

Having thought about the coupling constants and the dynamics of decays, let's now turn their kinematics. In quantum mechanics the Schroedinger equation with complex energy has a wave function solution which decays exponentially. That is the definition of the decay width Γ. The Fourier transform of the wave function into energy space yields the familiar Brite-Wigner resonance form:

$$
\begin{aligned}
\imath\partial\psi/\partial t &= H\psi, \psi = e^{-\imath Ht} \\
H &= M + \imath\Gamma/2 \\
|\psi|^2 &= e^{-\Gamma t} \\
|\psi|^2 &= 1/\left[(E-M)^2 + (\Gamma/2)^2\right]
\end{aligned}
\quad . \qquad \text{(A.12)}
$$

What about decay phase space? Non-relativistically phase space can be derived from the statement that all momenta are equally probable. Hence, the density is the joint probability of momentum elements in the three coordinates x, y, and z. The joint probability is just the volume element in three momentum space. This is a familiar form from statistical mechanics. Relativisitically one particle phase space is just the statement that all four momentum volume elements are equally probable. However, there is a constraint that the particle is on the mass shell. This leads to the form given in A.13 for the one particle volume element:

$$
\begin{aligned}
d\rho_1^{NR}(\vec{p}) &\sim d\vec{p} \\
d\rho_1(p) &\sim \delta(p^2 - m^2)d^4p = d\vec{p}/2E \\
&\sim dp_\perp^2 dy, \; y = \text{ rapidity}
\end{aligned}
\quad . \qquad \text{(A.13)}
$$

One of the implications of this result is that the invariant one particle inclusive cross-section should display a rapidity plateau. We know from the definition of rapidity that the width of this plateau should increase logarithmically with the energy. This means in turn that the mean charge multiplicity should increase logarithmically with the energy. In fact, this is actually observed as shown in Fig. A.2:

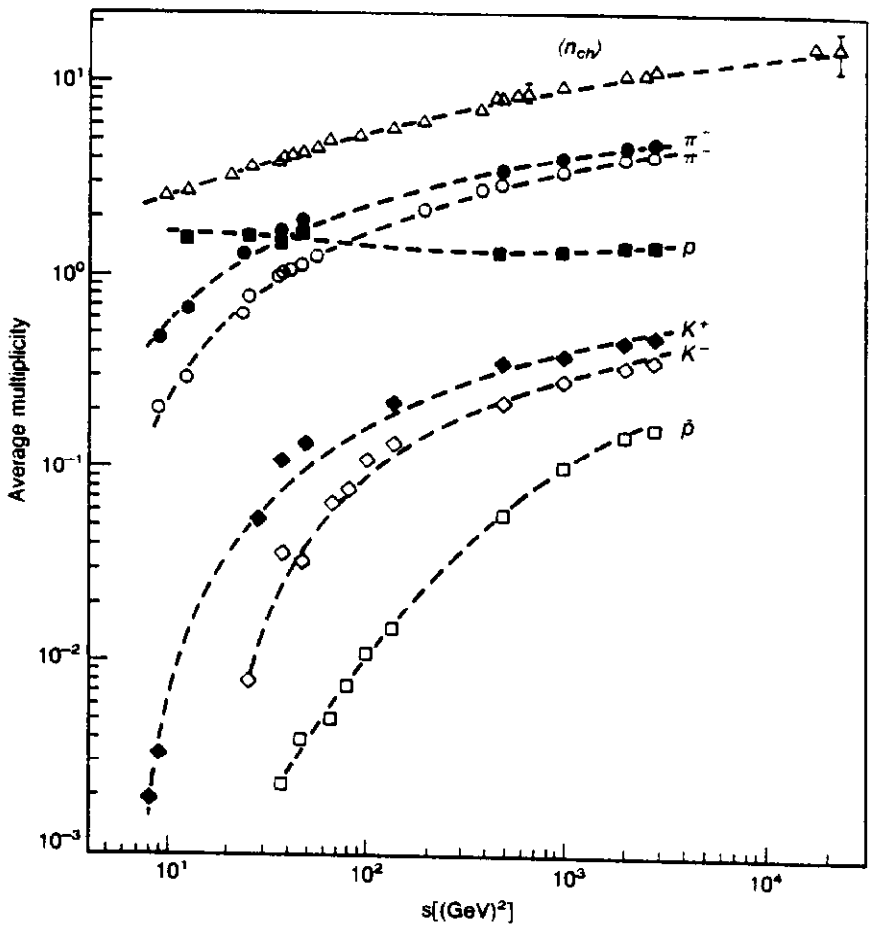

Fig. A.2: Mean charged multiplicity in pp collisions as a function of $\sqrt{s}$.

What about two particle phase space? As seen in Eq. A.14, for a two-body decay momentum conservation is imposed on the joint probability of two one particle phase spaces. Evaluating in the center-of-mass or starred system, we can integrate over p_2 using momentum conservation. We can then readily integrate over the angles of particle 1:

$$
\begin{aligned}
d\rho_2 &\sim \delta(\underline{P} - p_1 - p_2)\delta(p_1^2 - m_1^2)\delta(p_2^2 - m_2^2)d^4p_1 d^4p_2 \\
&= \delta(M - E_1^\star - E_2^\star)\delta(\vec{p}_1^\star + \vec{p}_2^\star)(d\vec{p}_1^\star/2E_1^\star)(d\vec{p}_2^\star/2E_2^\star) \\
\rho_2 &\sim \int \delta(M - E_1^\star - E_2^\star)\frac{d\vec{p}_1^\star}{2E_1^\star}(\frac{1}{2E_2^\star}) \\
&\sim \int \delta(M - E_1^\star - E_2^\star)\frac{4\pi p_1^{\star 2} dp_1^\star}{4E_1^\star E_2^\star}
\end{aligned}
\quad . \tag{A.14}
$$

Specializing to decays into equal masses, one can convert the integral over energy. We find that the relativistically invariant 2 particle phase space is proportional to the velocity of the decay particles in the center-of-mass system. It is intuitively clear that a decaying particle is more likely to go into light particles than heavy particles:

$$
\begin{aligned}
M &\rightarrow m + m, E_1^\star = E_1^\star = M/2 \\
\rho_2 &\sim \int \delta(M - 2E_1^\star)\left(\frac{\pi p_1^\star}{E_1}\right) dE_1^\star \\
&\sim \beta_1^\star
\end{aligned}
\quad . \tag{A.15}
$$

Let's look at a sample calculation which is first order in the weak interactions; the decay of a W boson into lepton pairs. The width is defined in Eq. A.16 below:

$$
\begin{aligned}
\Gamma_2 &\sim |A|^2\rho_2/M \\
&= \frac{1}{16\pi}|A|^2\frac{\beta^\star}{M}
\end{aligned}
\quad . \tag{A.16}
$$

The helicities and vertex factors are shown in Fig. A.3. We will be discussing the helicities implicit in the V-A weak interaction theory later. For now, you will just have to take it as given.

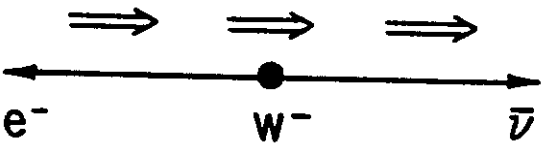

Fig. A.3.a: Helicity factors.

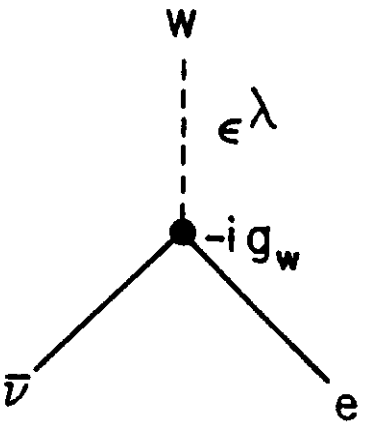

Fig. A.3.b: Vertex and polarization factors.

Fig. A.3: $W \rightarrow e\bar{\nu}$ decay.

The amplitude is proportional to the lepton current dotted into the W polarization with a vertex factor given by g_W. Squaring and summing over the spins one finds that $|A|^2$ is proportional to $g_W^2 M^2$. The decay width is proportional to the vertex factor squared times the mass. This is exactly what you would expect from purely dimensional arguments.

$$
\begin{aligned}
A &\sim J_\lambda \epsilon^\lambda \\
&\sim \frac{-ig_W}{2\sqrt{2}} \left[\bar{U}_e \gamma_\lambda (1-\gamma_5) U_\nu\right] \epsilon^\lambda \\
\sum |A|^2 &\sim g_W^2 M^2 \\
\Gamma_2 &= \left(\frac{g_W^2}{48\pi}\right) M
\end{aligned}
\qquad \text{(A.17)}
$$

Let us now turn to the cross-sections for processes which are strong, electromagnetic, or weak. Knowing about the coupling constants and the quark model, what can we say about total cross-sections? We can make a very crude assumption in meson-baryon and baryon-baryon scattering that there is an impulse approximation. Then what is important is the single scattering of the constituents. What is given on the accompanying table is the counting of the constituent quark-anti-quark, and quark-quark scattering.

Table A.1.
Constituent collisions in hadron-hadron scattering.

Beam	qq	$q\bar{q}$	$q\bar{s}$	qs	$\sigma(mb)$
π^+	3	3			25
π^-	3	3			25
K^+	3		3		17
K^-		3		3	20
p	9				40
$\bar{p}$		9			45
Λ	6			3	35

The strange quarks are treated differently from the up and down quarks. One thing you can see right away is that meson-proton cross-section is roughly 2/3 that of baryon-proton value. This is exactly what you expect from counting. In a little more detail, you can take the value of the total cross-section which is given on the table and extract cross-sections for the constituents given in Eq. A.18:

$$
\begin{aligned}
\sigma(qq) &\sim \sigma(\bar{q}q) \sim 4.5\ mb \\
\sigma(q\bar{s}) &\sim \sigma(\bar{q}s) \sim 2.2\ mb \\
&\sim \sigma(qs)
\end{aligned}
\qquad \text{(A.18)}
$$

The data is shown in Fig. A.4.

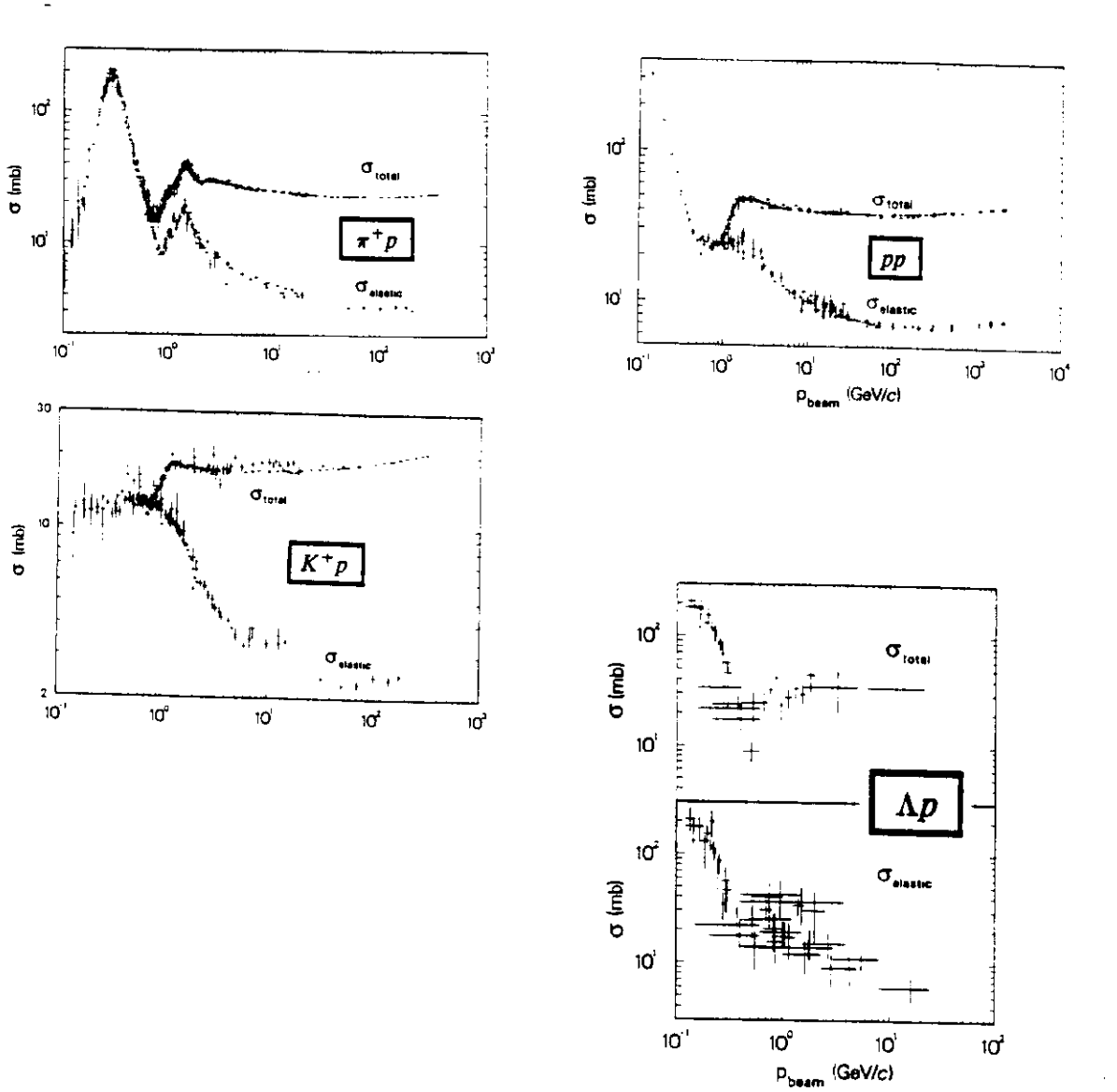

Fig. A.4: Compilation of meson-baryon and baryon-baryon cross-sections.

The quark-quark and quark-anti-quark scattering cross section for up and down quarks is about 4.5 millibarns, whereas the quark-strange or quark-anti-strange or anti-quark-strange cross-section is consistently smaller than that. It is about 2.2 millibarns. Those two numbers are sufficient to give you a good estimate of all measured meson-proton and baryon-proton scattering cross-sections. No dynamics have gone into that estimate of the cross-section. In fact, it is not at all clear that the impulse approximation or the additive quark model should be taken seriously. You can consider it a mnemonic device if you wish.

What about electromagnetic interactions? A first example is the total photon-proton cross-section. A diagram is shown in Fig. A.5.a. This is called the vector-dominance model. The couplings connecting photons to the vector mesons are all of order α, which means that the cross-section should be down from a typical meson-baryon cross-section by order α. If we take the πp cross-section we get a photon cross-section as given in Eq. A.19. The actual data is shown in Fig. A.6 and is surprisingly close to this estimate.

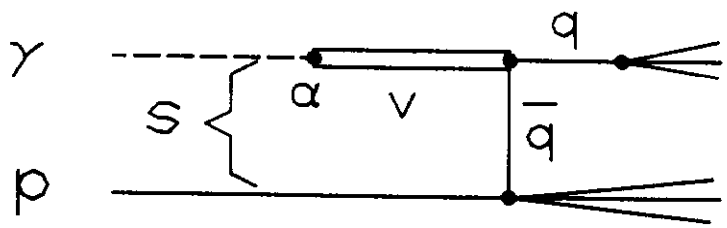

Fig. A.5.a: γp total cross section.

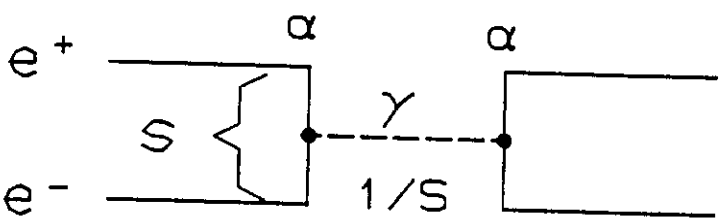

Fig. A.5.b: e^+e^- annihilation.

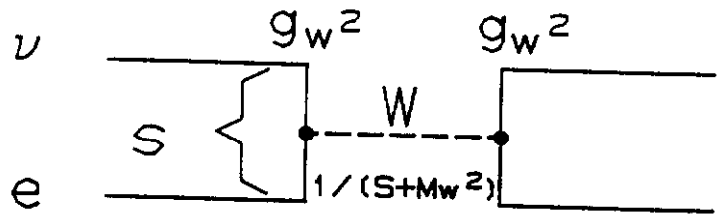

Fig. A.5.c: νe annihilation.

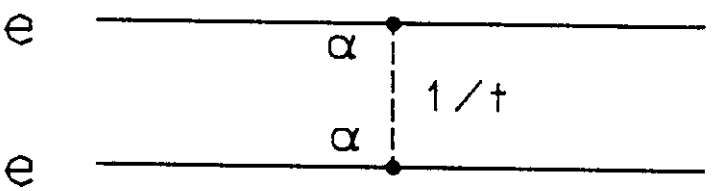

Fig. A.5.d: ee elastic scattering.

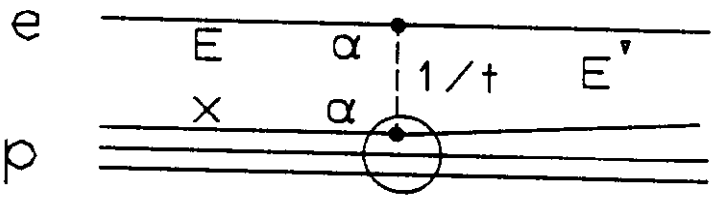

Fig. A.5.e: ep deep inelastic scattering.

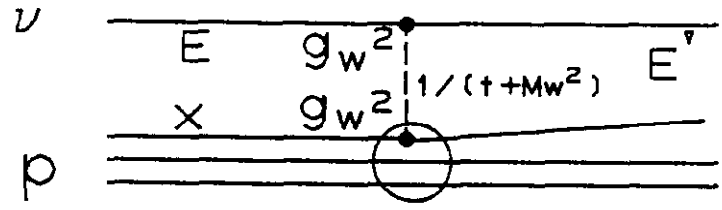

Fig. A.5.f: νp deep inelastic scattering.

Fig. A.5: Pointlike constituent scatterings.

Let us consider other point-like electromagnetic cross-sections. An example is e^+e^- annihilation. It is easy to get a dimensional estimate of the cross-section because there is only one length scale in a problem, the center-of-mass energy. We also know diagramatically that the cross-section should be proportional to α^2. The estimate would be that cross-section goes like $\frac{\alpha^2}{s}$. The exact result is given in Eq. A.19.

$$
\begin{aligned}
a) \quad \sigma(\gamma p) &\sim \alpha\sigma(\pi p) \\
&\sim 146\ \mu b \ , \\
b) \quad \sigma(ee) &\simeq 4\pi\alpha^2/3s \\
&= 87\ nb/s(GeV^2) \ , \\
c) \quad \sigma(\nu e) &\simeq 2g_W^4 s/\pi(s+M_W^2)^2 \to 2g_W^4/\pi s = 2\alpha_W^2/\pi s \\
&\to 2g_W^4 s/\pi M_W^4 \sim G^2 s/\pi \ , \\
d) \quad d\sigma/dt &\simeq 4\pi\alpha^2/t^2 \to \tfrac{4\pi\alpha^2}{t^2}\left[F^2(t)\right] \ , \\
e) \quad d^2\sigma/dtdx &= 4\pi\alpha^2/t^2\left\{F_1(x)\left[(E-E')/E\right]^2 + - - -\right\} \ , \\
f) \quad d^2\sigma/dtdx &= \alpha_W^2/64\pi(t+M_W^2)^2\left\{F_1(x)[(E'-E)/E]^2 + - - -\right\} \\
&= \tfrac{G^2}{2\pi}\left(\tfrac{M_W^2}{t+M_W^2}\right)^2\left\{F_1(x)\left[(E'-E)/E\right]^2 + - - -\right\} \ .
\end{aligned}
\tag{A.19}
$$

What about the total cross-section for neutrinos? In this case, one replaces (in A.19b) the photon by a W boson and the electromagnetic-coupling constant by the weak-coupling

constant as seen in Fig. A.5. In this case, there is another mass scale besides the center-of-mass energy which is the W mass. This leads to an expression for the cross-section given in Eq. A.19.c. The limit when the center-of-mass energy is well below the resonance at the W mass, is proportional to the center-of-mass energy. We expect low energy neutrino cross-sections to grow like the center-of-mass energy. This behavior is observed for the total cross-sections. We will say more about that later.

We will also mention differential cross-sections. Let's start with elastic point-like scattering. The paradigm for that is Rutherford scattering of electrons. Diagrammatically and dimensionally there is only the one scale which in this case, is the four momentum transfer t. Notice that if you turn the annihilation graph (Fig. A.5.b) on its side it is topologically the same graph so this is not a surprising statement. We expect that $d\sigma/\mathrm{dt}$ should be proportional to $\frac{\alpha^2}{t^2}$. The exact expression is given in Eq. A.19.d. One can also get that expression by realizing that the interaction energy is the Coulomb energy. In this case the scattering amplitude is the Fourier transform of the interaction energy which is $\frac{\alpha}{t}$. Therefore the square of the amplitude for this process is $\frac{\alpha^2}{t^2}$. This is familiar from Rutherford scattering. For extended objects, such as electron-proton scattering one has an elastic-proton form factor. It measures the faster fall-off with momentum transfer that one sees from an extended object with respect to point-like objects.

For inelastic-electromagnetic scattering one can see from looking at Fig. A.5 that this is very similar to elastic scattering. However, there is a new variable which is the fraction of the momentum carried by the quark or the x value that we talked about previously.

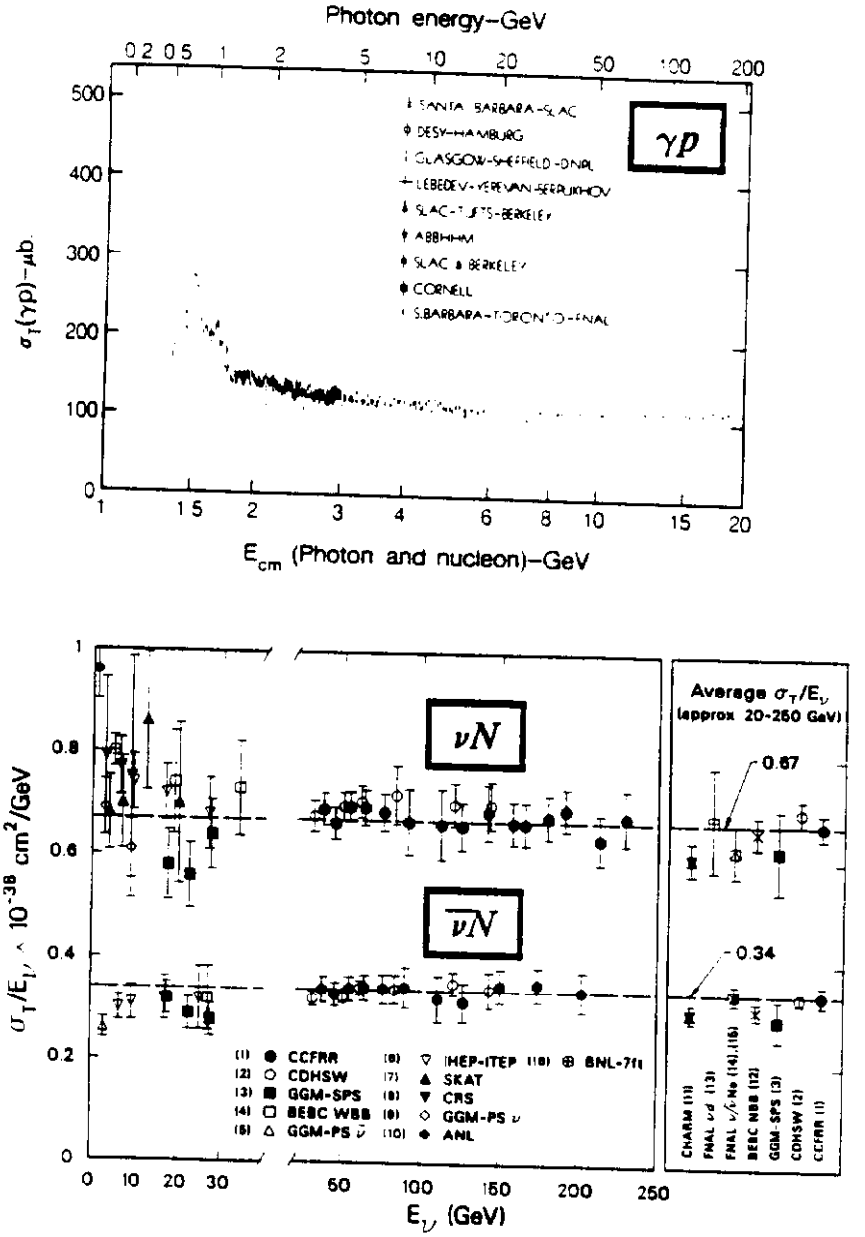

Fig. A.6: Compilation of total cross-sections for γp, νN, and $\bar{\nu}N$.

The doubly differential cross-section with this new variable and the momentum transfer is essentially the Rutherford scattering cross-section times the source function for quarks in the proton with that x value plus some other terms which are more complicated. The point is that this is just elastic scattering of point-like fermions with a source distribution.

For deep inelastic-neutrino scattering, one can appeal to electromagnetic scattering and

change the propagator and the coupling constant. One can then relate the coupling constant to the Fermi constant and obtain a completely analogous expression in the case of inelastic-neutrino scattering. However, in this case, at low energies, the propagator effect is very small as opposed to the situation in electromagnetism where you always have a factor $1/t^2$ in the cross-section. The differential cross-section becomes rather simple.

Again, the total cross-section increases linearly with the center-of-mass energy. It looks like the total neutrino-electron scattering except there is a source distribution for partons with the momentum fraction x. Integrating over t, since the upper limit on t is s, we get a cross-section which increases with s. We know the x range of the source function, integrating over all x, will just give us a number which leads us to believe that the neutrino nucleon total cross-section is just proportional to the Fermi constant squared and the center-of-mass energy. Data at low energies have been compiled and are presented in Fig. A.6. An estimate of the slope of the rise of the neutrino cross-section with s is given in Eq. A.20. It is gratifying to note that this estimate is within the ballpark of the data.

$$\begin{aligned} d^2\sigma/dtdx &\rightarrow \frac{G^2}{2\pi}\left\{[F_1(x)]\,(E' - E/E)^2 + - - -\right\} \\ d\sigma(\nu N)/dx &\sim \frac{G^2}{2\pi} s\,[F_1(x)] \\ \sigma(\nu N) &\sim G^2 s/\pi \qquad . \qquad \text{(A.20)} \\ \sigma(\nu N)/E_\nu &\sim 2G^2 M_N/\pi \\ &= 3.7 \times 10^{-38} cm^2/GeV \end{aligned}$$

Having built up a feeling for the coupling constants, the dynamics, and the kinematics with a few examples we can now go on to examine weak, electromagnetic, and strong decays of the hadronic systems that we studied in the first Section.

B. Weak Decays of Gauge Bosons, Leptons, & Hadrons

We are now armed with the coupling constants and phase space. Our goal is to explain, in this Section, the various weak decay rates and decay branching ratios of all of the particles. In the first Section, we tried to find a simple explanation for the quantum numbers and masses of the various composite hadrons in terms of the quark-quantum numbers. We were reasonably successful. Now we want to look at, for example in Fig. B.1, the lifetime and the decay modes of all the particles. We start with the gauge bosons since they have the simplest decays. We have already looked at the gauge boson couplings in the previous Section.

Particle	$I^G(J^{PC})$ [a]	Mass [b] (MeV)	Mean life [b] τ (sec) $c\tau$ (cm)	Partial decay modes: Mode	Fraction [b]		p (MeV/c) [c]
GAUGE BOSONS							
γ	$0,1(1^{--})$	$(< 3\times10^{-33})$	—	stable			
W	$J=1$	81.8 ± 1.5 GeV	$\Gamma<6.5$ GeV	$e\nu$	seen		40.9 GeV/c
				$\mu\nu$	seen		40.9
Z		92.6 ± 1.7 GeV	$\Gamma<4.6$ GeV	e^+e^-	seen		46.3 GeV/c
				$\mu^+\mu^-$	seen		46.3
LEPTONS							
ν_e	$J=\frac{1}{2}$	< 46 eV [d]	stable $[\tau > 3\times10^8 m_{\nu_e}$ sec (m_{ν_e} in MeV)]	stable			
e	$J=\frac{1}{2}$	0.5110034 ± 0.0000014 MeV	stable (> 2×10^{22} years)	stable			
ν_μ	$J=\frac{1}{2}$	< 0.25	stable $[\tau > 1.1\times10^5 m_{\nu_\mu}$ sec (m_{ν_μ} in MeV)]	stable			
			μ^- — (or μ^+ →chg. conj.)				
μ	$J=\frac{1}{2}$	105.65916 ± 0.00030 S=1.1[e]	2.19703×10^{-6} ± 0.00004	$e^-\bar{\nu}\nu$	(100)%		53
				†[$e^-\bar{\nu}\nu\gamma$	[e](1.4 ± 0.4)%		53
				$e^-\nu_e\bar{\nu}_\mu$	(<5)%]	LF	53
			$c\tau=6.5865\times10^4$	$e^-\bar{\nu}e^+e^-$	[e](3.4 ± 0.4)$\times10^{-5}$		53
				$e^-\gamma$	(<1.7)$\times10^{-10}$	LF	53
				$e^-e^+e^-$	(<2.4)$\times10^{-12}$	LF	53
				$e^-\gamma\gamma$	(<8.4)$\times10^{-9}$	LF	53

Fig. B.1: Table of particle properties for gauge bosons and first two lepton generations.

Let's start with the gauge bosons. The photon is the electromagnetic-gauge boson. We know that it is stable to the limit of our measurements. What about the electroweak gauge bosons, the W and the Z? We know that they couple with leptons through the weak coupling

constant which is of the same order of the electromagnetic coupling constant α. Therefore, we expect that first order weak transitions cause the decays of the W and the Z's into leptons and hadrons. The coupling scheme for the W and Z is shown in Fig. B.2. The charged W makes a charged current transition to all leptons pairs and all quark pairs which are allowed. We will discuss what allowed means later. We will assume that there is a universal coupling for all allowed charged pairs. The only proviso is that we need to count each color separately, so there is a factor of three for the three colors of the quarks relative to leptons.

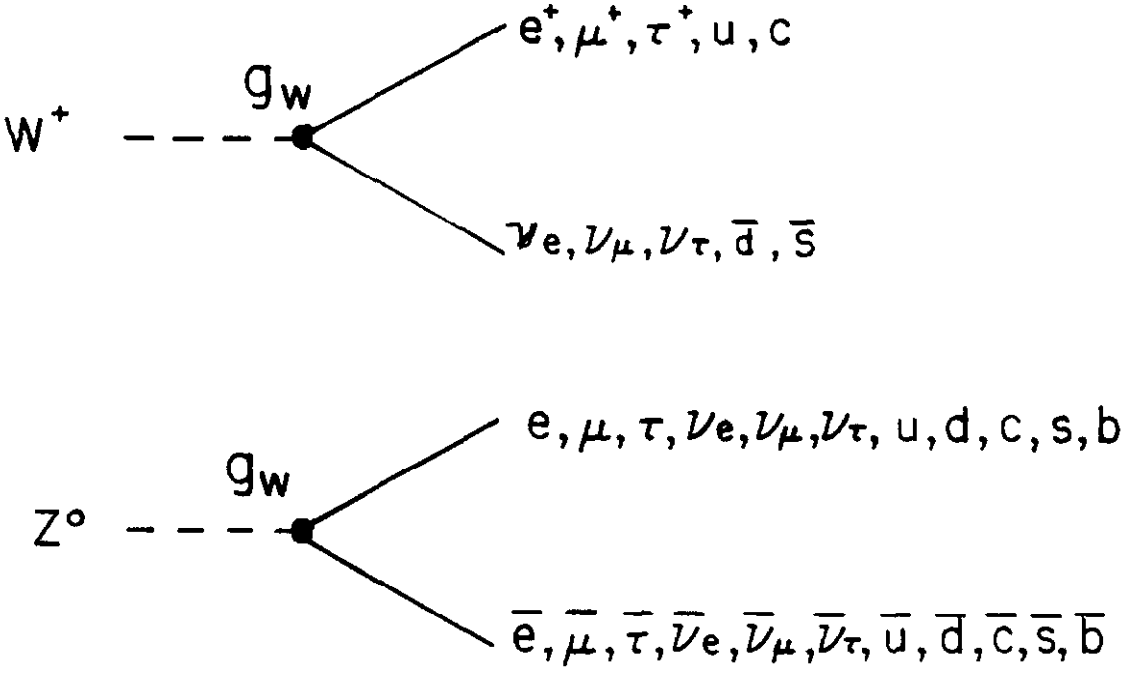

Fig. B.2: Coupling scheme for decays of W and Z mesons.

Dimensional arguments lead us to expect that the widths are proportional to g_W^2 and the mass of the parent. That is familiar from our discussion of phase-space. Electroweak unification means that α_W is some multiple of α. Hence, by dimensional arguments, an estimate of the width is shown in Eq. B.1:

$$\Gamma_W \sim g_W^2 M_W \sim \alpha M_W \ . \tag{B.1}$$

You recall from our discussion in Section A that knowing the Weinberg angle one can predict the W mass from the Fermi coupling constant. This mass turns out to be about 100 GeV

and that means that the W width is about 1 GeV. Note that this is a "weak" transition. However, we are at a mass where, by definition, the weak and electromagnetic strengths are comparable. For lower mass objects we expect to have a much narrower width for weak decays. As regards branching ratios, under the universality assumption, we just have to count final states weighted by the color factor. This ansatz leads to the branching ratio shown in Eq. B.2:

$$\begin{aligned} B(W \to \mu\nu) &\simeq 1/9 \\ B(Z \to \mu\mu) &\simeq 1/21 \end{aligned} \qquad \text{(B.2)}$$

These predictions for the masses and widths of the electroweak bosons have been spectacularly confirmed in the last few years at hadron colliders.

Now let's turn to lepton decays. We will assume the neutrinos to be massless and absolutely stable. In fact, there are only limits to the mass of the neutrinos. The electron is the lightest lepton and we assume that it is stable. The lightest non-trivial decay to consider is that of the μ lepton. The decay diagram for μ decay is shown in Fig. B.3.a. Obviously the way to make this decay is to take the W decay diagram that we have already talked about and sandwich it with lepton pairs on both ends. This means that lepton decays are second order in the weak interaction. Therefore, we expect the decay rates to be very reduced because the masses are light and Γ is proportional to α^2. Finally there is an enormous suppression factor due to the fact that the masses of leptons are light and therefore the intermediate W propagator factor will be tiny.

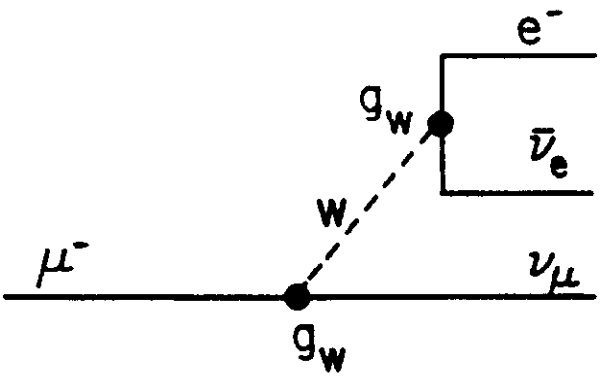

Fig. B.3.a: Decay diagram for μ decay.

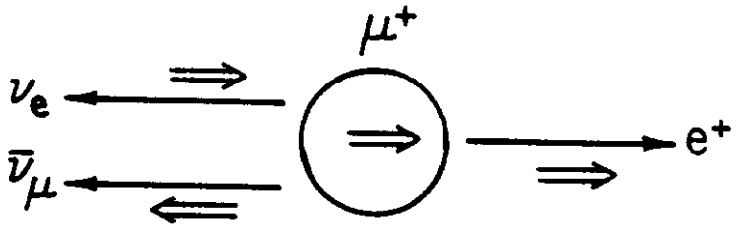

Fig. B.3.b: Helicity factors in μ decay.

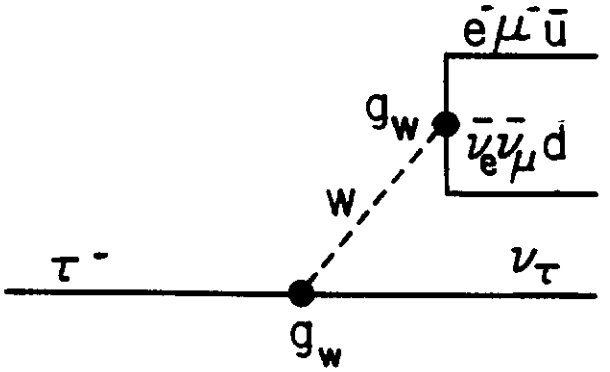

Fig. B.3.c: Decay diagram for τ decay.

Let's work this out in a little detail because it is very instructive. The current and differential decay rate are given in Eq. B.3:

$$\begin{aligned} G &= 1.2 \times 10^{-5}\ GeV^{-2} \\ J_\mu &\sim \ell\gamma_\mu(1-\gamma_5)\nu \\ d\Gamma &\sim \left(\frac{d\vec{p}_e}{E_e}\right)\left[\frac{1}{M_\mu}\right]\left\{G^2 M_\mu^4\left[x(3-2x)\right]\right\} \\ x &= p_e^*/(M_\mu/2),\ 0<x<1 \end{aligned} \tag{B.3}$$

We assume V-A coupling in the current. The differential width integrated over everything but the electron momentum is as given in Eq. B.3. The phase space factors are outside the parenthesis. Inside the parenthesis we have dynamical factors relating to the fact that we have a 4 point fermion coupling. This coupling gives us the M_μ^4. The V-A structure within

that 4 fermion coupling, in other words the Lorentz structure, is responsible for the factor x(3-2x). The reason for that factor is that the V-A theory imposes an helicity structure on the fermions. That structure is shown in Fig. B.3.b. The electron prefers to recoil against the 2 neutrinos, which means the electron will be fast, which is the x factor. If we now integrate over all possible electron momenta we find that the width is dimensionally proportional to the fermi constant squared times the parent mass to the 5th power.

Another way to see this dependence is to argue that since it is a second order process it should go like α^2 times phase space. Hence the width will be proportional to the mass and the propagator W for the available q value, the propagator squared is just $(M_\mu/M_W)^4$:

$$\begin{aligned} d\Gamma &\sim 4\pi p_e dp_e G^2 M_\mu^3 [x(3-2x)] \\ &\sim G^2 M_\mu^5 x^2(3-2x)dx \\ \Gamma &\sim G^2 M_\mu^5 \sim \left[\alpha_W (\frac{M_\mu}{M_W})^2\right]^2 M_\mu \end{aligned} \quad . \tag{B.4}$$

If there were no dynamics (that means if the factor in parenthesis in Eq. B.3 were just one), we would have the result shown in Eq. B.5. The width is just proportional to the mass:

$$\begin{aligned} d\Gamma &\sim \left(\frac{d\vec{p}_e}{E_e}\right)\frac{1}{M_\mu} \sim M_\mu x dx \\ \Gamma &\sim M_\mu \end{aligned} \quad . \tag{B.5}$$

Finally, how does this work? The observed lifetime is 3 x 10^{-19} GeV. That is because, in fact, the dimensional argument is true but there is an enormous numerical factor. If one does the numerical factor correctly we get the right value for the muon lifetime which is 2.2 microseconds:

$$\begin{aligned} \Gamma_\mu^{obs} &\stackrel{?}{=} 3 \times 10^{-19}\ GeV \\ \Gamma_\mu &= \frac{G^2 M_\mu^5}{192\pi^3},\ G^2 M_\mu^5 \sim 1.9 \times 10^{-15}\ GeV \end{aligned} \quad . \tag{B.6}$$

So in fact, the calculation of the muon lifetime works nicely.

What happens when we go to the next generation, the τ lepton? Are succeeding generations of leptons fundamentally different? The diagrammatic representation of that decay

is shown in Fig. B.3.c. In this case, since the τ is heavier it can decay into lepton pairs containing electrons, muons, and quarks. That means that we expect the branching ratio into electron and 2 neutrinos to be a fifth. This is very close to the observed branching fraction:

$$B(\tau \to e\bar{\nu}\nu) \simeq \frac{1}{5} \stackrel{?}{=} 0.17 \ . \tag{B.7}$$

One can easily scale the lifetime by observing that formally the τ decay is exactly the same as what we just did for the muon decay except that the parent mass is heavier. We would scale by the 5th power of the parent mass. The resultant decay width times branching ratio for the τ is exceedingly close to the observed value. Just as a reminder, this is an extrapolation over six orders of magnitude in decay width. Since it works out we can have some confidence that we understand the dynamics:

$$\Gamma(\tau \to e\bar{\nu}\nu) \simeq \Gamma_\mu \left(\frac{M_\tau}{M_\mu}\right)^5 = 3.4 \times 10^{-13}\ GeV \stackrel{?}{=} 4.2 \times 10^{-13} GeV \ . \tag{B.8}$$

The successes of these estimates lead us to believe that we understand the weak decays of gauge bosons and leptons. Flushed with this success, we want to begin to look at the weak decays of hadrons. In order to do that, first we have to understand the weak transitions between quarks. Observationally there are some rules which are obeyed in weak transitions:

$$\begin{aligned} \frac{\Gamma(K^0 \to \pi^+\pi^-)}{\Gamma(K^+ \to \pi^+\pi^0)} \sim 500, \quad & \Delta I = \frac{1}{2} \\ \Sigma^+ \not\to n e^+ \nu, \quad & \Delta S = \Delta Q \\ & \text{No Flavor Changing} \\ B(K_L^0 \to \mu^+\mu^-) = 9 \times 10^{-9} \quad & \text{Neutral Currents} \end{aligned} \ . \tag{B.9}$$

Experimentally, there is the $\Delta I = 1/2$ rule, which is seen in K decays, the $\Delta S = \Delta Q$ rule, and the absence of flavor changing neutral currents. We can begin to incorporate these rules by performing a Cabibbo rotation of the down and strange quarks by an angle θ_c. We identify the charged transitions with the SU(3) generators for I spin and V spin ladder operators. In this situation, the neutral currents which would occur between say $\bar{d}$ and $\bar{s}$ are cancelled by the existence of the charm quark. This is called the GIM mechanism and, in fact, the charm

quark was predicted in order to cancel flavor changing neutral currents. The currents are shown diagrammatically in Fig. B.4.

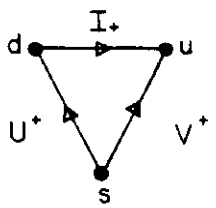

$$I^{\pm} \qquad V^{\pm}$$

$$J_h \sim \cos\theta_c \ (u\bar{d}) + \sin\theta_c \ (u\bar{s})$$

$$\begin{bmatrix} d' \\ s' \end{bmatrix} \equiv \begin{bmatrix} \cos\theta_c & \sin\theta_c \\ -\sin\theta_c & \cos\theta_c \end{bmatrix} \begin{bmatrix} d \\ s \end{bmatrix}$$

$$J_h \sim \cos\theta_c \ (u\bar{d} + c\bar{s}) + \sin\theta_c \ (u\bar{s} - c\bar{d})$$

$$J_h^{\circ} \sim u\bar{u} + c\bar{c} - d\bar{d} - s\bar{s}$$

Fig. B.4: SU(3) Generators for quark transitions. Quark weak current with Cabibbo rotations.

We have built in a mixing for the quark-weak transitions such that the strong eigenstates (quarks) are not the eigenstates which participate in the weak interactions. They are rotated by the Cabibbo angle. This is an arbitrary angle whose value we will have to determine. Writing the charged currents as SU(3) generators or in terms of fundamental quarks we build in $\Delta I = 1$ and $\Delta I = 1/2$ by using the I and V spin SU(3) generators. It is also fairly easy to see that we built in the $\Delta S = \Delta Q$ rule and that the flavor changing neutral currents are cancelled by the existence of the charm quark.

With these preliminaries out of the way let's look at charged pion decay. The quark diagrams and helicity structure for quark decays are shown in Fig. B.5. The helicity structure

implied by V-A means that leptons are left-handed and anti-leptons are right-handed if they are relativistic:

$$\begin{aligned} < \vec{\sigma} \cdot \vec{p} > &= \pm \beta \\ \pi &\not\to e\nu \end{aligned} \tag{B.10}$$

A glance at Fig. B.5 shows that the πs do not decay into electrons even though they have the larger phase space because this decay is helicity unfavored. Phase space also enormously disfavors $\pi^+ \to \pi^0 e^+ \nu$.

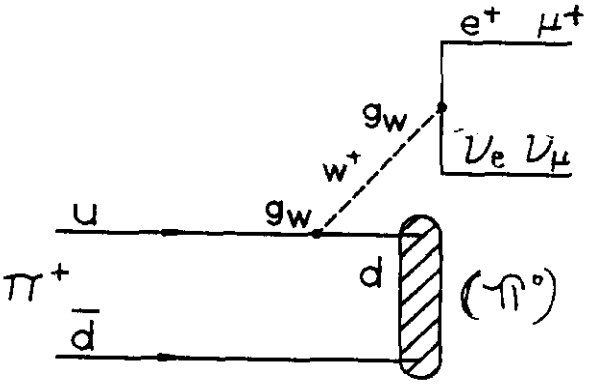

Fig. B.5.a: Quark diagram for π decay.

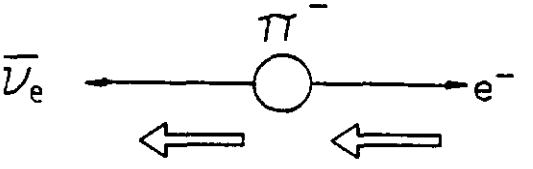

Fig. B.5.b: Helicity in π decay.

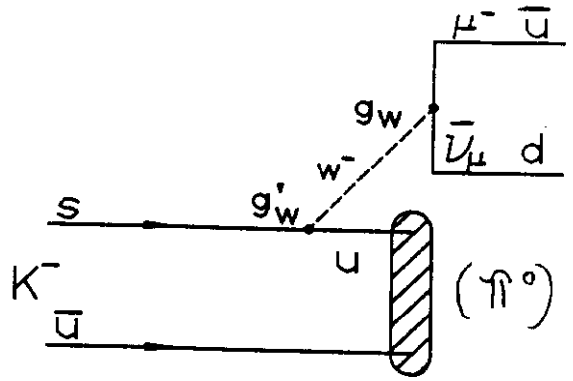

Fig. B.5.c: Quark diagram for K decay.

What about the π to $\mu + \nu$ decay? We attempt to scale the muon lifetime. Phase space scales as β^*. The propagator dynamics gives you a mass to the 4th power. Assuming the d is merely a spectator and somehow annihilates with the $\bar{d}$ with unity probability, we scale as in Eq. B.11:

$$\begin{aligned} \Gamma_\pi^{obs} &= 2.5 \times 10^{-17}\ GeV \\ \Gamma_\pi &\sim \Gamma_\mu \left[p_\pi^*/(M_\mu/2)\right] \left[\frac{m}{M_\mu}\right]^4, m = 300\ MeV \quad . \\ &\sim 1.1 \times 10^{-17}\ GeV \end{aligned} \tag{B.11}$$

In fact, this rough attempt at scaling turns out to be reasonably successful for the absolute decay rate. We also saw that the branching fractions could be explained entirely by helicity arguments and a V-A weak interaction theory.

Let's now try to estimate decays for charged kaons. The quark diagrams for this are shown in Fig. B.5. The strange quark is heavy and that means that the kaon can decay to $\mu\nu$ or quark anti-quark pairs. As with a charged pion, the electron is helicity disfavored. Ignoring the $u\bar{u}$ annihilation or continued propagation as a π^0, we expect and observe branching ratios as shown below:

$$\begin{array}{lcccl} B(K^- \rightarrow \mu^- \bar{\nu}) & & 1/4 & \stackrel{?}{=} & 0.63 \\ B(K^- \rightarrow \pi^- \pi^0) & = & 3/4 & & 0.21 \end{array} \quad . \tag{B.12}$$

These are certainly of the same order of magnitude but one obviously cannot claim any great success for the branching ratio argument. Remembering that the strange quark is Cabibbo mixed and unfavored for transition, we can estimate what the K leptonic rate is. For this we compare π and K decays as in Fig. B.5 and the equations below:

$$\begin{aligned} g'_W &\equiv g_W \tan\theta_c \\ \frac{\Gamma(K \to \mu\nu)}{\Gamma(\pi \to \mu\nu)} &\sim \tan^2\theta_c \left(\frac{p^*_K}{p^*_\pi}\right)(\gamma)^4\,,\ m_s = 500\ MeV \\ \Gamma_K^{obs} &= 3.4 \times 10^{-17}\ GeV \\ \theta_c &\sim 0.14(0.41 \text{ if no } \gamma \text{ factor}) \\ \tan\theta_c^{obs} &= 0.22 \end{aligned} \qquad \text{(B.13)}$$

Using the observed value of the leptonic width for the kaons we get an estimator (as we explain later) for the Cabibbo angle which is small. In fact, the exact result is within a factor of 2 of this estimate. This means that the favored transition is $u \to d$ whereas the unfavored transition, i.e., that with the $\sin\theta_c$ weight is $u \to s$. Another estimate of the Cabibbo angle can be had by comparing the semi-leptonic decay widths for $\pi^- \to \pi^0 e\bar{\nu}$ and $K^- \to \pi^0 e\bar{\nu}$. Although it is sketched in Fig. B.5 we did not discuss it since it is a very rare decay due to the small q value.

The neutral kaon system is rather more complicated but, of course, it is much richer. The K^0 and $\bar{K}^0$ strong eigenstates are not going to be the weak eigenstates. They mix due to the weak interactions, into what are approximately CP eigenstates the K_S and K_L. The mixing is via two $\Delta S = 1$ transitions. I am going to assume that we have a nodding acquaintance with the "classical" phenomena of kaon decay, CP violation, regeneration, and the like and concentrate on the box diagrams. They are more topical and are directly related to similar diagrams for b decays.

In both these systems you have a neutral system with a strong quantum number. There is a flavor which is different for the particle and anti-particle. However, they can mix through two sequential weak interactions. The quark diagrams are given in Fig. B.6. A rough estimate of the K_L decay width is given in Eq. B.14. Note that in three body semi-leptonic decays the helicity suppression of $e\nu$ is not operative. We scale Γ_π using Eq. B.11, Fig. B.5.a., and Fig. B.6.a:

$$
\begin{aligned}
a)\quad \Gamma^{obs}_{K_s} &= 7.4 \times 10^{-15}\ GeV \\
\Gamma^{obs}_{K_L} &= \Gamma_{K_S}/580 = 1.27 \times 10^{-17}\ GeV \\
\Gamma_K &\stackrel{?}{=} 5\Gamma_\pi\,[(M_K/2))/P^*_\pi]\,(\gamma)^4\theta_c^2 \\
&\stackrel{?}{=} 2.6 \times 10^{-16}\ GeV\ ,
\end{aligned}
\qquad \text{(B.14)}
$$

$$
\begin{aligned}
b)\qquad B(K_L \to \pi\mu\nu) &\quad 1/5 \quad 0.22 \\
B(K_L \to \pi e\nu) &= 1/5 \stackrel{?}{=} 0.39 \\
B(K_L \to 3\pi) &\quad 3/5 \quad 0.34\ .
\end{aligned}
$$

The factor 5 has to do with the fact that there are now five possible virtual W decays all with equal branching ratios and universal coupling. The mass to the 4th and Cabibbo angle factors are familiar from charged K decay. This estimate turns out to be fairly poor. The K_L meson lifetime is about 600 times longer than the K_S due to the fact that 2π decays are not accessible to the K_L if CP is a good quantum number. The relevant branching ratios are also given in Eq. B.14. We guess roughly 1/5 for each semi-leptonic decay and 3/5 for the non-leptonic decay. The observed ratios are at best within the right order-of-magnitude. For K_S, $B(K_S \to \pi\pi) \sim 1$ which is inexplicable at our level of discussion. This non-leptonic enhancement is still poorly understood.

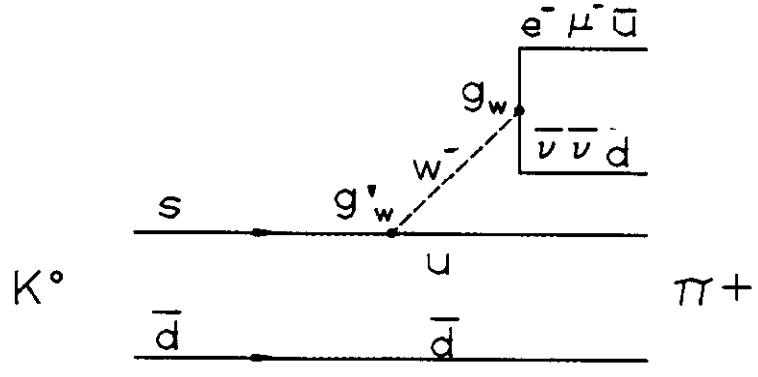

Fig. B.6.a: Quark diagram for $\bar{K}^0$ decay.

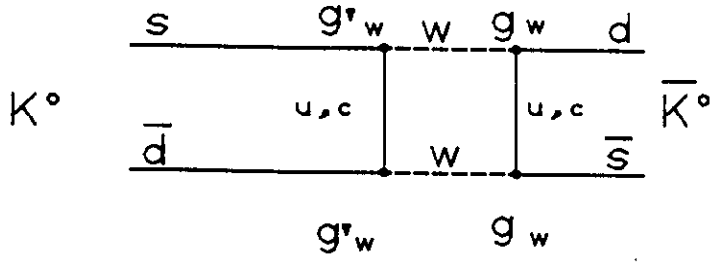

Fig. B.6.b: Box diagram for $K^0 - \bar{K}^0$ mixing.

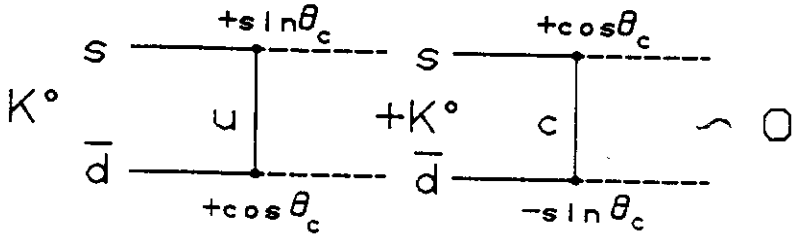

Fig. B.6.c: Suppression mechanism for $K^0\bar{K}^0$ mixing and flavor changing neutral current.

If we look at the box diagram for $K^0 - \bar{K}^0$ mixing and compare it to the decay diagram, it is easy to convince oneself that the mixing is comparable to the decay width:

$$\begin{aligned} A_{box} &\sim g_W^4 \sin^2\theta_c \\ A_{decay} &\sim g_W^2 \sin\theta_c \\ \Delta M &= M_{K_S} - M_{K_L} \sim \Gamma_{K_S} \\ \Delta M/\Gamma_{K_S} &\equiv x_{K_S} = 0.46 \end{aligned} \quad . \tag{B.15}$$

Since it is the weak interactions which cause the splitting of masses between the strong eigenstates, we expect the mass difference to be comparable to the K_S decay width and, indeed it is. In fact, the box diagram without the charm quark gives too large a $K_L - K_S$ mass splitting. As shown in Fig. B.6.c. it is the relative sign in the charged current (see Fig. B.4) between the up and the charm quark which causes a cancellation in the $K_L - K_S$ mass difference. Clearly that cancellation fails to the extent that the up and the charmed quarks have different masses and hence that their propagators behave differently.

$$\begin{aligned} A_{box} &\sim g_W^4 m^2 (1-\gamma_c)^2 (\sin\theta_c \cos\theta_c)^2 \\ &\sim [G \sin\theta_c \cos\theta_c m(1-\gamma_c)]^2 \end{aligned} \quad . \tag{B.16}$$

In principle the $K^0 - \bar{K}^0$ box diagram "predicts" the CP violating parameters in K decay. However, this is only true at the quark level. At the hadron level "chemistry" rears its ugly head. In any case, ϵ' has yet to be measured definitively. At Fermilab, E-731 is attempting such a measurement.

Historically, when charm was predicted to kill flavor changing neutral currents there was an upper limit put on the charm mass such that one would have the observed $K_S - K_L$ mass difference. If the charmed mass were too large then the GIM mechanism cancellation would be ruined by the difference in propagators and we would have too big a $K_S - K_L$ mass difference. What is amazing is that the numerical prediction for the charm quark mass turned out to be very good.

Now let's look at charmed meson decays. What we will do is merely scale up the results for semi-leptonic and non-leptonic K decays. In this case, the Cabibbo favored transition is $c \to s + W$:

$$
\begin{aligned}
a) \qquad W^- &\rightarrow e^-\bar{\nu}_e + \mu^-\bar{\nu}_\mu + 3\bar{u}d \\
\tfrac{B(D^+\rightarrow e^+)}{B(D^+\rightarrow K)} &= \tfrac{1/5}{3/5} \stackrel{?}{=} \tfrac{0.18}{0.64}, \\
\\
b) \quad \Gamma^{obs}(D^+ \rightarrow e^+) &= 2.6\times 10^{-13}\ GeV \stackrel{?}{=} (\gamma_c)^5\Gamma_{\pi+} = 7.8\times 10^{-14}\ GeV \\
m_c &= 1500\ MeV, \\
\\
c) \qquad \Gamma_{D+} & \quad 7.2 \quad c\bar{d} \\
\Gamma_{D^0} &= 15\times 10^{-13}\ GeV, \quad c\bar{u} \\
\Gamma_{F+} & \quad 23 \quad c\bar{s}.
\end{aligned}
\tag{B.17}
$$

We expect the branching ratio into electrons to be 1/5 and into hadrons (that means kaons plus some number of pions) to be 60%. For charged Ds these branching ratios are close to what is observed. As far as lifetime goes, we take the pion lifetime and scale by the quark mass to the 5th power. This result turns out to be within an order-of-magnitude which is an acceptable validation. Other charmed mesons, the D^0 and F^+ have lifetimes which are comparable to the D^+. There are details of factors of two and three. However, for the purposes of these rough "back of the envelope" estimates we can say that all of the lifetimes are the same and indicate the same underlying $c \rightarrow s + W$ transition.

Moving up the generations we expect no surprises, just as in going from μ to τ. For b decays, the basic quark transition is $b \rightarrow c + W$. The other quark in the b meson is assumed to be just a spectator. For b decays, the scaling is very similar to that for c decays. In this case, we have a new Cabibbo allowed pair which is kinematically available, the $\bar{c}s$ pair, but otherwise, the arguments go the same as in Eq. B.17.

$$
\begin{aligned}
a) \qquad W^- &\rightarrow e^-\bar{\nu}_e + \mu^-\bar{\nu}_\mu + \tau^-\bar{\nu}_\tau + 3(\bar{u}d + \bar{c}s) \\
\\
\tfrac{B(B\rightarrow e)}{B(B\rightarrow D)} &\simeq \tfrac{1/9}{1} \stackrel{?}{=} \tfrac{0.12}{0.80}, \\
\\
b) \qquad \Gamma_B &\sim \left(\tfrac{m_b}{m_c}\right)^5 \Gamma_D \\
4.7\times 10^{-13}\ GeV &\stackrel{?}{=} 6.2\times 10^{-10}\ GeV \\
\theta_b &\sim 0.03 \sim \theta_c^2\ .
\end{aligned}
\tag{B.18}
$$

The branching ratios are 9 to 1 and the underlying quark transition is $b \rightarrow W + c$. That certainly agrees with the observed branching ratios. However, when we do lifetime scaling we find a very large suppression. This means there is another angle for b decays; they are much longer lived than we expect. That angle is comparable to the square of the Cabibbo angle.

We don't know why the suppression exists and mapping out the elements of the complete mixing of the strong eigenstates into the weak eigenstates is a project which will occupy us for some time. The mixing matrix has many of its elements as yet only poorly determined.

So far we have discussed the non-leptonic and some of the leptonic decays of πs, Ks, Ds, and Bs. What about the purely leptonic decays which we have already looked at for the πs and Ks? The underlying quark diagram for such decays is shown in Fig. B.7. For pions the annihilation of the quark and anti-quark into W is Cabibbo favored whereas for Ks and Ds it is disfavored. In this case, there are strong interaction effects. We parameterize them as shown in Fig. B.7 with a phenomenological decay constant for the pseudoscalar. The leptonic piece is pointlike and we can treat it as such. The purely leptonic decay width is second order and goes like G^2. We take the Cabibbo factors into account and scale the phenomenological decay constant to the muon mass. The M_μ^2 factor is the helicity disfavored factor due to the V-A dynamics (see Eq. B.10). Overall the width is proportional to the pseudoscalar mass but that is just phase space. Using pion decays, we can find the decay constant, which is 138 MeV. The result (see Eq. B.13) for $K \to \mu\nu$ is $f_K \simeq f_\pi$. Emboldened by these results we assume flavor symmetry. Then all the decay constants are the same. Then it is easy to see from Fig. B.7 that the b leptonic decay rate goes like the mass of the parent.

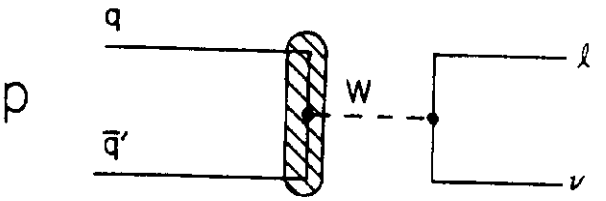

$$A \sim \frac{G}{\sqrt{2}} \langle 0|J_\mu^h|h\rangle \left[\bar{u}_\ell \gamma_\mu (1-\gamma_5) u_\nu\right]$$

$$\sim \frac{G}{\sqrt{2}} f_p\, q^\mu \begin{pmatrix} \sin\theta_c \\ \cos\theta_c \end{pmatrix} \left[\bar{u}_\ell \gamma_\mu (1-\gamma_5) u_\nu\right]$$

$$\Gamma \sim \left[\frac{G^2}{8\pi} f_p^2 \begin{pmatrix} \sin^2\theta_c \\ \cos^2\theta_c \end{pmatrix} M_\mu^2\right] M_p$$

Fig. B.7: Quark diagram for pseudoscalar meson leptonic decays.

$$
\begin{aligned}
f_\pi &= 138\ MeV \sim f_K \\
\frac{\Gamma(D^+ \to \mu^+ + \nu)}{\Gamma(K^+ \to \mu^+ + \nu)} &= \frac{M_D}{M_K}
\end{aligned}
\qquad \text{(B.19)}
$$

This is basically just two-body phase space. Since the non-leptonic and semi-leptonic rates scale as the 5th power of the mass, we expect that heavier flavors will have much reduced purely leptonic branching ratios. In fact, for charged D mesons there is only a 2% leptonic branching ratio upper limit. Purely leptonic D decays have yet to be observed.

Now a word about the neutral heavy flavored states. The strong eigenstates do not govern weak decay and are not the eigenstates of the weak decay. We have already seen how in the case of the neutral kaons the mass difference and decay width are comparable. The box diagram is such that we can make a statement about the charm-quark mass. There is a similar situation for Ds where in the box diagram connecting D^0 and $\bar{D}^0$ we have intermediate states with the b quark. The mixing box diagram is proportional to the b quark analog of the Cabibbo angle squared. Similarly for b quarks themselves, the b and $\bar{b}$ box diagram has intermediate top-quark states with their own analagous Cabibbo angle. The same arguments relating decay diagram and box diagrams lead us to believe that all the neutral heavy flavor particles will have weak mass differences comparable to their decay amplitudes. That means there will be mixing between the strong eigenstates in all the systems. This mixing for the b system means that if CP violation is small (as it is for the kaon system) and if one begins with a strong eigenstate at time zero (in other words, prepared by the strong interactions), as time evolves this state will become a mixture of B and $\bar{B}$s with the time evolution governed by the weak eigenstates. Assuming that the lifetimes for the weak eigenstates are very comparable, then the time evolution into charged leptons is shown below:

$$
\begin{aligned}
x &= \Delta M_B/\Gamma_B \\
\Gamma(B \to \ell^+) &\sim e^{-\Gamma t}[1 + \cos(\Delta M t)] \sim \Gamma(\bar{B} \to \ell^-) \\
\Gamma(B \to \ell^-) &\sim e^{-\Gamma t}[1 - \cos(\Delta M t)] \sim \Gamma(\bar{B} \to \ell^+) \\
\frac{B\bar{B} \to \ell^\pm \ell^\pm}{B\bar{B} \to \ell^+ \ell^-} &= x^2/(2 + x^2)
\end{aligned}
\qquad \text{(B.20)}
$$

At time zero we have a system decaying only into, say, positive leptons. As the system evolves with time we begin to get Bs decaying into negative leptons. This means that an

initial $B\bar{B}$ state integrated over all times will give us same sign di-leptons as shown in Eq. B.20. If one prepares $B\bar{B}$ pairs via the strong interactions and measures the like sign di-leptons, one can extract the mixing parameter. Recently there have been results from both UA1 and Argus that tell us that the mixing parameter for Bs is substantial:

$$\begin{aligned} \frac{\Delta M}{\Gamma} &\sim 0.03(m_t/40\ GeV)^2,\ x \sim 0.2\ to\ 0.4 \\ m_t &\gtrsim 100\ GeV \end{aligned} \quad . \tag{B.21}$$

Note that, the top quark is heavier than about 40 GeV. If it is heavier than M_W, then toponium spectroscopy will be wiped out by $t \to b + W$ decays. In that case, the rich spectroscopy of $t\bar{t}$ states will be killed by weak decays and the $q\bar{q}$ potential shown in Fig. D.7 of Section I will be hard to observe.

In fact, the mixing parameter is very comparable to that for the neutral kaon system. Since the box diagram is completely analagous to what we have discussed for the K_S, the fact that the mixing is large tells us that the top quark mass is fairly heavy. In fact, it looks as if Z^0 gauge bosons cannot decay into top pairs, as we have assumed previously.

Beyond mixing, there is also the possibility of observing CP violation in the $B^0\bar{B}^0$ system. Exactly as one does in the $K^0\bar{K}^0$ system, one writes the weak eigenstates. They are not, just as the K_S and K_L are not, CP eigenstates:

$$B_{\frac{1}{2}} \sim (1+\epsilon)B^0 \pm (1-\epsilon)\bar{B}^0 \quad . \tag{B.22}$$

If the same final state is accessible to both B and $\bar{B}$ and is a CP eigenstate, then the decay rate for B and $\bar{B}$ into that final state is given below:

$$\begin{aligned} \Gamma(B \to f) &\sim e^{-\Gamma t}\left[1 - \sin(\Delta M t) Im\left(\frac{1-\epsilon}{1+\epsilon}\right)\rho_f\right] \\ \Gamma(\bar{B} \to f) &\sim e^{-\Gamma t}\left[1 + \sin(\Delta M t) Im\left(\frac{1-\epsilon}{1+\epsilon}\right)\rho_f\right] \\ \rho_f &= A(\bar{B} \to f)/A(B \to f) \sim 1 \\ \frac{(\Gamma_B - \Gamma_{\bar{B}})}{(\Gamma_B + \Gamma_{\bar{B}})} &\sim x Im\left(\frac{1-\epsilon}{1+\epsilon}\right)\rho_f \end{aligned} \quad . \tag{B.23}$$

These equations are very much like the equations for K_S and K_L decays into a common accessible final state of 2 pions. The asymmetry between B and $\bar{B}$ integrated over all times

is proportional to the mixing parameter and the CP violating parameter ϵ. Recall that in the neutral-kaon system the CP violating parameter ϵ is 2×10^{-3}. So far this is the only example of CP violation that we have measured.

Clearly the ψK_s system is accessible to both B^0 and $\bar{B}^0$ as we see in Fig. B.8. Not only that but the transition elements are all Cabibbo favored. For reasons that are too complicated to go into here, using the Standard Model parameters one can estimate the size of ϵ for Ds. It is expected to be one part in 1000, similar to that for Ks. For Bs people expect it to be a few tenths. As we have seen, the mixing parameter is also at the level of a few tenths. This means that one expects for fairly rare decays such as ψK_s (which may have a branching ratio of one part in 10,000) that the CP asymmetry, as defined in Eq. B.23, will be quite large. It will be of order of a few percent. This is certainly an exciting possibility; examining CP violation in some system other than the neutral-kaon system. For kaons people have been working since 1964 and have extracted basically one number, ϵ. There is another number in CP violation but after many years it is still not clear that this number is not 0. Hopefully, within the next couple of years experiments such as E-731 here at Fermilab can clear this up. For the B system the fixed-target program is only now gearing up to begin a series of exploratory measurements of B physics production, mixing, and CP violation.

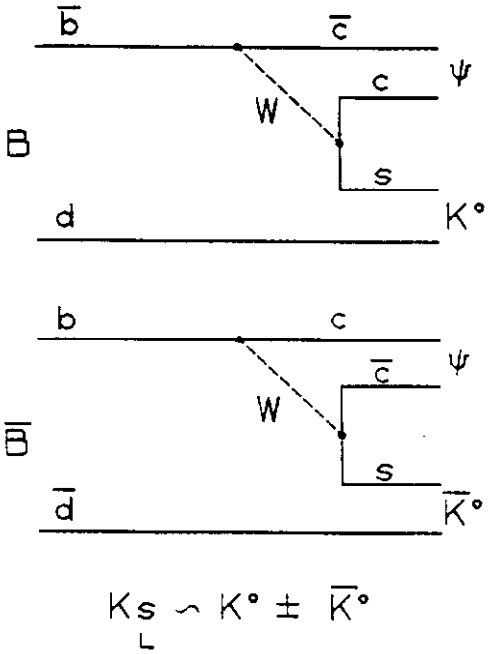

Fig. B.8: B and $\bar{B}$ decay schemes leading to the same final state CP eigenstate ψK_S.

So far we have said nothing about weak decays of baryons. We will not really say much in great detail about them because they are more complicated. We just want to draw the analogy with the decays of mesons. In studying the Dirac equation, one finds the solutions for particle and anti-particle in a particular representation. They are given below:

$$\begin{aligned} u &= \chi \begin{bmatrix} 1 \\ \frac{\vec{\sigma}\cdot\vec{p}}{E+m} \end{bmatrix}, v = \chi \begin{bmatrix} \frac{-\vec{\sigma}\cdot\vec{p}}{E+m} \\ 1 \end{bmatrix} \\ \bar{u}'\gamma_\mu g_V u &\rightarrow g_V \chi^{*\prime}\chi \\ \bar{u}'\gamma_\mu\gamma_5 g_A u &\rightarrow g_A \chi^{*\prime}\vec{\sigma}\chi \end{aligned} \quad . \tag{B.24}$$

Defining phenomenological couplings for the hadrons for vector and axial vector coupling, one can look at the non-relativistic limit which is applicable in baryon decays because the q value is rather low. For vector coupling only the time component is important, whereas for axial vector coupling the space components of $\gamma_\mu\gamma_5$ are important.

We have already mentioned that the weak current for $\Delta S = 0$ transitions is proportional to the isotopic spin ladder operators I^+I^-, while the strangeness changing weak currents are proportional to the V^+ and V^- operators. Combining the SU(3) flavor operators with the Lorentz spin operators, we get the expression for the ratio of axial to vector coupling for $\Delta S = 0$ and $\Delta S = 1$ transitions given below:

$$\begin{aligned} g_A/g_V &= \frac{< B'|I_+\sigma_Z|B >}{< B'|I_+|B >}, \ \Delta S = 0 \\ &= \frac{< B'|V_+\sigma_Z|B >}{< B'|V_+|B >}, \ |\Delta S| = 1 \end{aligned} \quad . \tag{B.25}$$

For pointlike leptons the coupling is V minus A so the ratio of axial to vector coupling is 1. However, for the baryons we have strong interaction effects which can change this ratio. We can use SU(3) Clebsch-Gordan algebra to relate the matrix elements of transitions within a multiplet, because all of those transitions are related by I spin, U spin, or V spin ladder operators. However, we see that it is only the vector current which is proportional to an SU(3) generator. Hence, it is only that coupling which has a conserved generator current. This is called the conserved vector current. For the axial decays, we have mixtures of both kinds of octets. The baryons have mixed symmetry. The axial vector generator, although it is proportional to V^+ also has a σ_Z piece, so it is not a pure SU(3) generator. This means the axial current is not conserved. All in all, the weak decays for the baryon octet are rather complicated for both semi-leptonic and non-leptonic decays. Although we have sketched out

what one does, in practice it is a messy business. Fermilab has a long history of hyperon-decay measurements, the latest in that series is E-715 which was looking at the β decay of the Σ.

Suffice it to say that in a spectator model, we expect the decay rates for semi-leptonic and non-leptonic decays of mesons and baryons to be rather similar. Representative spectator quark diagrams are shown in Fig. B.9.

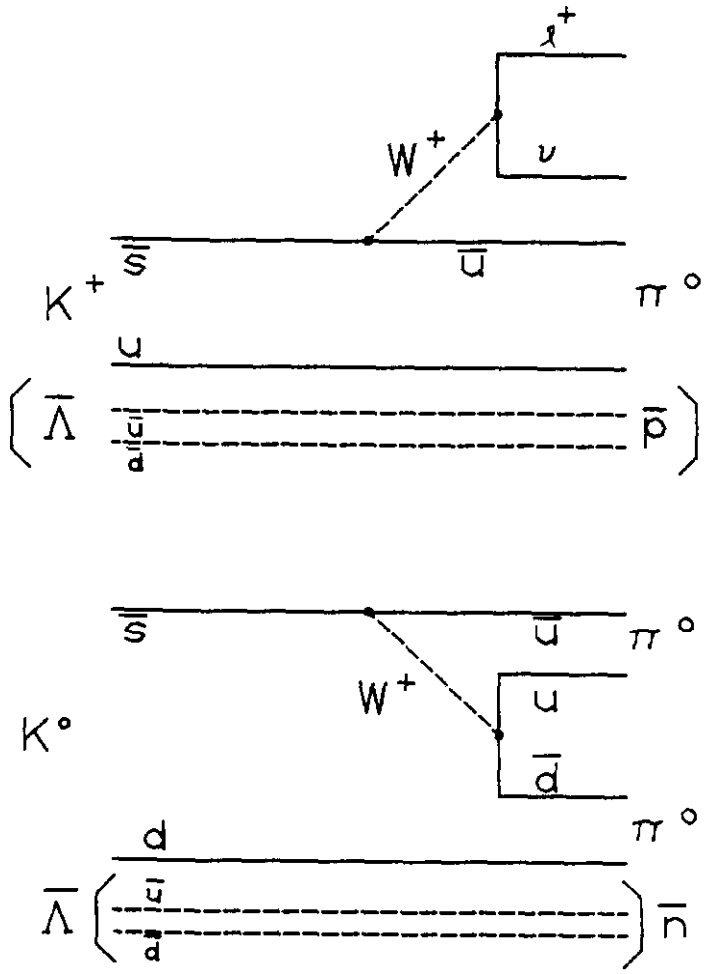

Fig. B.9: Spectator quark diagrams for semi-leptonic and non-leptonic weak decays comparing K and Λ decays; $K^+ \to \pi^0 \ell^+ \nu$ vs $\bar{\Lambda} \to \bar{p} \ell^+ \nu$ and $K^0 \to \pi^0 \pi^0$ vs $\bar{\Lambda} \to \bar{n} \pi^0$

In Table B.1, we show a comparison of the meson and baryon semi-leptonic decays. From the quark diagram it is clear that the underlying mechanism is that $s \to u + W$ followed by $W \to \ell\nu$. To the extent that this proceeds as a spectator diagram, we expect the decay widths to be comparable. They are certainly all of order a few times 10^{-18} GeV which lends credence to this model. Similarly for the non-leptonic weak decays, Table B.2, the quark diagrams for spectators are again completely similar. In this case, the meson and baryon rates are comparable and they are all a few times 10^{-15} GeV. There is a nonleptonic enhancement that one really doesn't understand particularly well and that we have glossed over. However, for the purposes of comparison between the mesons and baryons it is clear that a spectator model where one quark decays inside a hadron and the other quarks act effectively as spectators works out rather well.

Table B.1.

Comparison of meson and baryon semi-leptonic decays.

Decay Mode			$\Gamma(GeV)$ $\times 10^{18}$
K^+	$\to$	$\pi^0\ell^+\nu$	4.3
K_L	$\to$	$\pi^+\ell^-\bar{\nu}$	8.4
Λ	$\to$	$p\ell^-\bar{\nu}$	2.5
Σ^-	$\to$	$n\ell^-\bar{\nu}$	6.5
Ξ^-	$\to$	$\Lambda\ell^-\bar{\nu}$	3.6
Ω^-	$\to$	$\Xi^0\ell^-\bar{\nu}$	0.9

Table B.2.

Comparison of meson and baryon non-leptonic decays.

Decay Mode			$\Gamma(GeV)$ $\times 10^{15}$
K_S	$\to$	$\pi\pi$	7.4
Λ^0	$\to$	$n\pi$	2.5
Σ^+	$\to$	$n\pi$	8.2
Σ^-	$\to$	$n\pi^-$	4.4
Ξ^0	$\to$	$\Lambda\pi^0$	2.3
Ξ^-	$\to$	$\Lambda\pi^-$	4.0
Ω^-	$\to$	ΛK^-	8.0
	$+$	$\Xi\pi$	

Dimensional analysis can be very useful in estimating rare decays. For example, at Brookhaven Lab, much attention is focussed on rare K decays. The lepton number violating decay $K_L^0 \to \mu e$, if mediated by a heavy particle of mass M_F with coupling g, would imply

a lifetime $\Gamma(K_L \rightarrow \mu e) \sim (g^2/M_F^2)^2 M_K^5$. If we assume $g = g_W$ then $B(K_L \rightarrow \mu e) \sim (M_W/M_F)^4$. Hence a limit of $B \sim 10^{-8}$ probes a mass $M_F \sim 10\ TeV$. Clearly, very high mass scales are being probed in these experiments.

The second order nature of the weak decays makes the neutron very long lived. At the quark level $u \rightarrow d\ e\nu$ which is driven only by the $M_p - M_n$ electromagnetic mass difference. We roughly expect a neutron with lifetime scaled up from Γ_μ by $\left[M_\mu^{-1}(M_p - M_n)\right]^5 = 3.6 \times 10^9$. This is an enormous factor, scaling $1/\Gamma_\mu = 2.2\mu\ sec$ to $1/\Gamma_n = 7930\ sec$. The observed lifetime is 898 sec which is close for 9 decades of extrapolation. Another example of a rare decay is proton decay, mediated by a super heavy particle M_x at unification masses. At that mass, all coupling constants have run together to $g^2 \sim \alpha$. The familiar propagator and phase space arguments yield $\Gamma_p \sim (g^2/M_x^2)^2 M_p^5 \sim (\alpha^2/M_x^4) M_p^5$. For $M_x \sim 10^{14}\ GeV$, $\Gamma_p \sim 10^{-60}\ GeV$. This rate is $\sim 10^{45}$ times slower than Γ_Λ. In fact that the heavy M_x propagator factor slows down the rate, means that a sensitive measurement of $1/\Gamma_p$ probes fantastically high mass scales which are inaccessible to brute force techniques.

If we now look at the particle properties table we realize that we have worked our way through almost all of the particles which decay predominately by the weak interactions. We have come to a fairly successful explanation of the lifetimes, the decay modes, and branching ratios based on very simple minded arguments.

C. Electromagnetic Decays

Let us now begin to look at the electromagnetic decays of hadrons. The lightest particles which decay electromagnetically with significant branching fractions are the π^0 and η, decaying into two photons. The observed decay rates are given below:

$$\begin{aligned} \Gamma(\pi^0 \to \gamma\gamma) &= 7.6\ eV \\ \Gamma(\eta^0 \to \gamma\gamma) &= 0.41\ keV \end{aligned} \quad . \tag{C.1}$$

First look at the π^0 decay with a crude model; see Fig. C.1.a. We will treat the quark anti-quark system as we did in positronium and estimate the decay rate that way. Taking a binding radius for the quark anti-quark system compatible with the numbers we got in the first Section we can estimate the wave function at the origin. Thus, we get an estimate for pion decay rate which is unfortunately 200 kilovolts. This is a large discrepancy and, in fact, it is too large even for an "abacus" estimate:

$$\begin{aligned} \Gamma(^1S_0 \to \gamma\gamma) &= \frac{4\alpha^2}{M^2}|\psi(0)|^2 \\ a_0 &\sim 0.8\ fm \\ |\psi(0)|^2 &\sim (1/0.8\ fm)^3 \sim 0.016\ GeV^3 \\ \Gamma(^1S_0 \to \gamma\gamma) &\sim 200\ keV \end{aligned} \quad . \tag{C.2}$$

Why is this not working out particularly well? We know there are strong interactions and so we know there are multiple gluon effects which are important. In particular, the pion is as we know, anomalously light. That might mean that the mass scale is smaller, and that the coupling constants are larger.

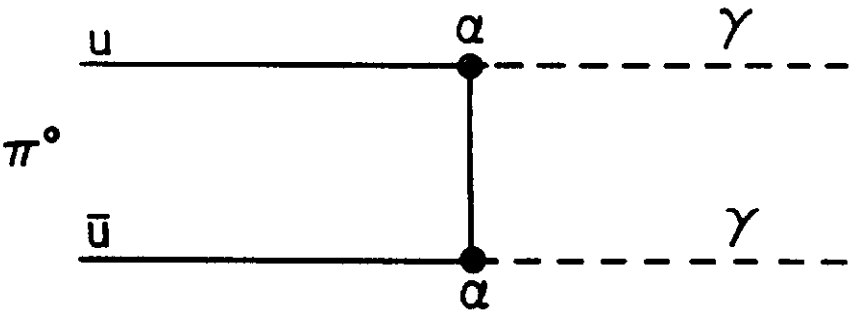

Fig. C.1.a: Quark diagram for π^0 decay.

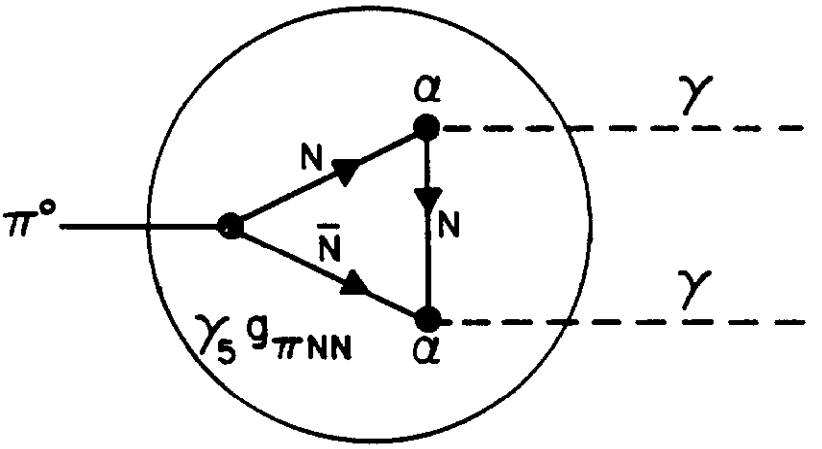

Fig. C.1.b: Strong interaction corrections for π^0 decay.

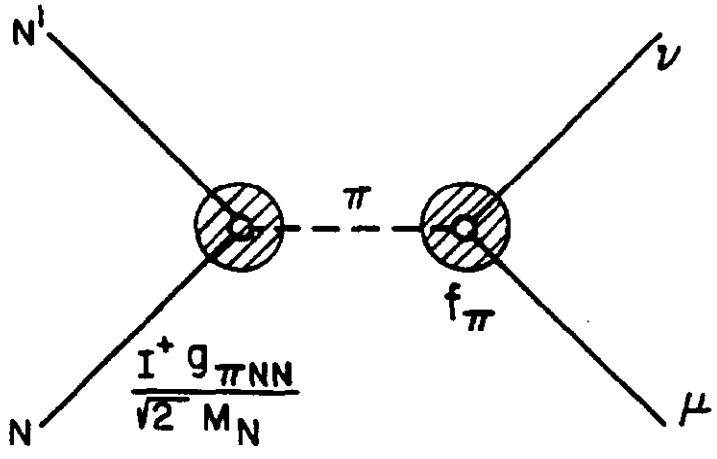

Fig. C.1.c: Relation of π leptonic decay to nucleon β decay.

These considerations lead us to believe that we are going to have to face up to strong interaction effects. We are going to have to do "chemistry" at some level in order to understand the system. The first attempt at estimating the strong interaction effects is seen in Fig. C.1.b. We insert a phenomenological pseudoscalar coupling of the pion to the nucleon anti-nucleon system and work out the decay rate. Note that this phenomenological coupling constant is large, $g^2_{\pi NN}/4\pi \sim 15$. This means we are indeed in a nonperturbative regime:

$$\Gamma(\pi^0 \to \gamma\gamma) \sim \frac{\alpha^2}{16\pi^2}\left(\frac{g^2_{\pi NN}}{4\pi}\right)\frac{M^3_\pi}{M^2_N}, \quad \frac{g^2_{\pi NN}}{4\pi} \sim 15 \ . \tag{C.3}$$

Now we have an expression for the $\pi^0 \to \gamma\gamma$ transition rate in terms of the pion nucleon coupling constant. We would like to relate that to some other process we have already seen. The diagram for this relationship is shown in Fig. C.1.c. We use the definition that we made in Section B for a pion decay constant which was appropriate to the leptonic decay of the pion. Diagrammatically, we have a relationship between nucleon β decay and pion leptonic decay. If we assume that the nucleon β decay axial coupling is dominated by the pion pole, we derive the relationship seen in Eq. C.4:

$$
\begin{aligned}
\Gamma(\pi \to \mu\nu),\ f_\pi &= 138\ MeV \\
A_\beta(N \to N'\ell\nu) &\sim \left(\frac{g_{\pi NN}}{\sqrt{2}M_N}\right)\left(\frac{M_\pi^2}{q^2+M_\pi^2}\right) f_\pi \\
&\equiv g_A \qquad . \qquad \text{(C.4)} \\
g_A &\stackrel{?}{=} \frac{g_{\pi NN} f_\pi}{\sqrt{2}M_N} \\
1.18 &\stackrel{?}{=} 1.42
\end{aligned}
$$

Since the momentum transfer scale for β decay is low, we can make an approximation to the propagator. Therefore, we have a relationship between the axial-vector coupling constant and the pion-nucleon coupling constant. This relationship is fairly well obeyed. It is called the Goldberger-Trieman relation. Notice that as we discussed in Section B, the axial-vector coupling is not strictly 1 as it is for leptons because of strong interaction effects between the quarks. Using this relationship we can express the pion-electromagnetic decay in terms of electromagnetic-coupling constant, the axial weak decay constant, the pion decay constant, and the relevant mass scales. The result does not refer to nucleons. In fact, we can replace them by quarks. Assuming a color factor of three summation we get an estimate for the width of 14 electron volts which is quite close to the observed value:

$$
\begin{aligned}
\Gamma(\pi^0 \to \gamma\gamma) &= \left\{\frac{9 < Q^2 > \alpha^2}{32\pi^3}\left[g_A\left(\frac{M_\pi}{f_\pi}\right)\right]^2\right\} M_\pi \\
&= 14\ eV \qquad . \qquad \text{(C.5)} \\
e_q &\equiv Qe
\end{aligned}
$$

Of course, the axial-coupling constant and the pion-decay constant are merely parameterizations of our ignorance of the strong interactions. This means what we have done is relate different classes of ignorance in some successful fashion. An a priori calculation from first principles will have to wait for a real lattice engine. We defer discussion of $\eta \to \gamma\gamma$, Eq. C.1, until later. For decay modes discussed in the rest of this Section, the branching fractions are small.

Let us now turn to the consideration of vector-meson decays into lepton pairs. A tabulation of the data is given in Table C.1 and the relevant quark diagram for this process is shown in Fig. C.2.

Table C.1.
Vector meson decays into e^+e^-.

Meson	M(GeV)	$< Q^2 >$	$\Gamma(keV)$	$\lvert\psi(0)\rvert^2(GeV^3) \times 10^{-2}$
ρ	0.770	$\frac{1}{2}$	6.5 $\pm$0.8	0.29
ω	0.783	$\frac{1}{18}$	0.76 $\pm$ 0.17	0.31
ϕ	1.020	$\frac{1}{9}$	1.34 $\pm$ 0.08	0.47
ψ	3.095	$\frac{4}{9}$	4.8 $\pm$ 0.06	3.9
ψ'	3.684	$\frac{4}{9}$	2.1 $\pm$ 0.3	2.4
Υ	9.460	$\frac{1}{9}$	1.2	40.6

A rough estimate is given below:

$$\begin{aligned} \Gamma(\rho \to ee) \simeq 7\ keV &\stackrel{?}{=} \alpha^2 |\psi(0)|^2 / M_\rho^2 \\ &\stackrel{?}{=} \left[\alpha^2 \alpha_s^3\right] M_\rho = 1.1\ keV \quad . \\ \alpha_s &\sim 0.3 \end{aligned} \tag{C.6}$$

The width is proportional to α^2, the wave function at the origin, and the mass of the system. Making a simple assumption of strong binding and taking the strong coupling to be 1/3 we get an estimate of 1.1 kilovolt which is certainly in the same order-of-magnitude as of the observed widths.

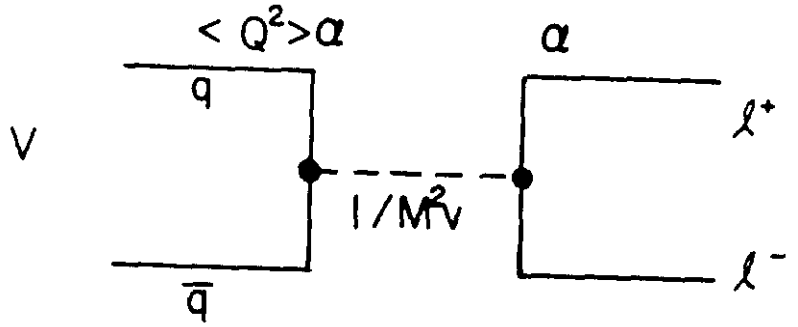

Fig. C.2: Quark diagram for vector-meson decays into lepton pairs.

Note that the α^2/M^2 factor is the same as we saw for the total cross-section for lepton pairs. It is basically the propagator of the virtual photon which, when we were discussing cross-section went like $\frac{\alpha^2}{s}$; in this case s is M_V^2. The other modification is that what one needs to change a cross section to a reaction rate is the flux which is the wave function at the origin[2]. In order to evaluate these rates we need the average value of the squared charge of the vector-mesons. We can get that for the vector meson octet using the wave functions we derived in Section I under the assumption of magic mixing. These charges are worked out in Eq. C.7:

$$\begin{aligned}
\Gamma(V \to \ell^+\ell^-) &= 16\pi\alpha^2 < Q^2 > \frac{|\psi(0)|^2}{M_V^2} \\
< Q^2 > = & \left|\frac{1}{\sqrt{2}}\left(\frac{2}{3}+\frac{1}{3}\right)\right|^2, \qquad \rho = \frac{1}{\sqrt{2}}(u\bar{u} - d\bar{d}) \\
& \left|\frac{1}{\sqrt{2}}\left(\frac{2}{3}-\frac{1}{3}\right)\right|^2, \qquad \omega = \frac{1}{\sqrt{2}}(u\bar{u} + d\bar{d}) \\
& \left|\frac{1}{3}\right|^2, \qquad \phi = s\bar{s} \\
& \left|\frac{2}{3}\right|^2, \qquad \psi = c\bar{c} \\
& \left|\frac{1}{3}\right|^2, \qquad \Upsilon = b\bar{b}
\end{aligned} \tag{C.7}$$

The results are fairly straight forward to derive. For example, we expect the ρ to ϕ width to be 9 to 1, and we observe a factor of about 5.3. There is more that we can do with this data to give us a confirmation of the underlying dynamics. We can extract the wave function of the origin instead of just the ratios and plot those as a function of the quark anti-quark system mass. We find that the wave function at the origin squared scales very closely as the square of the mass. If you recall, we showed in the first Section that one gluonic exchange gives us a mass cubed scaling, while a confining string potential gave a linear scaling with mass. This is additional evidence for a combination of Coulomb potential from one gluon exchange plus a confining potential:

$$\begin{array}{c} |\psi_{q\bar{q}}(0)|^2 \sim M^2 \\ M^3 \text{ for } OGE,\ M \text{ for string} \end{array} \quad . \tag{C.8}$$

Finally, for heavy quark anti-quark systems one can combine hadronic and electromagnetic decay widths to extract the strong coupling constant. Recall that the ψ cannot decay into two gluons. It decays into three gluons and we transcribed the positronium formula in the first Section. The total ψ decay rate is proportional to the wave function at the origin squared. We have just derived the fact that the dilepton decay rate of the ψ is also proportional to the wave function at the origin. The ratio is then independent of the mass of the state and the wave function at the origin; we have removed the internal dynamics and only the ratio of the coupling constants is left:

$$\begin{aligned} \Gamma(\psi \to ggg) &= \frac{\alpha_s^2 |\psi(0)|^2}{M^2} \left[\frac{\alpha_s 4(\pi^2 - 9)}{9\pi} \right] \\ \Gamma(\psi \to ee) &= 16\pi\alpha^2 < Q >^2 |\psi(0)|^2 / M^2 \\ \frac{\Gamma(\psi \to \text{Hadrons})}{\Gamma(\psi \to ee)} &= 13.4,\ \alpha_s = 0.19 \\ \Gamma(\eta_c \to gg) &= 16\pi\alpha_s^2 |\psi(0)|^2 / M^2 \\ &= 7\ MeV \stackrel{?}{\leq} 11 \pm 4\ MeV \end{aligned} \quad . \tag{C.9}$$

Given α_s and the wave function at the origin from the dilepton rate we can predict the η_c rate which is about the η_c total width into two gluons. It turns out to be about 7 MeV. The data for the total width is not yet good enough to really confront this prediction but there is a limit which is compatible with this prediction. For amusement one can perform the

same sort of operations for the ϕ meson. In this case, the ratio of hadron decays to lepton decays is much larger. That tells us that α_s is larger. If one takes it literally, it looks as if α_s is increasing as the mass scale decreases which is just what one expects for asymptotic freedom:

$$\frac{\Gamma(\phi \to KK)}{\Gamma(\phi \to ee)} = 3221, \ \alpha_s = 0.47 \ . \tag{C.10}$$

In Section I, we derived the relationship between spin-spin mass splitting and the wave function at the origin. In this case we take the charm quark mass to be 1.5 GeV which is just about half of the ψ mass. This is an assumption that the system is quite non-relativistic. We can eliminate the wave function at the origin by using the dilepton decay rate. We then have a relationship between the spin-spin mass splitting coupling constants, and the observed dilepton rate. We get a consistent value for α_s of 0.2 again. The upshot of all of these manipulations is that the dilepton decay rate for vector mesons validates the dynamics that we did in the first Section for quark anti-quark bound systems. We obtain the same wave function at the origin and the same coupling constant:

$$\begin{aligned} M_\psi - M_{\eta_c} &= 115 \ MeV \simeq \frac{M_{ss}}{4} \\ &= \frac{32\pi\alpha_s}{9m_c^2}|\psi(0)|^2 = \frac{M_\psi^2 \alpha_s \Gamma(\psi \to ee)}{2m_c^2\alpha^2} \ . \\ &= \left[\frac{8}{9}\frac{\alpha_s}{\alpha^2 < Q >^2}\right]\Gamma(\psi \to ee) \\ \alpha_s &= 0.2 \end{aligned} \tag{C.11}$$

Let's turn our attention now to the decays of vector mesons to pseudoscalar mesons plus photons. The spin diagrams for that and the related decay of pseudoscalar into two photons are shown in Fig. C.3. Also shown in that figure is the diagram for the experimental method of measuring such decay rates. In this case, one produces the vector meson in the Coulomb field of the nucleus. The virtual proton target in a heavy Z nucleus is scattered by the incident pseudoscalar meson producing a vector meson. This cross-section can be substantial because although one is down by a factor of α there are Z protons and using a heavy nucleus $Z\alpha$ can be close to 1. The virtual photon also constrains the process to be very forward, so all of the cross-section is in a very small region of phase space. Fermilab has a history of doing such experiments, starting out with E-272 and continuing in the fixed-target program.

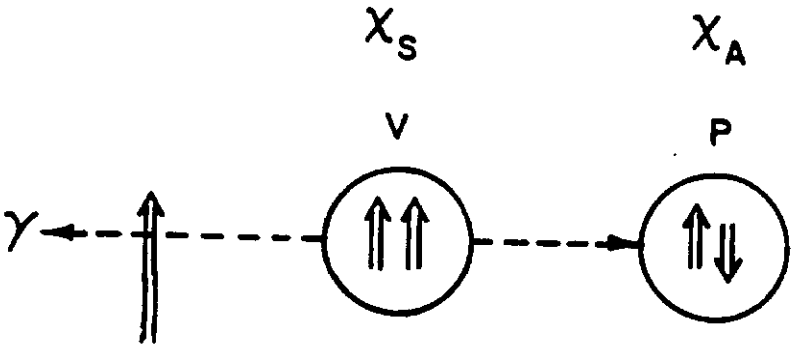

Fig. C.3.a: Spin orientations for $V \rightarrow P\gamma$.

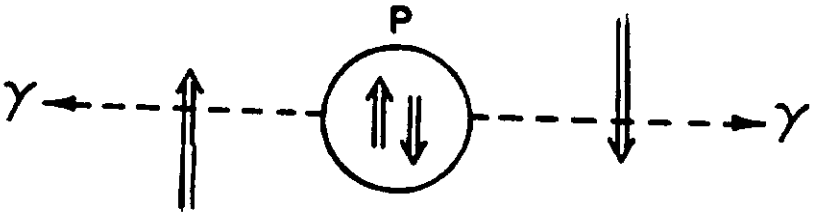

Fig. C.3.b: Spin orientations for $P \rightarrow \gamma\gamma$.

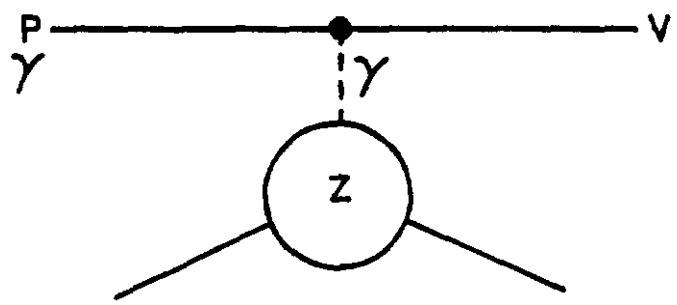

Fig. C.3.c: Primakoff diagram for V production in the Coulomb field of a nucleus.

We can start off with a very rough estimator for the decay rate. This is a magnetic dipole transition so you know that in the long wavelength approximation of classical electromagnetism that the width goes like the q value cubed. Again, looking at coupling, it is proportional to α so the decay rate is as shown below. We can get within an order of magnitude of the observed rate in this fashion:

$$\begin{aligned} V &\rightarrow P\gamma \\ \Gamma(M1) &\sim \alpha[(M_V - M_P)/M_V]^3 M_V \\ \Gamma(\rho \rightarrow \pi\gamma) &\sim 600\ keV \\ &\stackrel{?}{=} 70\ keV \end{aligned} \qquad \text{(C.12)}$$

We have an interaction energy between the electric field of the photon and the electric dipole moment. We assume the usual relationship between the moment and the spin. The final state photon is decomposed into spin directions Jz of +1, -1, and zero. The polarization vector, $\vec{\epsilon}$, is as shown in Eq. C.13:

$$
\begin{aligned}
A &= < P \left| \vec{\mu} \cdot \vec{E} \right| V > \\
\vec{\mu} &= \tfrac{e}{2m} Q \vec{\sigma} \\
V(J_Z = 1), \vec{\epsilon} &= (1, \imath, o) \left(-\tfrac{1}{\sqrt{2}} \right) \\
\vec{\sigma} \cdot \vec{\epsilon} &= -\tfrac{1}{\sqrt{2}} (\sigma_x + \imath \sigma_y) = \sqrt{2} \sigma_+
\end{aligned}
\qquad \text{(C.13)}
$$

This means that the amplitude is proportional to the spin-flip (or spin-ladder) operators. That is not surprising when you look at Fig. C.3 because what you are doing is taking one of the spins in the vector meson, flipping it to make a pseudoscalar meson, and giving off a photon in order to conserve spin. Defining the magnetic moment μ in Eq. C.14 and working out the operators of the up ladder we get the amplitude shown below:

$$
\begin{aligned}
A_+ &= \frac{\sqrt{2}e}{2m} \sum_i < P|Q\sigma_+|V >, \ \mu = \frac{|e|}{2m} \\
&= \mu [< P|Q_1|V > - < P|Q_2|V >] \ . \qquad \text{(C.14)} \\
< \chi_S|\sigma_+^1|\chi_A > &= - < \chi_S|\sigma_+^2|\chi_A > = \frac{-1}{\sqrt{2}}
\end{aligned}
$$

The amplitude is simply proportional to the magnetic moment for quark and anti-quark sandwiched between the vector and pseudoscalar states. In order to work out the algebra for the spin ladder operators one needs the symmetric and anti-symmetric wave functions which we have already given in the first Section when working out the spectroscopy of the pseudoscalar and vector octet. Let's go through the calculation in some detail for $\omega \rightarrow \pi\gamma$ decay. The wave functions and charges are:

$$
\begin{aligned}
\omega &= (u\bar{u} + d\bar{d})/\sqrt{2} \\
\pi &= (-u\bar{u} + d\bar{d})/\sqrt{2} \\
< \omega|Q_1|\pi > &= \left[-(+\frac{2}{3}) + (-\frac{1}{3}) \right] /2 \ . \qquad \text{(C.15)} \\
< \omega|Q_2|\pi > &= \left[-(-\frac{2}{3}) + (+\frac{1}{3}) \right] /2 \\
A_+ &= \mu
\end{aligned}
$$

Evaluating the charge of the first parton (quark) and the second parton (anti-quark) sandwiched between the ω and π states we get the result that the transition amplitude for the ω in a spin up state is just equal to the magnetic moment. Similarly, the amplitude for the ω with spin minus 1 in the z direction is equal to μ. The amplitude for a vector meson in a spin zero state along the z axis is 0 because you cannot get a transverse photon by spin-angular momentum conservation. Summing over the final states and averaging over the initial polarization states we get the result shown below:

$$\begin{aligned} A_- &= A_+, A_0 = 0 \\ \sum_f |A(\omega \to \pi\gamma)|^2 &= \tfrac{2}{3}\mu^2 \end{aligned} \qquad \text{(C.16)}$$

Let's look at a few other vector mesons. The ϕ is very simple because in the magic mixing scheme it is a pure $s\bar{s}$ state. Since the photon conserves flavor the amplitude is 0. Experimentally the rate for $\phi \to \pi\gamma$ is rather small:

$$\begin{aligned} A(\phi \to \pi\gamma) &\stackrel{?}{=} 0 \\ \frac{\Gamma(\phi \to \pi\gamma)}{\Gamma(\omega \to \pi\gamma)} &\simeq 0.006 \end{aligned} \qquad \text{(C.17)}$$

This experimental ratio supports the idea of magic mixing which we have already come to by considerations of the OZI rule. Finally what about the ρ decay? The spin considerations are the same as for $\omega \to \pi\gamma$. The only difference is in the expectation value of the quark and anti-quark charges. They are shown below:

$$\begin{aligned} \rho &= (-u\bar{u} + d\bar{d})/\sqrt{2} \\ < \rho|Q_1|\pi > &= \left[+(\frac{2}{3}) + (-\frac{1}{3})\right]/2 \\ < \rho|Q_2|\pi > &= \left[+(-\frac{2}{3}) + (\frac{1}{3})\right]/2 \\ \frac{\Gamma(\rho \to \pi\gamma)}{\Gamma(\omega \to \pi\gamma)} &= \frac{1}{9} \end{aligned} \qquad \text{(C.18)}$$

The ratio is of $\rho \to \pi\gamma$ to $\omega \to \pi\gamma$ is expected to be 1/9.

A compilation of the data for these electromagnetic decays is given in Table C.2. We can see that indeed the ω width is about 9 times larger than the ρ width. Note that the sign of the terms of the wave function is quite important because this is exactly the inverse of the behavior we saw for dilepton decays where the ρ had a 9 times higher width than the ω.

Table C.2.
Decay Rates for $V \to P\gamma$.

Decay Mode	$\Gamma(keV)$	A/μ
$\omega \to \pi^0\gamma$	890	1
$\rho \to \pi\gamma$	70	$\frac{1}{3}$
$\phi \to \pi\gamma$	5.5	0
$\rho \to \eta\gamma$	50	$\frac{1}{\sqrt{3}}(\cos\theta_0 + \sqrt{2}\sin\theta_0)$
$\omega \to \eta\gamma$	3	$\frac{1}{3\sqrt{3}}(\cos\theta_0 + \sqrt{2}\sin\theta_0)$
$\phi \to \eta\gamma$	62	$\frac{2}{3\sqrt{3}}(-\sqrt{2}\cos\theta_0 + \sin\theta_0)$
$\eta' \to \omega\gamma$	7.6	$\frac{1}{3\sqrt{3}}(\sqrt{2}\cos\theta_0 - \sin\theta_0)$
$\eta' \to \rho\gamma$	83	$\frac{1}{\sqrt{2}}(\sqrt{3}\cos\theta_0 - \sin\theta_0)$
$K^{*+} \to K^+\gamma$	60	$\frac{1}{3}(1 + 1/\gamma)$
$K^{*0} \to K^0\gamma$	75	$\frac{1}{3}(-2 + 1/\gamma)$

$$\gamma \equiv ms/mu \sim 1.5$$

The situation for vector mesons containing strange quarks is very similar to what we have already done. The magnetic moment of the strange quark is down by a factor of γ on the average from that of the up and down quarks because it is heavier. Hence the charge is weighted by the γ factor in the expression for the decay amplitude. We work out the amplitude for K^{*0} and K^{*+} in Eq. C.19:

$$
\begin{aligned}
\mu_s &\equiv \frac{e}{2m_s}Q\vec{\sigma} = \frac{e}{2m\gamma}Q\vec{\sigma} = \frac{\mu}{\gamma}Q\vec{\sigma} \\
A_+ &= \mu[< P|Q_1/\gamma_1|V > - < P|Q_2/\gamma_2|V >] \\
K^{*0} &= d\bar{s} \\
A_+ &= \mu\left[-\frac{1}{3} - (\frac{1}{3}\gamma)\right] = \frac{-\mu}{3}\left[1 + \frac{1}{\gamma}\right] \\
K^{*+} &= u\bar{s} \\
A_+ &= \mu\left[\frac{2}{3} - (-\frac{1}{3}\gamma)\right] = \frac{-\mu}{3}\left[-2 + \frac{1}{\gamma}\right]
\end{aligned}
\qquad \text{(C.19)}
$$

Mixing result for the pseudoscalar mesons can be found using definitions from Section I. The resulting fit to θ_0 confirms the value found previously.

Data given in the Table C.1 allow us to extract γ which turns out to be about 5/3. This is close to the value of about 3/2 that we got from spectroscopy. The agreement helps us believe the picture of these kinds of decays; a single quark making a transition within the meson is a reasonable approximation to the reality of the situation. The logical extrapolation of this behavior occurs in the charm-vector mesons. We have already noted that the heavier quarks have a less mobile spin in that the magnetic moment is reduced. That means that in the limit of very heavy quarks only the light quark flips its spin. The charm quark is inert; it just sits there. The relevant factor in the decay width is just the square charge of the light quark:

$$
\gamma \to \infty, \frac{\Gamma(D^{*0}(c\bar{u}) \to D^0\gamma)}{\Gamma(D^{*+}(c\bar{d}) \to D^+\gamma)} = 4 \; . \qquad \text{(C.20)}
$$

In the limit where γ becomes very large we have the ratio of D^{*0} to D^{*+} at 4 which is just the square ratio of the light quark charges. We get the same result for the kaon system (see Table C.1) if γ becomes large. Unfortunately, since there doesn't exist a good experimental measure of the widths of the charged and neutral D^*s, we cannot confront this prediction with experimental data.

A word about units. This is a magnetic dipole transition. The scales are α times the squared charge of the quarks. We have to sum over the final states so we have a $(2J_f + 1)$ factor. Electromagnetic dipole transitions have a q^3 scaling, and we need a $1/M^2$ to bring the dimensions out properly. The rate then is proportional to the magnetic moment squared times the q value to the third power:

$$
\begin{aligned}
\Gamma(M1) &= \frac{4}{3} < Q >^2 \alpha(2J_f+1)\frac{k^3}{M^2} \sim \mu^2(2J_f+1)k^3 \\
k &= M_V - M_P \\
Q &= \frac{2}{3}, m_c = M_\psi/2 = 1550\ MeV \\
k &= M_\psi - M_{\eta_c} = 116\ MeV \\
\Gamma(\psi \to \gamma\eta_c) &= 0.71\ keV \stackrel{?}{=} 0.80\ keV
\end{aligned}
\qquad . \qquad \text{(C.21)}
$$

For the ψ decay into $\eta_c\gamma$ we know the charge of the charm quark. We take the mass to be half of the ψ mass for non-relativistic binding. This gives us a q value of 116 MeV. One can make a sharp prediction that the radiative decay width down to the η_c is 0.7 keV. That is very close to the observed value for this transition.

What about the baryon radiative decays? One can measure them directly in hyperon beams or using the Primakoff effect with nucleon beams. A collection of some of the radiative decays is given in Table C.3 with a comparison to typical meson radiative decays. They are certainly of a comparable scale. Just as in the case with weak semi-leptonic decays and non-leptonic decays, we take this as evidence that the underlying dynamics is a single quark transition with some spectator quarks lurking around and not doing too much to effect things.

Table C.3.
Comparison of Meson and Baryon Radiative Decays

Decay Mode	$\Gamma(keV)$
$\omega \to \pi\gamma$	850
$\rho \to \pi\gamma$	70
$\Delta(1232) \to N\gamma$	690
$\Delta(1620) \to N\gamma$	42
$N(1440) \to p\gamma$	190
$N(1520) \to p\gamma$	600
$\Lambda(1520) \to \Lambda\gamma$	125
$\Sigma \to \Lambda\gamma$	11

Of course there are still many radiative transitions which have not been measured and there is a long standing program of hyperon beam physics at Fermilab to make such measurements. For example, E-761 is the current experiment in a long line. We expect further increases in our knowledge of radiative baryon decays from E-761.

There are a related set of decays for which we can take over the formalism we have developed above fairly easily. These are the decays of pseudoscalars into two photons. Recall that the photon is a U spin singlet. It is easy to remember that it is the flavorless quark anti-quark combination weighted by the charge of the quark as shown below:

$$\begin{aligned} \gamma &= \sqrt{\frac{3}{2}}\left(\frac{2}{3}u\bar{u} - \frac{1}{3}d\bar{d} - \frac{1}{3}s\bar{s}\right) \\ A_+ &= \mu[< P|Q_1|\gamma > - < P|Q_2|\gamma >] \\ A_+^{\pi^0} &= \frac{\mu\sqrt{3}}{2}\left[\frac{2}{3}(-\frac{2}{3}) - \frac{1}{3}(-\frac{1}{3})\right]2 \\ &= -\frac{\mu}{\sqrt{3}} \end{aligned} \qquad \text{(C.22)}$$

What one does is use the amplitude for vector meson into pseudoscalar plus photon and merely insert the photon as the vector. Starting from Eq. C.19, substitute the wave functions to get the amplitude for $\pi^0 \rightarrow \gamma\gamma$. This amplitude is again proportional to the quark magnetic moment as it should be. In exactly the same way, we can use the singlet and octet wave functions to derive the transition amplitudes for a singlet or octet into two photons. Recalling that the physical η is a mixture of the SU(3) singlet and octet we get the expression for the relative amplitudes for the η and the π as shown in Eq. C.23:

$$\begin{aligned} A_+^{\eta_8} &= -\frac{1}{\sqrt{3}}A_+^{\pi^0} \\ A_+^{\eta_1} &= -2\sqrt{\frac{2}{3}}A_+^{\pi^0} \\ \frac{A(\eta \rightarrow \gamma\gamma)}{A(\pi \rightarrow \gamma\gamma)} &= \frac{-1}{\sqrt{3}}(\cos\theta_0 + 2\sqrt{2}\sin\theta_0) \\ \theta_0 &\sim 15^0 \end{aligned} \qquad \text{(C.23)}$$

We can use the data quoted in Eq. C.1 to solve for the pseudoscalar mixing angle.

We find an angle of 15^0 from this ratio. Within errors and approximations this is in good agreement with the 24^0 angle we got from the pseudoscalar nonet mixing. This is a reasonable confirmation of the mixing value that we got from an entirely different viewpoint, looking at the systematics of the mass relations in the pseudoscalar nonet.

Let's turn now to the consideration of baryon magnetic moments. Normally, one thinks of this as a static property of the baryons. However, it does represent the interaction of a quark in the baryon with a magnetic field, i.e., photons. Therefore, we might expect that it is related to the electromagnetic transitions we have just been discussing. Indeed, they have all had amplitudes which are directly proportional to the quark-magnetic moment. The first thing we need is the SU(6) wave function for the baryons. In the first Section we found the spin wave functions for the proton. We did this by looking at the coupling of 2 spin $\frac{1}{2}$ to form spin 0 and spin 1. Then we recoupled to a third quark to give us spin $\frac{3}{2}$ and spin $\frac{1}{2}$:

$$\begin{aligned} 3 \otimes 2 &= 2 \oplus 4, 1 \otimes 2 = 2 \\ (uu) \otimes d & \\ P \Uparrow &= \tfrac{1}{\sqrt{6}}(2u \Uparrow u \Uparrow d \Downarrow - u \Uparrow u \Downarrow d \Uparrow - u \Downarrow u \Uparrow d \Uparrow) \\ N \Uparrow &= \tfrac{1}{\sqrt{6}}(2d \Uparrow d \Uparrow u \Downarrow - d \Uparrow d \Downarrow u \Uparrow - d \Downarrow d \Uparrow u \Uparrow) \end{aligned} \quad . \tag{C.24}$$

If (uu) are symmetric there is still an overall anti-symmetry. When color is taken into account the flavor-spin is symmetric. The (uu) are in a spin one state and when recoupled to the d quark go to a spin $\frac{1}{2}$ state. If the (uu) are anti-symmetric, they are in a spin 0 state, and recouple to the d quark to get a total spin $\frac{1}{2}$ state. These wave functions were quoted in Fig. C.3 of Section I already. The linear sum of the symmetric and anti-symmetric octets gives us the wave functions shown in Eq. C.24. The equation for the neutron comes from isotopic spin symmetry, where one merely exchanges all u with d and vice-versa.

For the magnetic moment we assume that only a single quark at a time interacts. We will make the impulse approximation and sum over all the quarks in the hadron as in Eq. C.25:

$$\begin{aligned} \mu_h &= \sum_i < h, S_Z | \mu_i \sigma_Z^i / \gamma_i | h, S_Z > \\ &= \frac{|e|}{2m} \sum_i < h, S_Z | Q_i \sigma_Z^i / \gamma_i | h, S_Z > \\ \mu_p &= \frac{\mu}{6}\left[4(\frac{2}{3}+\frac{2}{3}+\frac{1}{3}) + (\frac{2}{3}-\frac{2}{3}-\frac{1}{3}) + (-\frac{2}{3}+\frac{2}{3}-\frac{1}{3}\right] \\ \mu_n &= \frac{\mu}{6}\left[4(-\frac{1}{3}-\frac{1}{3}-\frac{2}{3}) + (-\frac{1}{3}+\frac{1}{3}+\frac{2}{3}) + (\frac{1}{3}-\frac{1}{3}+\frac{2}{3})\right] \\ \mu_p &= \mu, \mu_n = -\frac{2}{3}\mu \end{aligned} \quad . \tag{C.25}$$

We have assumed that the quarks are pointlike Dirac fermions with a g factor of 2. The explicit result for the proton and the neutron are given in Eq. C.25. It is merely a matter of keeping track of the charge and the spin direction for the u and the d quarks. The result is the famous relationship that the ratio of the proton to neutron-magnetic moments is $-\frac{3}{2}$ which is in very good agreement with the experimental result.

Years ago this was considered a great triumph for SU(6). In addition, there is the absolute value of 2.79 nuclear magnetons for the proton-magnetic moment. If we equate that to the quark-magnetic moment, we get a constituent quark mass of 340 MeV. This is in good agreement with what we found from baryon spectroscopy:

$$\begin{aligned} \mu_p/\mu_n &= -\frac{3}{2} \stackrel{?}{=} \frac{-2.79}{1.91} = -1.46 \\ \mu_p &= 2.79|e|/2M_p = |e|/2m \quad . \\ m &= 340\ MeV \end{aligned} \tag{C.26}$$

One can continue through the baryon octet and decuplet to find magnetic moments for baryons containing strange quarks. For the Λ, which is a strange iso-singlet, the u and d must be in an isotopic singlet state. Therefore, since they are I = 0 they don't contribute to the magnetic moment. This means that the only contributor is the strange quark. We obtain the prediction that the Λ magnetic moment is just the strange quark magnetic moment. It is the magnetic moment μ reduced by γ times the charge of the strange quark:

$$\begin{aligned} \Lambda &= (ud)s \qquad \Omega^- = sss \\ (ud), \quad I &= 0 \\ \mu_\Lambda &= \mu\left(\frac{-1}{3\gamma}\right) \qquad \mu_\Omega = \frac{\mu}{\gamma}\left(\frac{-1}{3}+\frac{-1}{3}+\frac{-1}{3}\right) \quad . \\ &= -\mu/3\gamma \\ \gamma &= 1.52 \end{aligned} \tag{C.27}$$

The measured value shown in Table C.4 gives us another estimator of γ, which is $\gamma = 1.52$.

Table C.4.
Magnetic moments of octet and decuplet baryons.

Baryon	μ_h	SU(6), μ_h/μ
p	2.79	1
n	-1.9	$-\frac{2}{3}$
Λ	-0.61	$-\frac{1}{3\gamma}$
Σ^+	2.33	$\frac{1}{9}\left[\frac{4}{3}+\frac{1}{\gamma}\right]$
Σ^-	-1.41	$\frac{4}{9}\left[-1+\frac{1}{3\gamma}\right]$
Ξ^0	-1.25	$-\frac{4}{9}\left[\frac{2}{3}--\frac{1}{\gamma}\right]$
Ξ^-	-0.69	$\frac{4}{9}\left[1-\frac{1}{\gamma}\right]$
Ω^-	E-756?	$-\frac{1}{\gamma}$

This is at least in rough agreement with what we got from spectroscopic considerations. Finally, there is a prediction for the Ω which consists of three strange quarks in an entirely symmetric state. The prediction is just that that is the strange quark magnetic moment times three. It is interesting to note that there has been a long tradition of magnetic moment measurements at Fermilab. The latest in that series is E-756 whose goal has been to measure the Ω magnetic moment precisely enough to make incisive discrimination between various models which are more detailed and which make more strict predictions about the magnetic moments of the hyperons.

If one looks at the particle property tables in the blue book it is clear that we have now considered essentially all of the electromagnetic decays of both the mesons and the baryons and some of the static electromagnetic properties such as the magnetic moments of the hyperons. Everything we have done has served to confirm the picture of hadrons as systems of quarks with constituent masses that can be found from spectroscopy and whose decays can be understood using coupling constants and single quark dynamics to give us the observed decay rates.

D. Strong Hadronic Decays

We now come to the consideration of strong decays of the hadrons. This will be a short section because this task is roughly equivalent to that of trying to understand atomic physics from a study of the residual Van der Waals forces between molecules. As such, the study is not going to yield any particularly fruitful insights into the dynamics of the quarks and the gluons inside our hadron molecules. Of neccesity this will be a very brief and superficial discussion.

First let's just remind ourselves of G parity. G parity is like C parity for photons in that for a system of n pions the G parity is $(-1)^n$, just the way the C parity for a system of n photons is $(-1)^n$. The same situation in C obtains for gluons as for photons. In the first section, we did mention already the OZI rule which tells us that ϕ mesons can decay into a K^+K^- pair via two gluon coupling but that the $s\bar{s}$ pair in the ϕ can annihilate (since it is a C = 1 state) only into three or more gluons. That leads us to expect that the amplitude into two bodies is down by a factor of α_s for $\rho\pi$ with respect to KK after one has taken out the phase space factors. The phase space factor is just the velocity of the final state in the center-of-mass as we derived in Section A of the second Section:

$$\begin{aligned} \frac{\Gamma(\phi \to KK)}{\Gamma(\phi \to \rho\pi)} &= \frac{0.84}{0.15} \sim \frac{|A_{KK}|^2 P^*_{KK}}{|A_{\rho\pi}|^2 P^*_{\rho\pi}} \\ \frac{|A_{KK}|}{|A_{\rho\pi}|} &\sim 4.6 \sim (\alpha_s)^{-1} \end{aligned} \quad . \tag{D.1}$$

We estimate the strong coupling constant to be of order 0.2.

Another manifestation of the OZI rule is something we have already quoted. The ψ goes into 3 gluons and has a total width of 63 kilovolts while the η_c can go to 2 gluons and has a width of order 10 MeV. The ratio of those two widths taken over from the positronium formula also gives us a strong coupling constant of order 0.2:

$$\begin{aligned} \frac{\Gamma_\psi}{\Gamma_{\eta_c}} &\sim \frac{63\ keV}{10\ MeV} \sim \frac{\alpha_s 4(\pi^2 - 9)}{9\pi} \\ \alpha_s &\sim 0.2 \\ \Gamma^{4^{++}}_{h(2030)} &\sim 200\ MeV \end{aligned} \quad . \tag{D.2}$$

For comparison, without such a suppression, the typical hadronic width of say the h(2030)

is about 200 MeV. Note that the $D\bar{D}$ is not available to the ψ because it is below threshold, whereas the $K\bar{K}$ is available to the ϕ although it is only slightly above threshold.

Let's look at vector meson decays and try to get some feeling for the widths and the systematics. The spin diagrams for vector goes to pseudoscalar plus pion is shown in Fig. D.1.

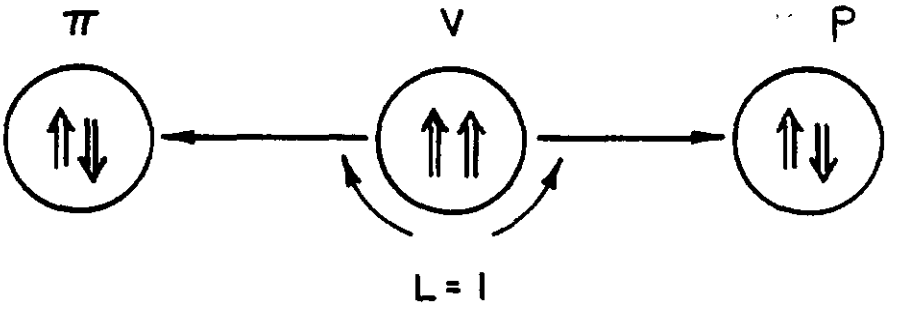

a) V$\rightarrow P\pi$ decays.

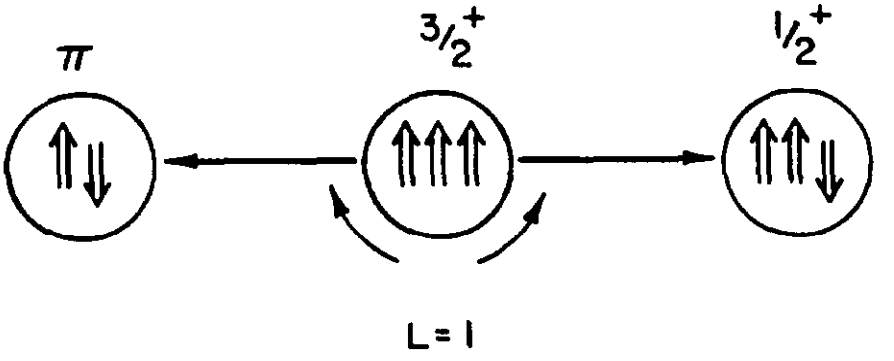

b) $\frac{3}{2}^+ \rightarrow \frac{1}{2}^+\pi$ decays.

Fig. D.1: Spin diagram for

This is supposed to be the analog of the electromagnetic decay vector goes to pseudoscalar plus photon. In fact, the typical width of 100 MeV is something like the typical electromagnetic decay width of 1 MeV scaled up by the ratio of the coupling constants which in this case is α (assuming $\alpha_s \sim 1$):

$$\begin{aligned} V &\rightarrow (P\pi)_{L=1} \\ \Gamma &\sim 100\ MeV \sim \Gamma(V \rightarrow P\gamma)/\alpha \end{aligned} \quad . \tag{D.3}$$

In this case, the colorless π is the "residual Van der Waals" force carrier at long range made up of composites of color forces. Table D.1 gives the results for ρ decay and K^* decay into $K\pi$. The ω has to go to 3π because it has G parity of -1 whereas the ρ has the G parity of +1. The widths are all of order 100 MeV. One can always get a rough estimate of what kinds of decays will happen by drawing quark diagrams. For example, for $K^* \rightarrow K\pi$, the quark diagram is shown in Table D.1. In this case, one is boiling quark anti-quark pairs out of the vacuum. The gluons which are the agents of the coupling are traditionally not shown in such diagrams.

Table D.1.
$V \rightarrow P\pi$ Widths.

$V \rightarrow P\pi$	BR	$\Gamma(MeV)$
$\rho \rightarrow \pi\pi$	1.0	153
$\omega \rightarrow 3\pi$	0.9	9.8
$K^* \rightarrow K\pi$	1.0	51

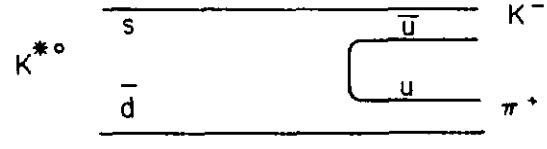

What about P wave states? The P states are 1^{++}, 2^{++}, for example, which we have already looked at when discussing spin-orbit coupling in spectroscopy in the first Section. One might expect these P wave states to decay down to S states by spitting out a pion in a cascade mechanism. In fact, as seen in Table D.2 there is some evidence that the 2^{++} and 1^{++} decay down to vector meson + pion, which in turn decays to pseudoscalar + another pion. There are no particularly obvious systematics to the branching ratio and decay widths. Again the branching ratios to cascade are reasonably large and all the decay widths are at the 100 MeV level, which is typical for hadronic decay.

Table D.2.
$(L=1) \rightarrow (L=0) + \pi$ widths.

J^{PC}	Mode	BR	$\Gamma(MeV)$
2^{++}	$f \rightarrow \pi\pi$	0.84	176
	$A_2 \rightarrow \rho\pi$	0.70	110
$(^3P_2)$	$f' \rightarrow K\bar{K}$	?	70
	$K^* \rightarrow K^*\pi$	0.24	100
	$A_1 \rightarrow \rho\pi$	1.0	316
1^{++}	$D \rightarrow \eta\pi\pi$	0.49	25
$(^3P_1)$	$Q \rightarrow K^*\pi$	0.94	184

$$2S + 1P_J \rightarrow \begin{matrix} ^3S_1 + \pi \\ ^3S_0 + \pi \end{matrix}$$

For the decuplet baryons there is a tendency to proceed in an analogous fashion, $\frac{3}{2}^+ \rightarrow \frac{1}{2}^+ \pi$, as seen in Fig. D.1. For example, as seen in Table D.3, $\Delta \rightarrow N + \pi$, $\Sigma^* \rightarrow \Lambda + \pi$ and $\Xi^* \rightarrow \Xi + \pi$. These decays all occur with branching ratios near 1 and with widths in order 100 MeV. A typical quark diagram for decuplet goes to octet plus π is shown in Table D.3. Again, one boils quark anti-quark pairs out of the vacuum and combines them in all ways to get the final states.

Table D.3.
$\frac{3}{2}^+ \rightarrow \frac{1}{2}^+ \pi$ widths.

$\frac{3}{2}^+ \rightarrow \frac{1}{2}^+$ Mode	BR	$\Gamma(MeV)$
$\Delta \rightarrow N\pi$	1.0	110
$\Sigma^* \rightarrow \Lambda\pi$	0.88	36
$\Xi^* \rightarrow \Xi\pi$	1.0	148

$$10 \rightarrow 8 + \pi$$

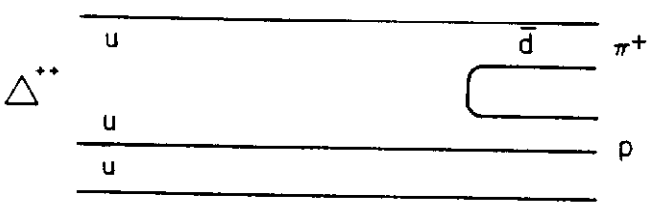

Finally, for P wave baryons one has the quantum numbers shown below:

$$L = 1 \qquad \begin{matrix} \frac{1}{2}^-, \frac{3}{2}^-, \frac{5}{2}^- \\ N, \Delta, \Sigma, \Xi, \Lambda \end{matrix} \quad . \tag{D.4}$$

Within those quantum number multiplets there are different flavor catagories. Nucleon, $(I = \frac{1}{2})$, Δ, $(I = \frac{3}{2})$, Σ, Λ and Ξ.

Table D.4.

$(L = 1) \rightarrow \begin{matrix} (L = 0) + P \\ (L = 0) + V \end{matrix}$ widths.

Typical Mode	Typical Γ (MeV)
N(1520)$\rightarrow N\pi$	120
$N\eta$	
ΛK	
$\Delta\pi$	
$N\rho$	
$\Delta \rightarrow N\pi$	200
ΣK	
$N\rho$	
$\Sigma \rightarrow \Sigma\pi$	200
$\Lambda\pi$	
NK	
$\Xi \rightarrow \Xi\pi$	20
ΛK	
ΣK	
$\Lambda \rightarrow \Sigma\pi$	200
NK	

There is some tendency for the octets and decuplets in the higher angular momentum state to decay into $\frac{1}{2}^+$ octets plus vector or pseudoscalar mesons. The SU(3) factors for that are in $8 \otimes 8$ then which contains both the octet and decuplet in higher angular momentum states:

$$
\begin{aligned}
(8,10)_L \rightarrow \quad & 8_{\frac{1}{2}+} + V \\
& 8_{\frac{1}{2}+} + P \qquad . \qquad \text{(D.5)} \\
8 \oplus 8 = 1 \quad \oplus \quad & 8 \oplus 8 \oplus 10 \oplus 27
\end{aligned}
$$

Typical kinds of decay modes are taken from the table of particle properties. The widths are of order 200 MeV and there is no particular systematics to the decay modes beyond this. The quark diagrams which were used to categorize the decays are also useful for examining various dynamical questions. An example of this is shown in Fig. D.2 where a K^* to $K^0\pi$ decay is shown. Also shown is the scattering $\pi + p \rightarrow K + \Sigma$ via the annihilation into an s channel Δ. These quark diagrams are useful mnemonics and can be used to give an idea of decay branching ratios of new heavy flavors.

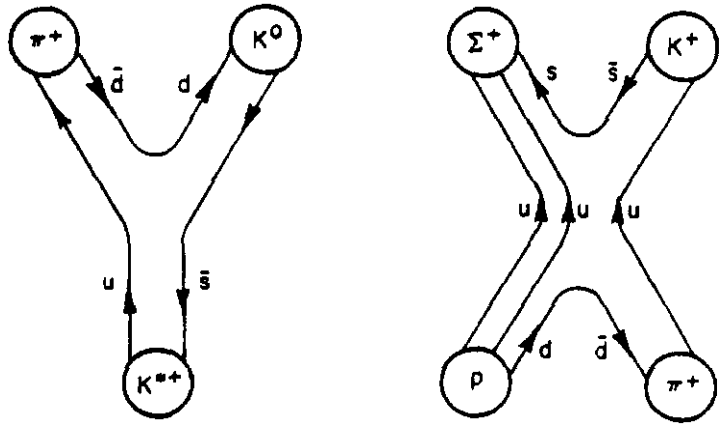

Fig. D.2: Quark diagrams for decays and 2 body scattering.

This seems a good place to stop because our Van der Waals chemistry is threatening to become organic chemistry. It is leading us rather far afield from our attempt to understand the molecular physics of hadrons using the atomic physics of quarks.

Summary

What we have attempted to do is to provide a simple but superficial framework for any particular particle. Thus, without undue reference to the blue book, one can put it into a SU(3) category. Therefore, we can understand it's quark content, and it's quantum numbers by putting it into an octet or a decuplet or a singlet. The mass can be understood knowing its strange quark content since the constituent masses and the spin-spin splitting depend on strangeness. For higher excitations, the spin-orbit splitting has been estimated. In this way, you can make a very quick estimate of the mass of this hadron. We found the coupling constants; the weak coupling 4 fermion dynamics, or the electromagnetic or hadronic dynamics. Knowing the mass and coupling, one should be able to make a good estimate of the decay width. By drawing particular sets of diagrams one should also be able to get a plausible idea of the relevant branching ratios into different final states. With these preliminaries, after a moments thought in order to orient oneself, one can go look in the blue book without any hesitation that the answers that one finds are explicable in an intuitive way. By intuition in this case we just mean internalized repetitive experiences.

The hope is that now there are no major mysteries to be found in the particle properties blue book. We presume that our trip to the zoo has been a pleasant and rewarding excursion. We now understand the kingdom / phylum / order / family / genus / species classification of the hadrons that we have met at the zoo.

References

1. Phys. Lett. 170B, April 1986, "Review of Particle Properties" and Particle Properties Data Booklet, Particle Data Group.

2. C. Quigg, "Models for Hadrons," FNAL CONF-81/78-THY, Nov. 1981.

3. F. E. Close, "An Introduction to Quarks and Leptons," Academic Press (1979).

4. I.S. Hughes, "Elementary Particles," Cambridge University Press (1985).

5. K. Gottfried, "Concepts in Particle Physics," Clarendon Press (1986).

6. I.B. Okun, "Particle Physics, The Quest for the Substance of Substance," Harwood (1984).

7. F. Halzen and A. Martin, "Quarks and Leptons: An Introductory Course in Modern Particle Physics," Wiley (1984).

8. D. Perkins, "Introduction to High Energy Physics," Addison Wesley (1982).